A bird's eye view: global analysis of nuclear and electroweak properties and the role of CEνNS

Matteo Cadeddu
matteo.cadeddu@ca.infn.it

INFN CAGLIARI

STVDIORVM UNIVERSITAS CARALITANA

In collaboration with
M. Atzori Corona, N. Cargioli, F. Dordei, C. Giunti

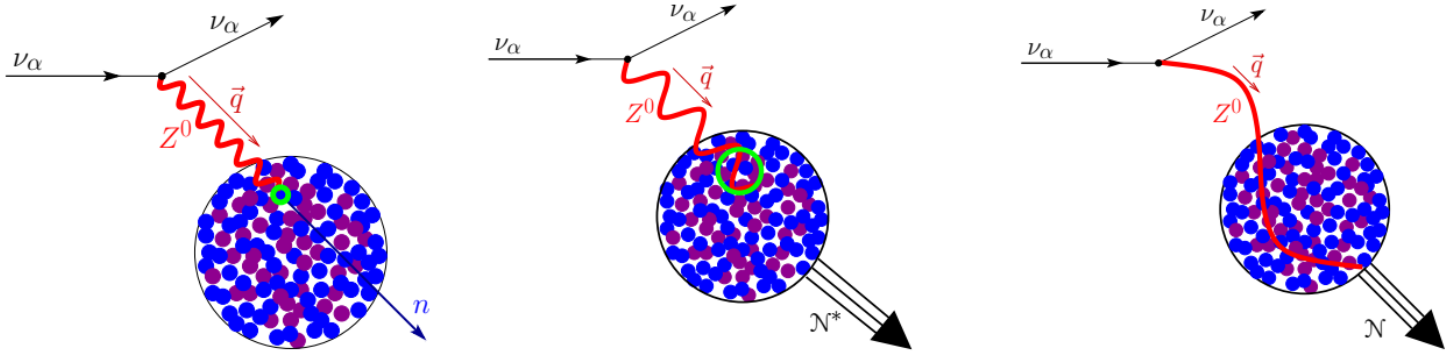

For a recent review see Europhysics Letters, Volume 143, Number 3, 2023 (EPL 143 34001), arXiv:2307.08842v2

Coherent elastic neutrino nucleus scattering (aka CEνNS)

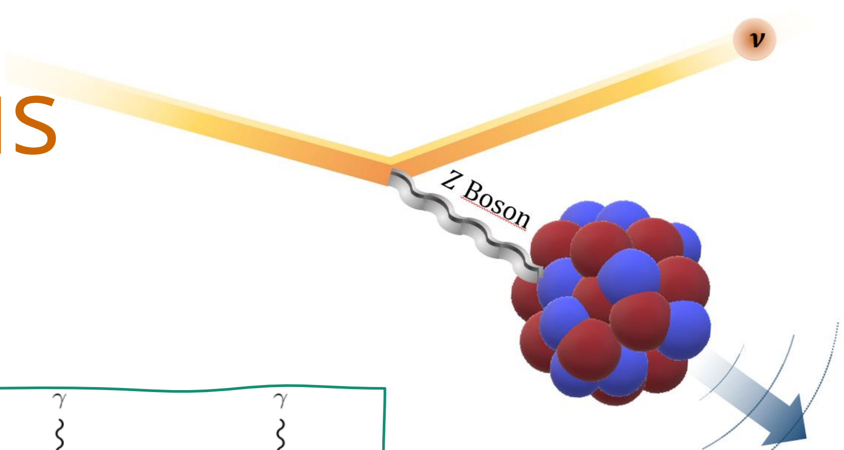

+A pure weak neutral current process

$$\boxed{\frac{d\sigma_{\nu_\ell\text{-}\mathcal{N}}}{dT_{\rm nr}}(E,T_{\rm nr}) = \frac{G_{\rm F}^2 M}{\pi}\left(1-\frac{MT_{\rm nr}}{2E^2}\right)\left(Q_{\ell,\rm SM}^V\right)^2}$$

+Weak charge of the nucleus

$$Q_{\ell,\rm SM}^V = \Big[\underbrace{g_V^p\left(\nu_\ell\right) Z F_Z\left(|\vec{q}|^2\right)}_{\text{protons}} + \underbrace{g_V^n N F_N\left(|\vec{q}|^2\right)}_{\text{neutrons}}\Big]$$

In general, in a weak neutral current process which involves nuclei, one deals with **nuclear form factors** that are different for protons and neutrons and cannot be disentangled from the neutrino-nucleon couplings!

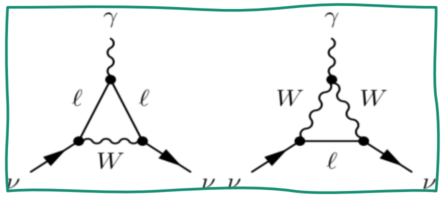

J. Erler and S. Su. *Prog. Part. Nucl. Phys.* 71 (2013). arXiv:1303.5522 & PDG2023 and **M. Atzori Corona et al. arXiv:2402.16709**

+ Neutrino-nucleon tree-level couplings

$$g_V^p = \frac{1}{2} - 2\sin^2(\vartheta_W) \cong \mathbf{0.02274}$$

$$g_V^n = -\frac{1}{2} = -0.5$$

See F. Dordei's talk on radiative corrections

+ Radiative corrections are expressed in terms of WW, ZZ boxes and the neutrino charge radius diagram → Flavour dependence

$$g_V^p(\nu_e) \simeq 0.0381,\ g_V^p(\nu_\mu) \simeq 0.0299 \quad g_V^n \simeq -0.5117$$

Nuclear physics, but since $g_V^n \approx -0.51 \gg g_V^p(\nu_\ell) \approx 0.03$ neutrons contribute the most

$$\boxed{\frac{d\sigma}{dE_r} \propto N^2}$$

What we can learn from CEνNS

M. Cadeddu et al., JHEP 01 (2021) 116, arXiv:2008.05022

O. G. Miranda et al., JHEP 05 (2020) 130, arXiv:2003.12050

M. Atzori Corona et al., JHEP 05 109 (2022), arXiv:2202.11002

C. Giunti, *PRD* 101 (2020) 3, 035039, arXiv:1909.00466

D. K. Papoulias and T. S. Kosmas, PRD 97, 033003 arxiv:1711.09773

D. A. Sierra et al., PRD 98, 075018 (2018) arXiv:1806.07424

L. J. Flores et al., JHEP 06 (2020) 045, 2002.12342

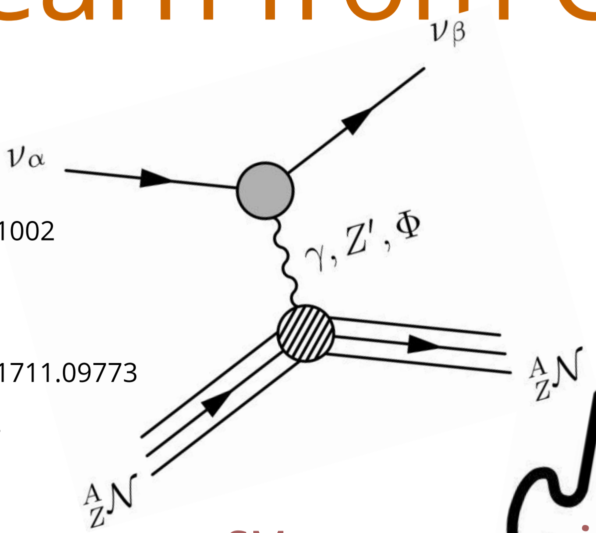

O. G. Miranda et al., JHEP 05 (2020) 130, arXiv:2003.12050

B. Dutta et al., Phys. Rev. Lett. 123, 061801 (2019)

O. G. Miranda et al., JHEP 07 (2019) 103, arXiv: 1905.03750

D. Aristizabal Sierra et al., Phys. Rev. D 98, 075018 (2018)

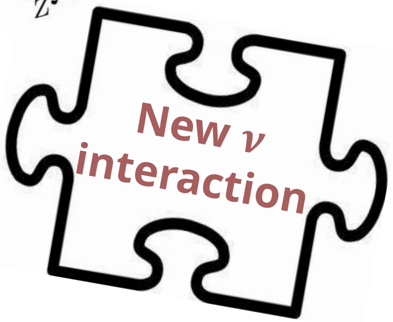

Neutrino energy

Mass of the nucleus

SM vector proton coupling

SM vector neutron coupling

$$\frac{d\sigma^{CE\nu NS}(E_\nu, E_r)}{dE_r} \cong \frac{G_F^2\, m_N}{\pi}\left(1 - \frac{m_N E_r}{2E_\nu^2}\right)\left[g_V^p\left(\sin^2(\vartheta_W)\right) Z\, F_Z(|\vec{q}|^2) + g_V^n\, N\, F_N(|\vec{q}|^2)\right]^2 + \dots$$

Weinberg angle

Proton Form Factor

Neutron Form Factor

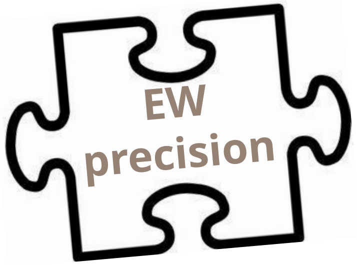

D. Papoulias et al., PLB 800 (2020) 135133, arXiv:1903.03722

Coloma et al., JHEP 08 (2020) 08, 030, arXiv:2006.08624

D. A. Sierra et al., JHEP 1906:141 (2019) arXiv: 1902.07398

B. Canas et al., PRD 101, 035012 (2020), arXiv:1911.09831

K. Patton, J. Engel, G. C. McLaughlin, and N. Schunck, Phys. Rev. C 86, 024612 (2012).

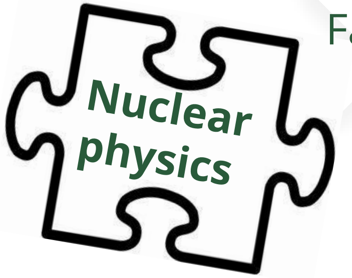

Interplay between nuclear and electroweak physics

+ This feature is always present when dealing with electroweak processes.

- Atomic Parity Violation (APV): atomic electrons interacting with nuclei- **Cesium (Cs)** and **lead (Pb)** available.
- Parity Violation Electron Scattering (PVES): polarized electron scattering on nuclei- **PREX(Pb)** & CREX(Ca)
- Coherent elastic neutrino-nucleus scattering (CEνNS)- **Cesium-iodide (CsI),** argon (Ar) and germanium (Ge) available.

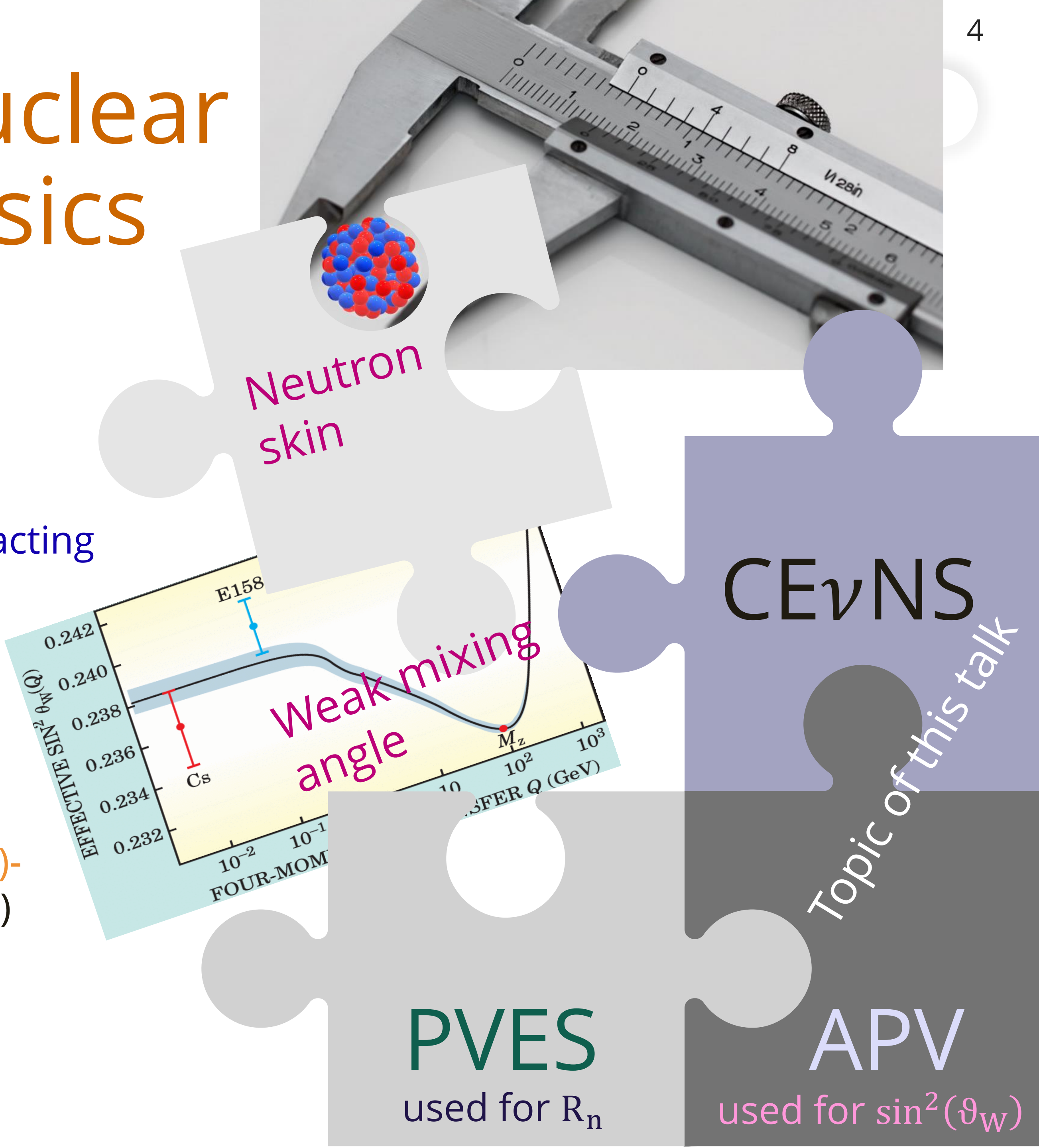

Where did we leave off at the last MG7 edition?

Neutron form factor dependence in CEνNS cross section

$$\frac{d\sigma^{CE\nu NS}(E_\nu, E_r)}{dE_r} \cong \frac{G_F^2\, m_N}{\pi}\left(1 - \frac{m_N E_r}{2E_\nu^2}\right)\left[g_V^p\left(\sin^2(\vartheta_W)\right) Z\, F_Z(|\vec{q}|^2) + g_V^n\, N\, F_N(|\vec{q}|^2)\right]^2$$

Neutron form factor (R_n) to be fitted

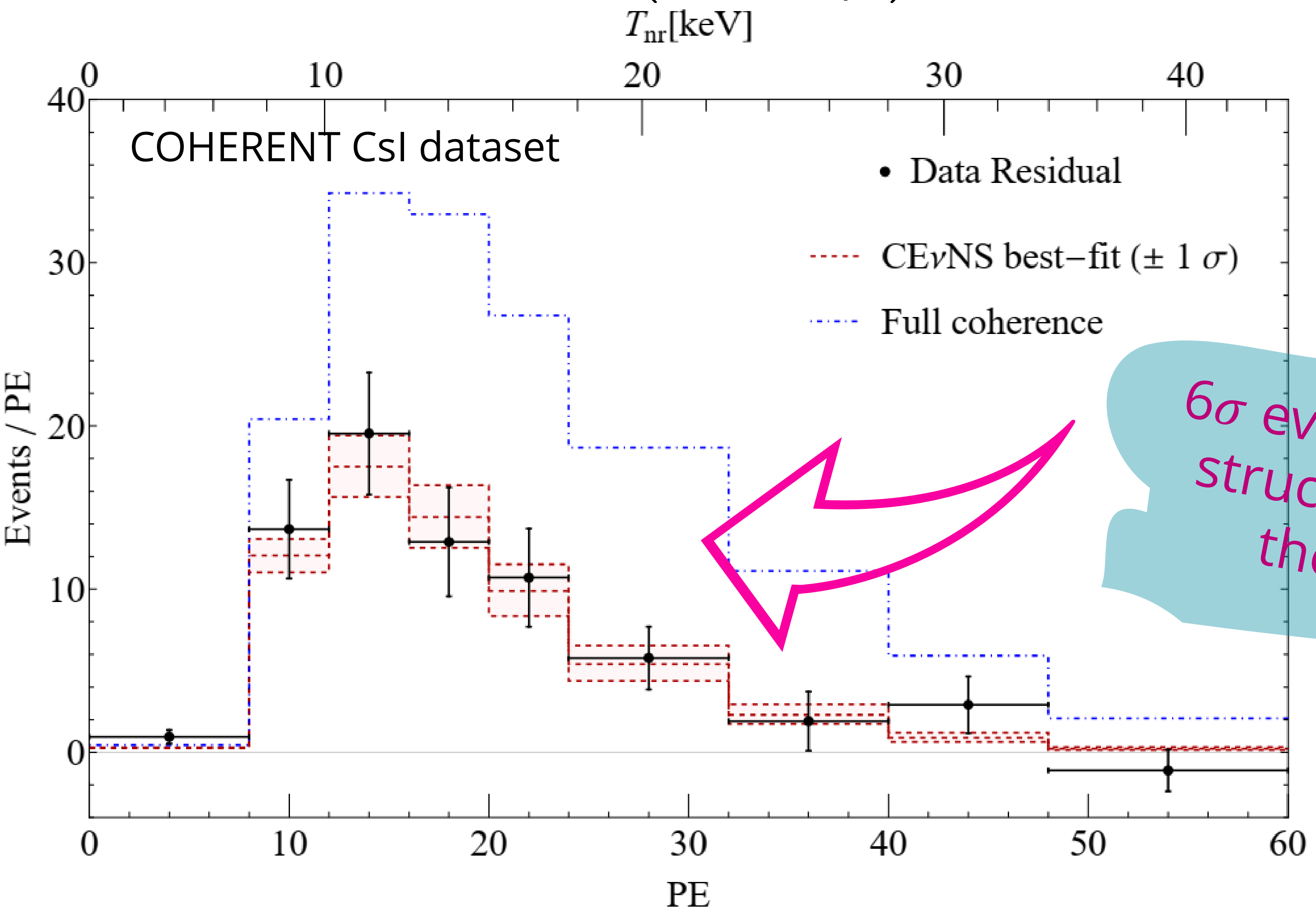

6σ evidence of the nuclear structure suppression of the full coherence!

See also:

Rossi et al. PRD 109, 095044 (2024) arXiv:2311.17168

De Romeri et al. JHEP04(2023)035 arXiv:2211.11905

D. Papoulias et al., PLB 800 (2020) 135133, arXiv:1903.03722

M. Atzori Corona et al., EPJC 83 (2023) 7, 683. ArXiv:2303.09360

The CsI neutron skin fixing $\sin^2(\vartheta_W)$

If we fix the value of $\sin^2\vartheta_W$ at the SM prediction ($0.23863(5)$) then we obtain (1D fit):

M. Atzori Corona et al., EPJC 83 (2023) 7, 683
arXiv:2303.09360

$$R_n\ (\mathrm{CsI}) = 5.47 \pm 0.38\ \mathrm{fm}$$

$\sim$7% precision

Neutron skin: R_n (CsI)- R_p (CsI)

$$\Delta R_{np}(\mathrm{CsI}) = 0.69 \pm 0.38\ \mathrm{fm}$$

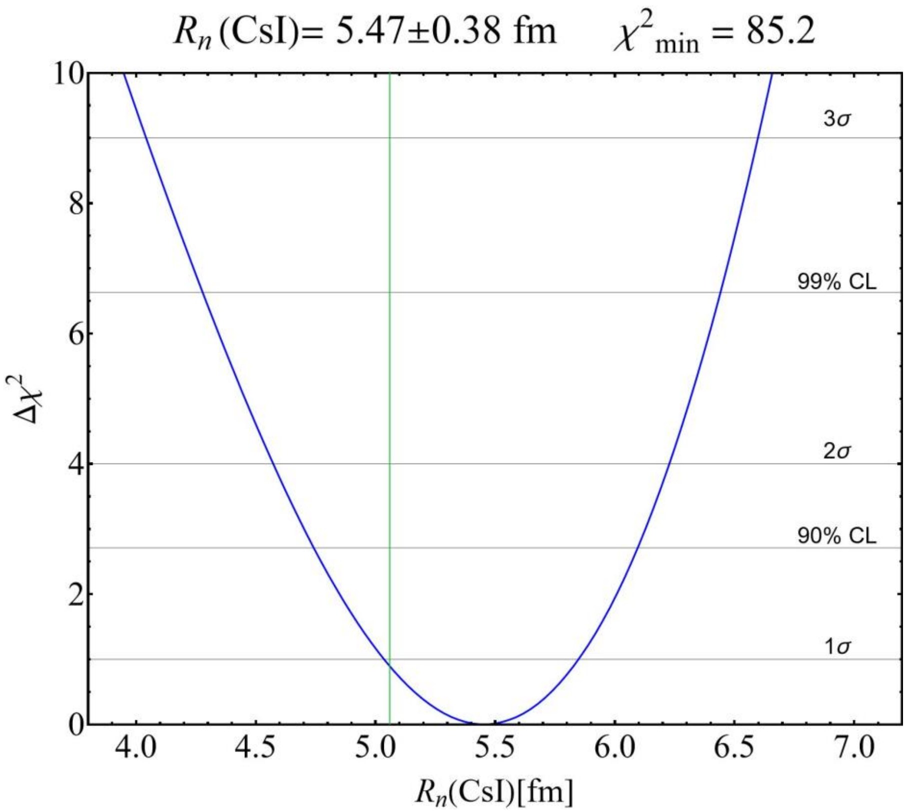

Theoretical values of the neutron skin of Cs and I obtained with nuclear mean field models. The value is compatible with all the models...

$$0.12 < \Delta R_{np}^{CsI} < 0.24\ \mathrm{fm}$$

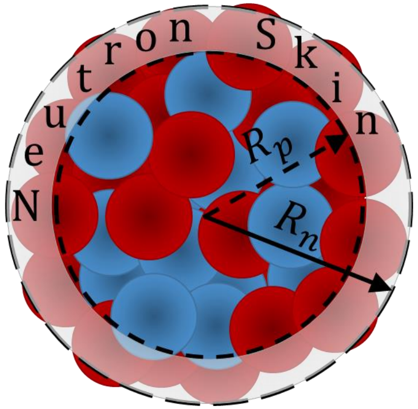

	^{127}I						^{133}Cs					
Model	R_p^{point}	R_p	R_n^{point}	R_n	$\Delta R_{np}^{\mathrm{point}}$	ΔR_{np}	R_p^{point}	R_p	R_n^{point}	R_n	$\Delta R_{np}^{\mathrm{point}}$	ΔR_{np}
SHF SkI3 [81]	4.68	4.75	4.85	4.92	0.17	0.17	4.74	4.81	4.91	4.98	0.18	0.18
SHF SkI4 [81]	4.67	4.74	4.81	4.88	0.14	0.14	4.73	4.80	4.88	4.95	0.15	0.14
SHF Sly4 [82]	4.71	4.78	4.84	4.91	0.13	0.13	4.78	4.85	4.90	4.98	0.13	0.13
SHF Sly5 [82]	4.70	4.77	4.83	4.90	0.13	0.13	4.77	4.84	4.90	4.97	0.13	0.13
SHF Sly6 [82]	4.70	4.77	4.83	4.90	0.13	0.13	4.77	4.84	4.89	4.97	0.13	0.13
SHF Sly4d [83]	4.71	4.79	4.84	4.91	0.13	0.12	4.78	4.85	4.90	4.97	0.12	0.12
SHF SV-bas [84]	4.68	4.76	4.80	4.88	0.12	0.12	4.74	4.82	4.87	4.94	0.13	0.12
SHF UNEDF0 [85]	4.69	4.76	4.83	4.91	0.14	0.14	4.76	4.83	4.92	4.99	0.16	0.15
SHF UNEDF1 [86]	4.68	4.76	4.83	4.91	0.15	0.15	4.76	4.83	4.90	4.98	0.15	0.15
SHF SkM* [87]	4.71	4.78	4.84	4.91	0.13	0.13	4.76	4.84	4.90	4.97	0.13	0.13
SHF SkP [88]	4.72	4.80	4.84	4.91	0.12	0.12	4.79	4.86	4.91	4.98	0.12	0.12
RMF DD-ME2 [89]	4.67	4.75	4.82	4.89	0.15	0.15	4.74	4.81	4.89	4.96	0.15	0.15
RMF DD-PC1 [90]	4.68	4.75	4.83	4.90	0.15	0.15	4.74	4.82	4.90	4.97	0.16	0.15
RMF NL1 [91]	4.70	4.78	4.94	5.01	0.23	0.23	4.76	4.84	5.01	5.08	0.25	0.24
RMF NL3 [92]	4.69	4.77	4.89	4.96	0.20	0.19	4.75	4.82	4.95	5.03	0.21	0.20
RMF NL-Z2 [93]	4.73	4.80	4.94	5.01	0.21	0.21	4.79	4.86	5.01	5.08	0.22	0.22
RMF NL-SH [94]	4.68	4.75	4.86	4.94	0.19	0.18	4.74	4.81	4.93	5.00	0.19	0.19

Weak mixing angle from CEνNS only

$$\frac{d\sigma^{CE\nu NS}(E_\nu, E_r)}{dE_r} \cong \frac{G_F^2\, m_N}{\pi}\left(1 - \frac{m_N E_r}{2E_\nu^2}\right)\left[g_V^p\left(\sin^2(\vartheta_W)\right) Z\, F_Z(|\vec{q}|^2) + g_V^n\, N\, F_N(|\vec{q}|^2)\right]^2$$

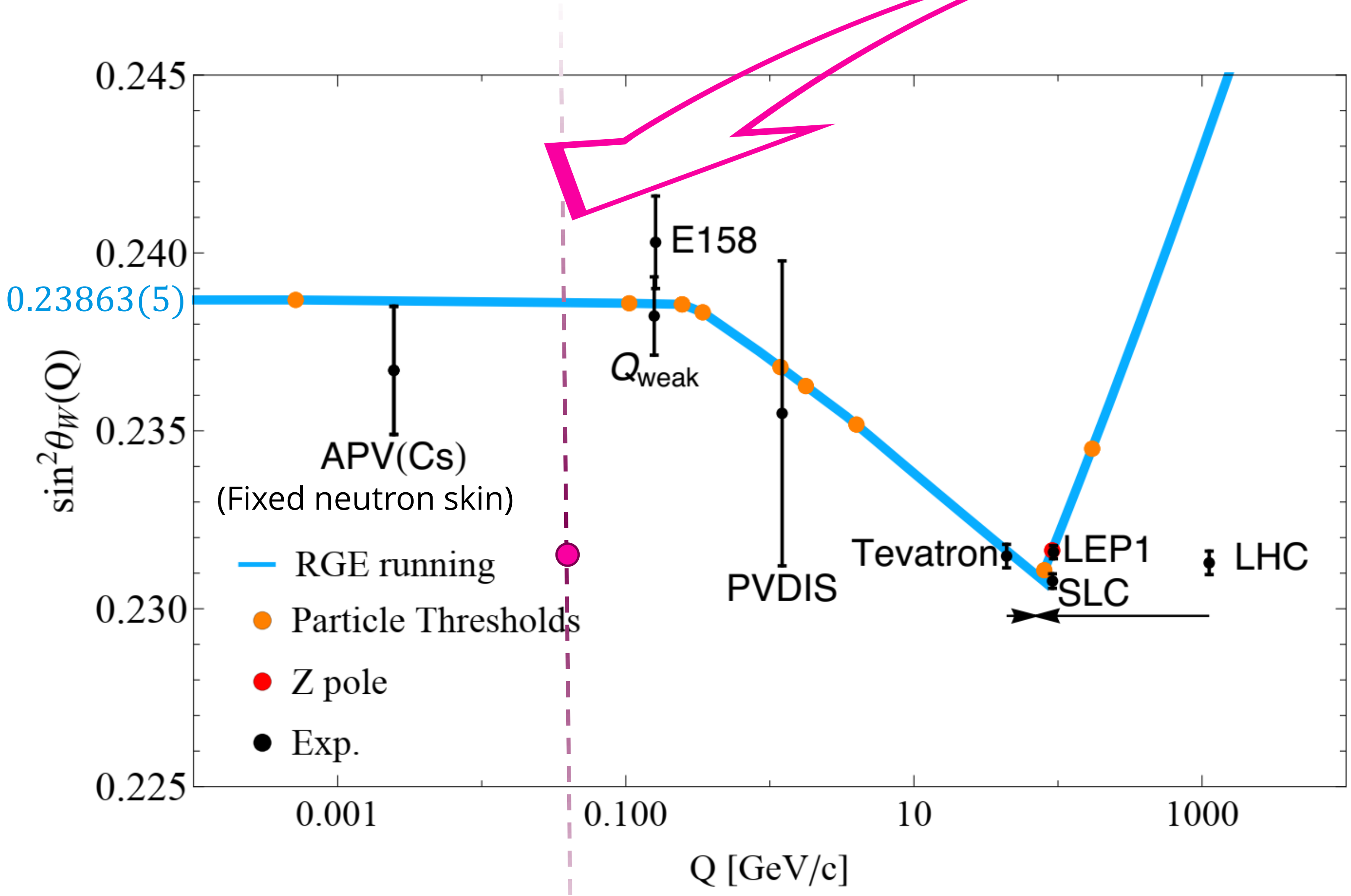

If we fix the value of the neutron radius of Cs and I and we fit for the weak mixing angle only we obtain:

$$\sin^2\vartheta_W = 0.231^{+0.027}_{-0.024}$$

The precision on the weak mixing angle using CEνNS is poor because of the neutrino-proton coupling suppression!

M. Atzori Corona et al., EPJC 83 (2023) 7, 683. ArXiv:2303.09360

The strategy

APV (Cs)

+ Sensitive to the weak mixing angle
+ Similarly sensitive to the neutron skin

COHERENT (CsI)

+ CEνNS is sensitive to the neutron skin
+ But less sensitive to the weak mixing angle

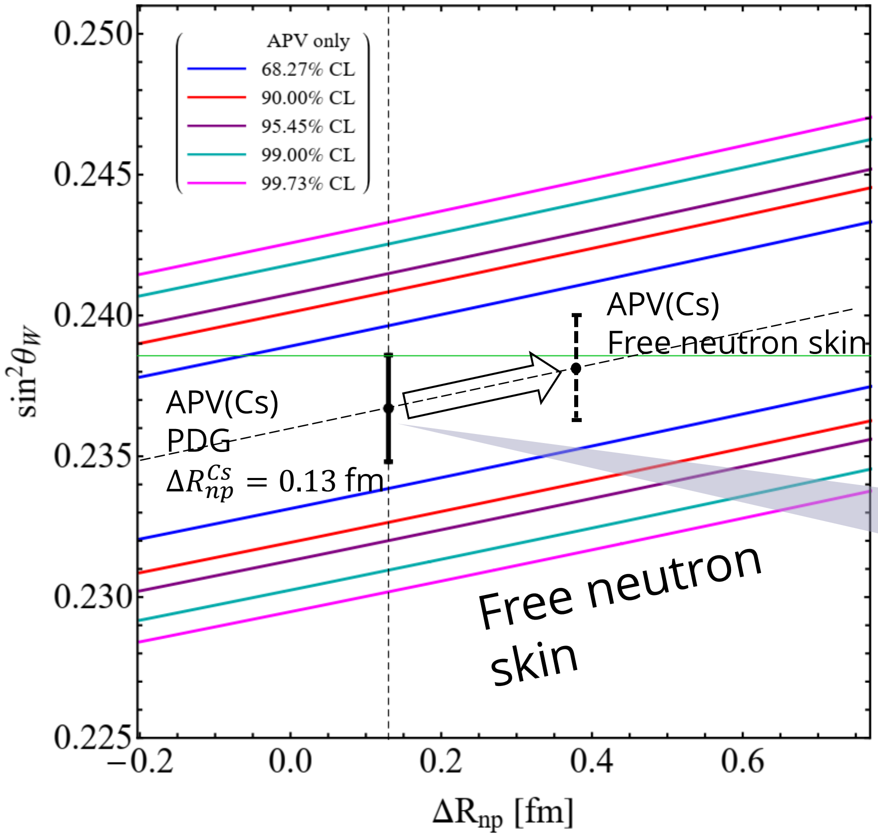

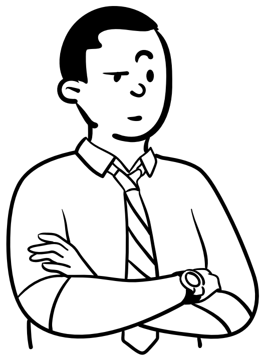

APV(Cs) PDG corresponds to $\Delta R_{np}^{Cs}(\text{Extr.}) = 0.13$ fm

Extrapolated from antiprotonic atoms...

$$\sin^2 \vartheta_W(\text{COH}-\text{CsI}) = 0.231^{+0.027}_{-0.024}(1\sigma)^{+0.046}_{-0.039}(90\%\text{CL})^{+0.058}_{-0.047}(2\sigma)$$

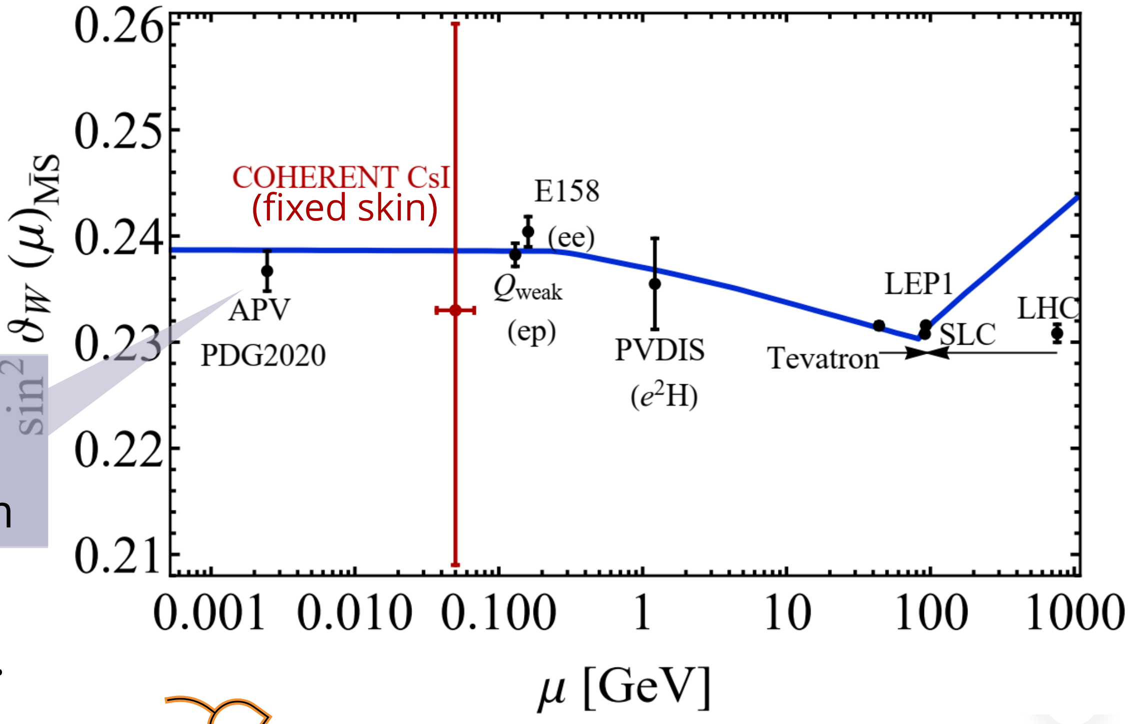

Why not combining them?

Combined fit of COHERENT and APV(Cs)

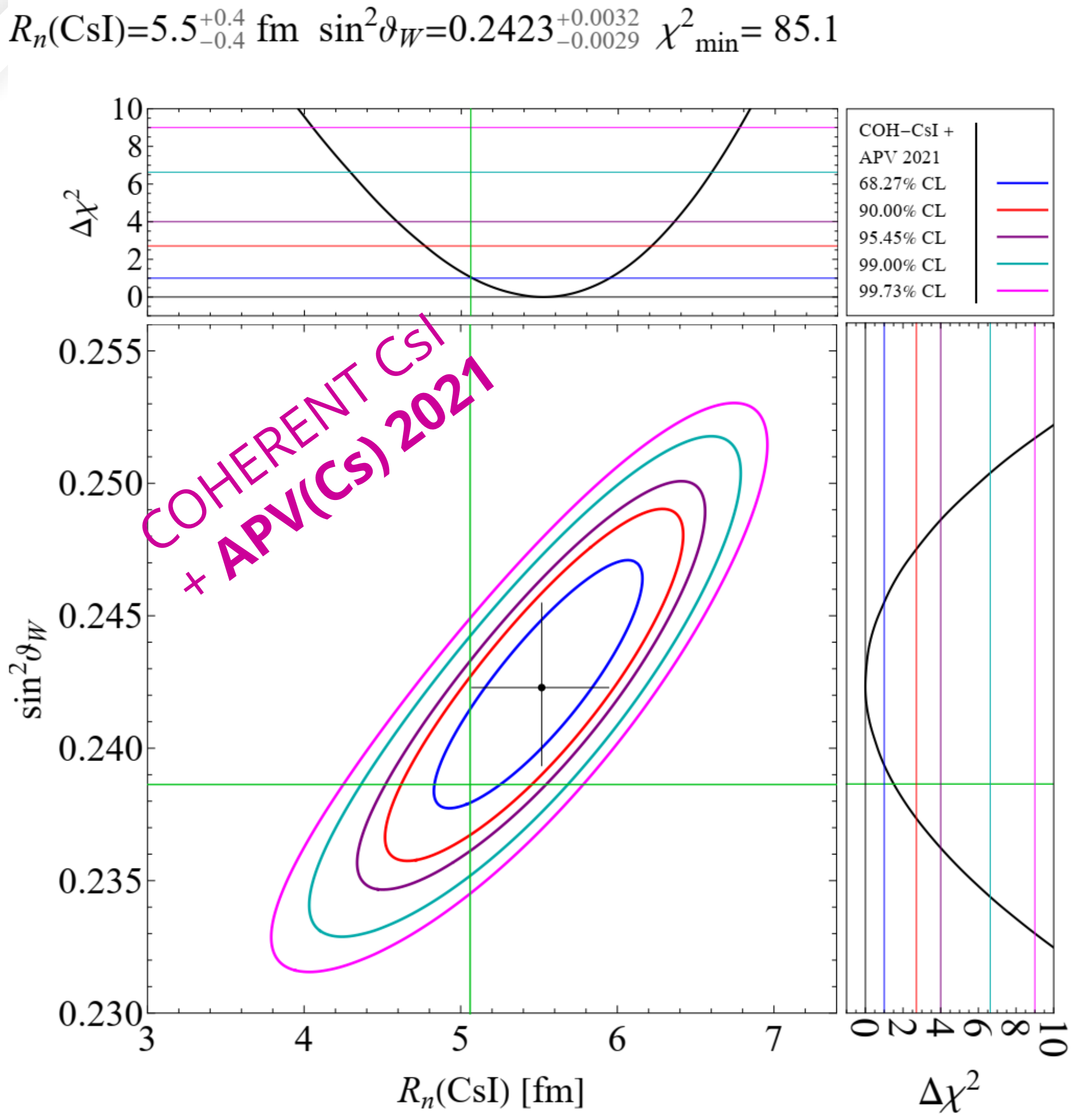

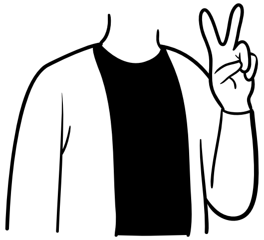

No assumptions on the Cs neutron skin are made. The neutron skin is taken directly from CEνNS experimental data

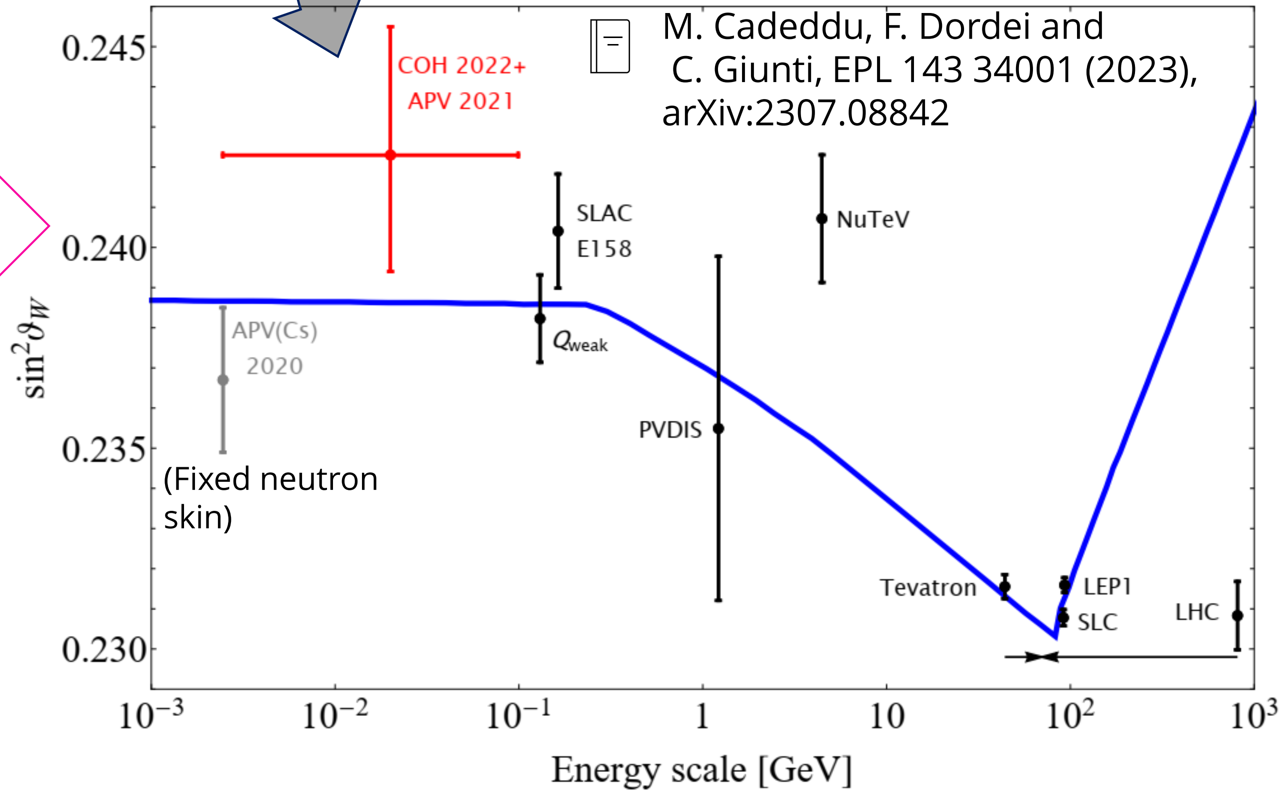

M. Cadeddu, F. Dordei and C. Giunti, EPL 143 34001 (2023), arXiv:2307.08842

M. Atzori Corona et al., EPJC 83 (2023) 7, 683, arXiv:2303.09360

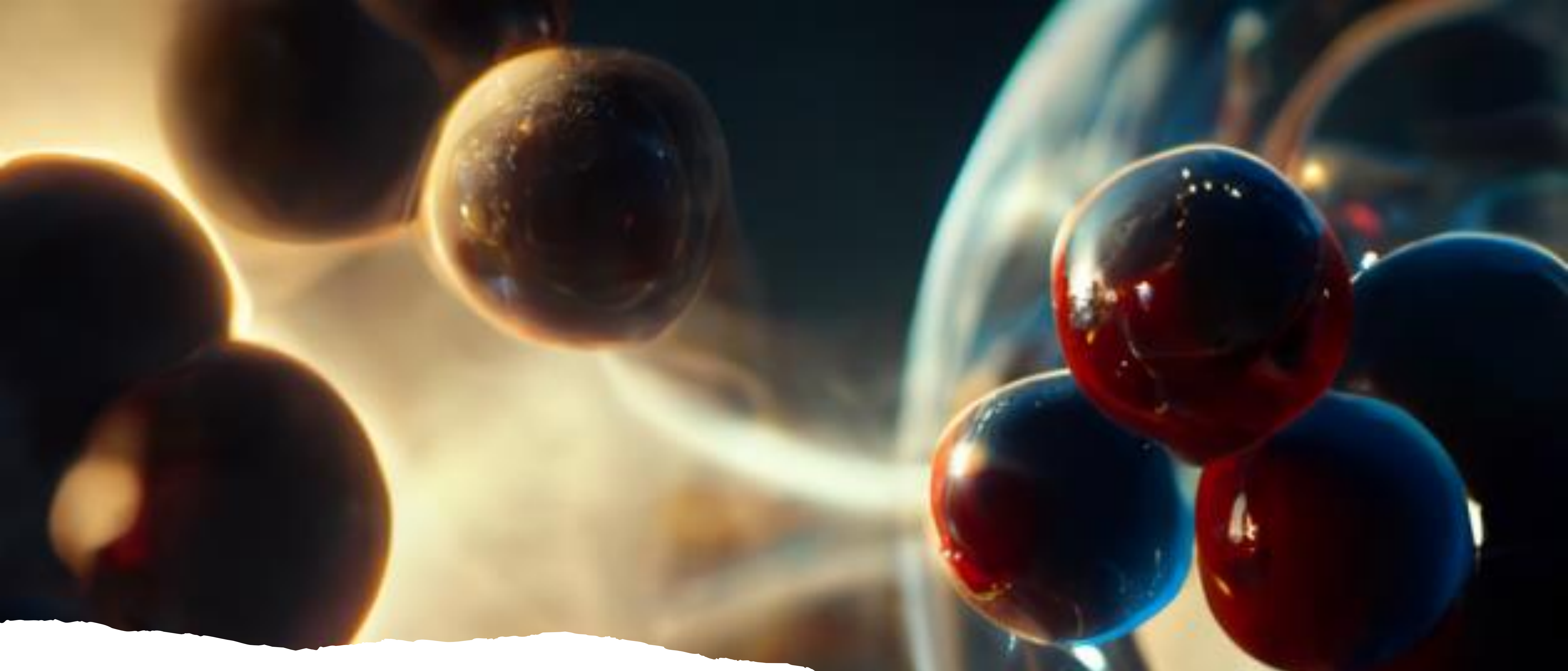

Where are we now?

M. Atzori Corona et al. Refined determination of the weak mixing angle at low energy, arXiv:2405.09416 (2024)

Cs neutron skin from proton-elastic scattering

New measurement from **proton-cesium elastic scattering at low momentum transfer** using an in-ring reaction technique at the **Cooler Storage Ring** (**CSRe**) at the Heavy Ion Research Facility in Lanzhou, which can be included in the derivation of $\sin^2\vartheta_W$. The authors employed this value to re-extract the COHERENT $\sin^2\vartheta_W$ value by fitting the CEνNS CsI dataset, finding $\sin^2\vartheta_W$ = 0.227 ± 0.028.

New direct measurement of the cesium-133 neutron skin, $\Delta \boldsymbol{R}_{\boldsymbol{np}}(\mathbf{Cs}) = \mathbf{0.12 \pm 0.21}$ **fm** available!

+ Experiments with hadronic probes are more precise BUT result interpretation of hadronic probe experiments is difficult due to the complexity of strong-force interactions.

Hovever, this is the first **DIRECT** determination of R_n(Cs)!

Huang et al.
arXiv:2403.03566v2

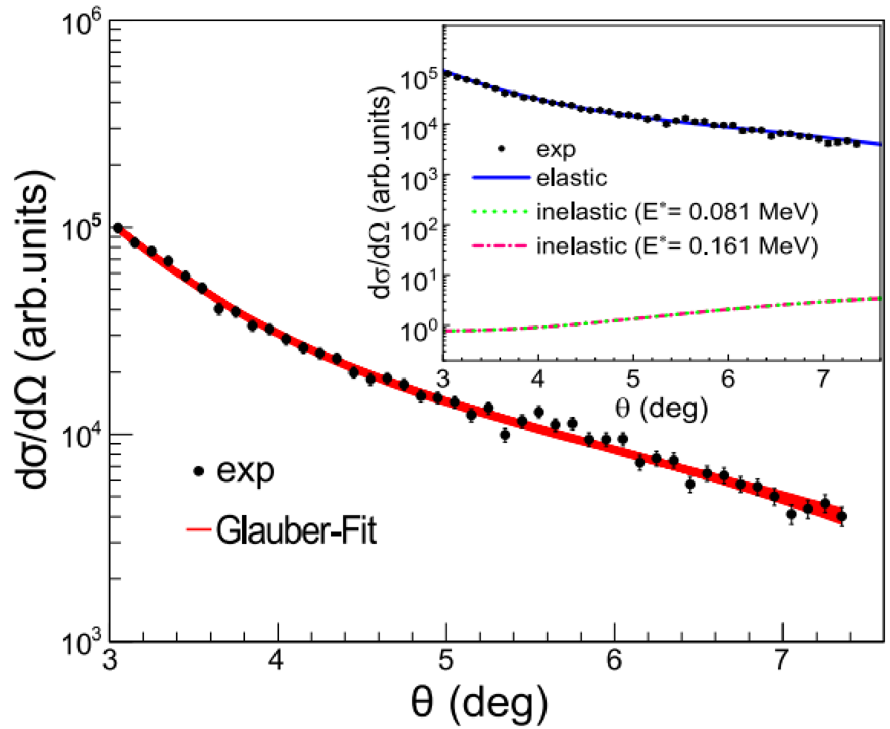

“Cesium neutron radius determination with hadronic probes has been historically experimentally challenging due to the low melting point and spontaneous ignition in air.“

First results: fit using R_n(Cs) from CSRe

+ We combine APV(Cs) and COHERENT CsI adding a prior on R_n(Cs)= 4.94 ± 0.21 fm coming from the **Cooler Storage Ring** (**CSRe**)

$\sin^2\vartheta_W$	$\mathrm{R_n}(^{133}\mathrm{Cs})[\mathrm{fm}]$
$0.2396^{+0.0020}_{-0.0019}$	5.04 ± 0.19

Big improvement with respect to our previous result (arXiv:2303:09360):

$$\sin^2\vartheta_W = 0.2423^{+0.0032}_{-0.0029}, \quad R_n(\mathrm{CsI}) = 5.5^{+0.4}_{-0.4}\ \mathrm{fm}$$

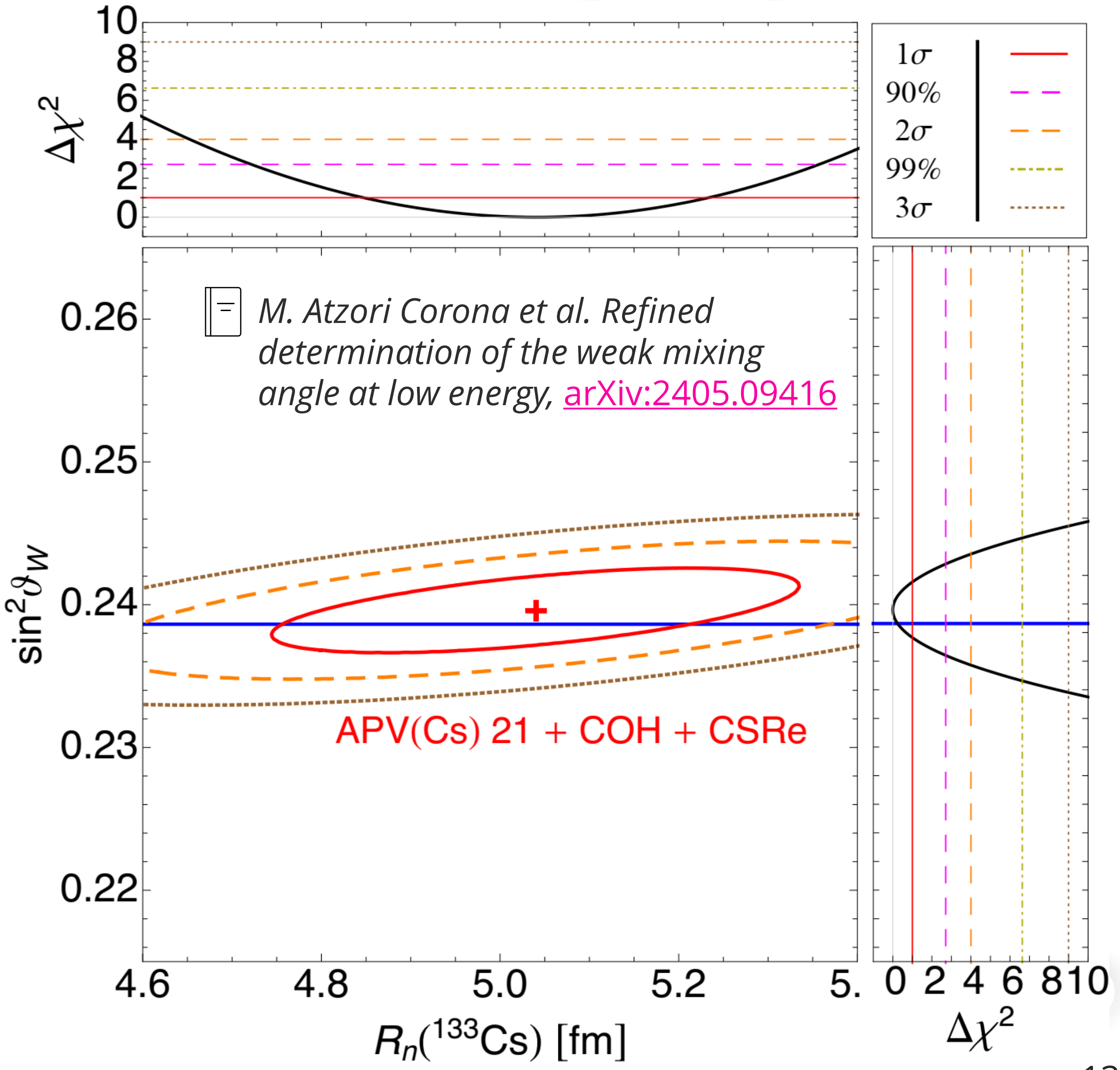

✓ Pros: For the first time a direct measurement on R_n(Cs) is used

❖ Cons: CSRe R_n(Cs) still comes from hadronic probes…

Can we use electroweak only inputs?

ElectroWeak only fit

+ We perform a fit using Electroweak (EW) only information removing the R_n(Cs) input from CSRe
+ APV(Cs) 21
+ COHERENT CsI
+ APV(Pb)+PREX-II

M. Atzori Corona et al. PRC 105, 055503 (2022), Arxiv: 2112.09717,

- APV has been measured also using lead.
- Moreover PREX-II has measured the Pb neutron skin with Parity Violation Electron Scattering (PVES).

We can profit from a very nice correlation between R_n(Cs) and R_n(Pb) within many theoretical nuclear models to translate R_n(Pb) to R_n(Cs)

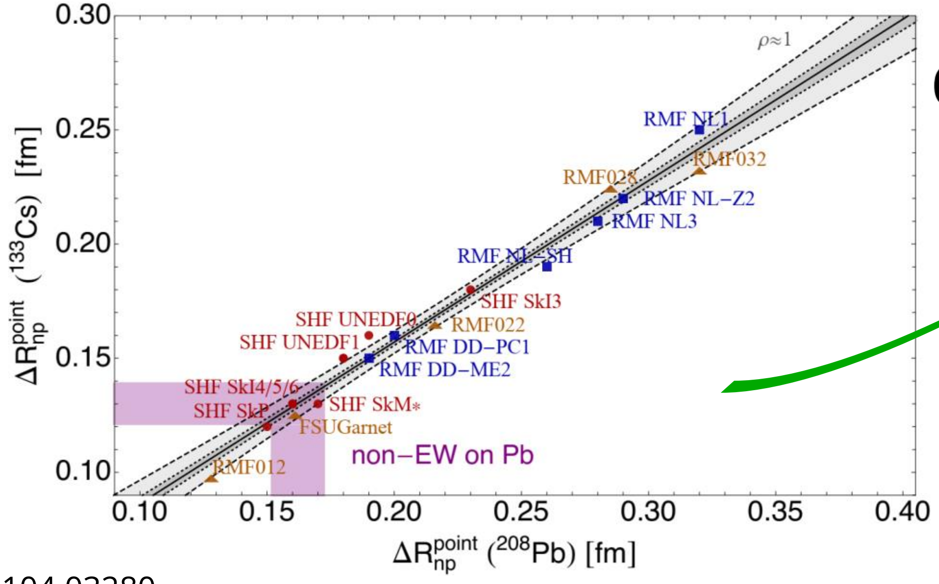

M. Cadeddu et al. PRD **104**, 011701 (2021), arXiv:2104.03280

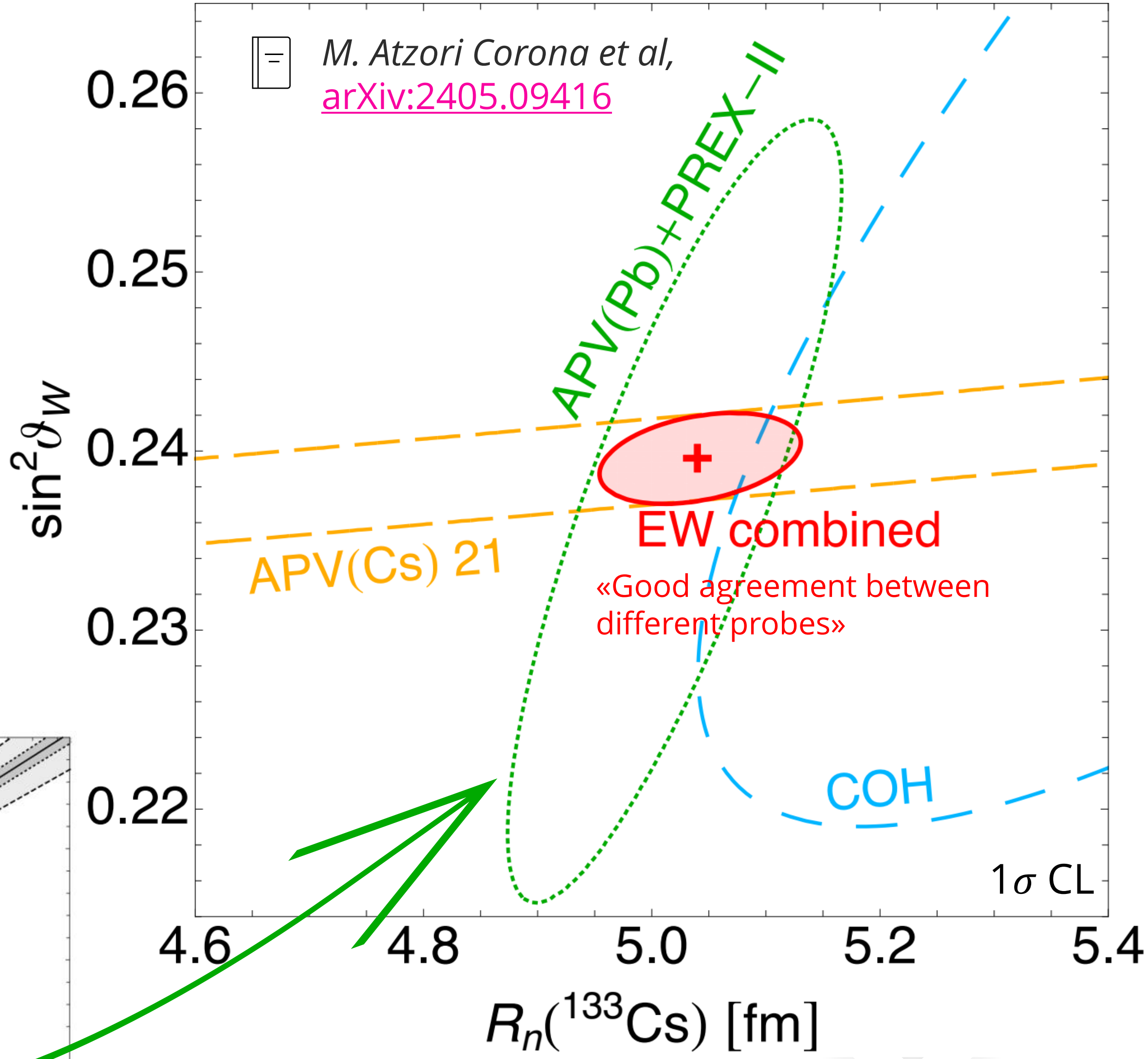

- ✓ Pros: only electroweak probes used
- ❖ Cons: we should trust the theoretical nuclear models for the translation of R_n(Pb) to R_n(Cs)

Comparison between the two results

A very nice agreement between the EW fit and that using R_n(Cs) from proton scattering is achieved!

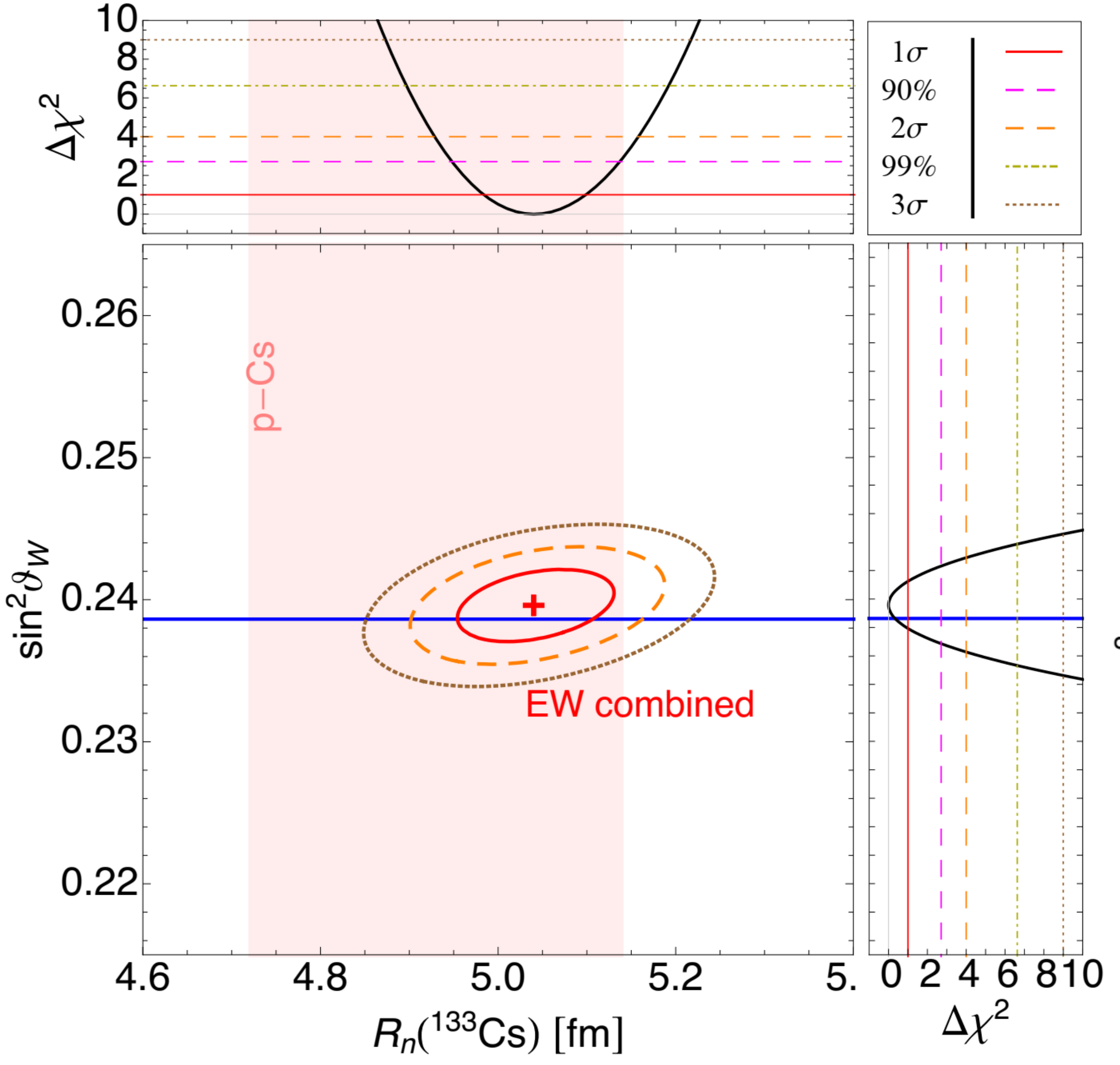

$$\sin^2\vartheta_W = \begin{cases} \boxed{0.2396 \pm 0.0017\,(\text{EW combined})} \\ \boxed{0.2396^{+0.0020}_{-0.0019}\,(\text{APV(Cs)} + \text{COH} + \text{CSRe})} \end{cases}$$

✓ same central values different uncertainties.

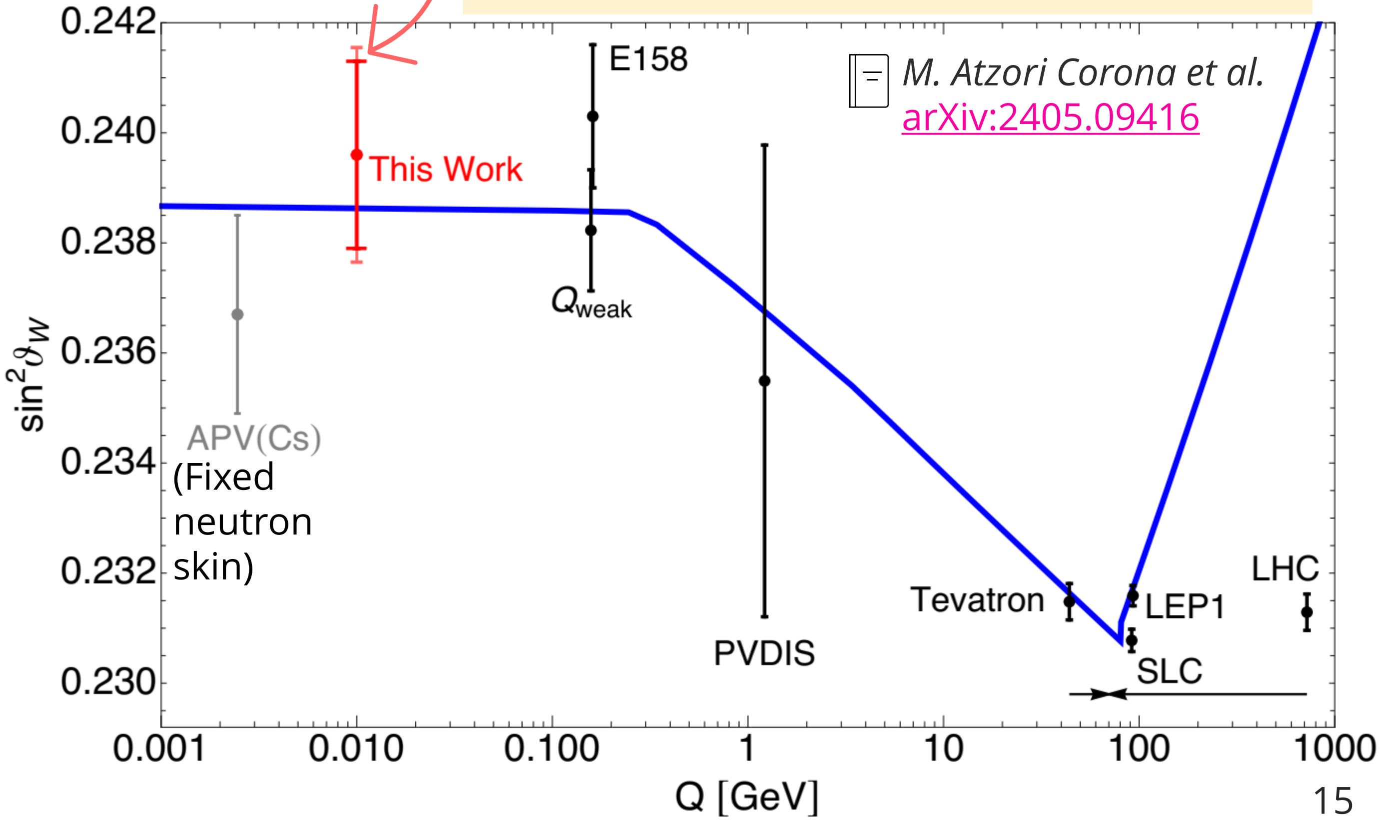

M. Atzori Corona et al.
arXiv:2405.09416

Conclusions for R_n(Cs)

	$\sin^2\vartheta_W$	$R_n(^{133}Cs)$[fm]	
APV(Cs)+COH+CSRe	$0.2396^{+0.0020}_{-0.0019}$	5.04 ± 0.19	3.8%
EW combined	0.2396 ± 0.0017	5.04 ± 0.06	1.2%

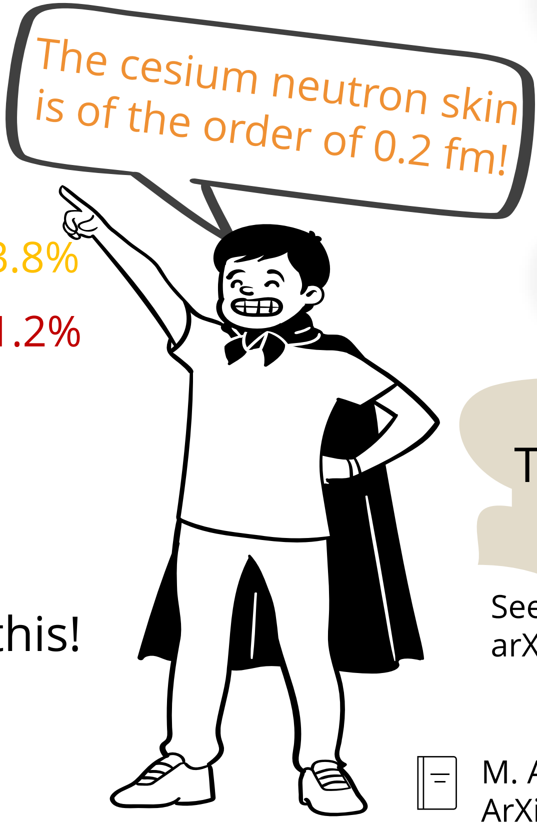

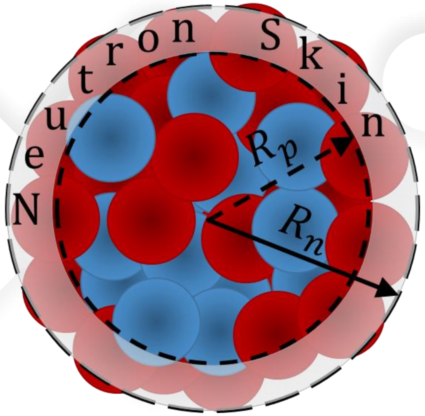

The neutron radius (or skin) of ^{133}Cs tends to be «large» but we cannot conclude more than this.

The COHERENT program for R_n(Cs) for is exciting!

See details in D. Akimov et al., arXiv:2204.04575 (2022)

✓ **We need** precise CEνNS measurements on this!

✓ With COH-CryoCsI-I we can reach same R_n(CsI) precison of the current EW combined fit (3.7%) and with COH-CryoCsI-II a better precision of the EW combined fit (0.5%)

M. Atzori Corona et al., EPJC 83 (2023) 7, 683. ArXiv:2303.09360

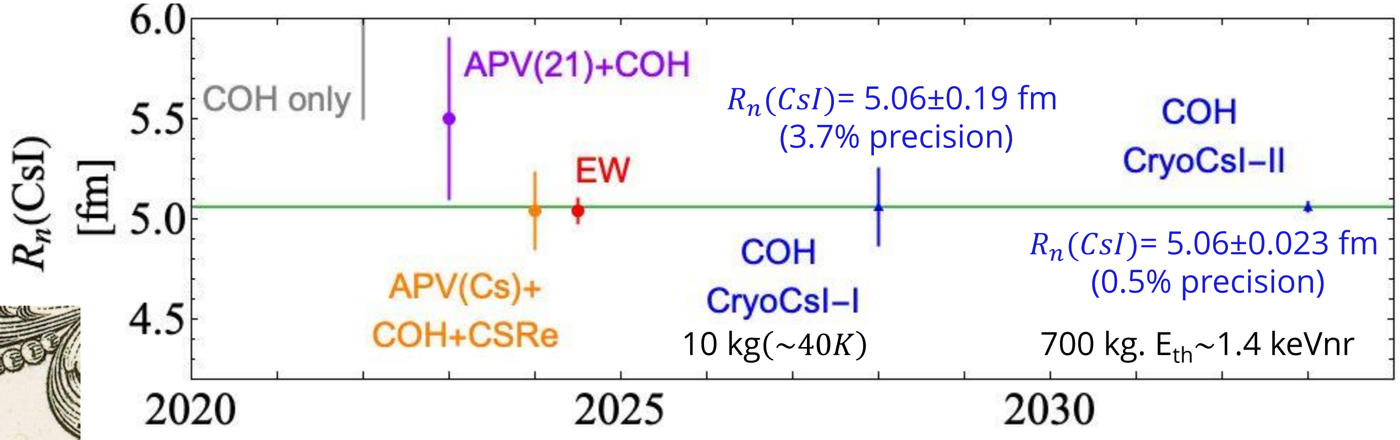

Conclusions for $\sin^2\vartheta_W$

Take home message 2

	$\sin^2\vartheta_W$
APV(Cs)+COH+CSRe	$0.2396^{+0.0020}_{-0.0019}$
EW combined	0.2396 ± 0.0017

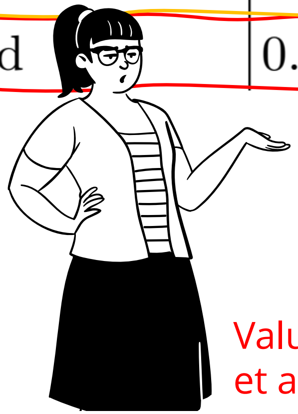

The biggest «uncertainty» comes from the theoretical calculation of the amplitude of the electric dipole transition $\mathbf{Im}\ \boldsymbol{E_{PNC}}$ used in **APV(Cs)** for which two different versions are available.

Value of Im E_{PNC} from B. K. Sahoo et al. PRD 103, L111303 (2021).

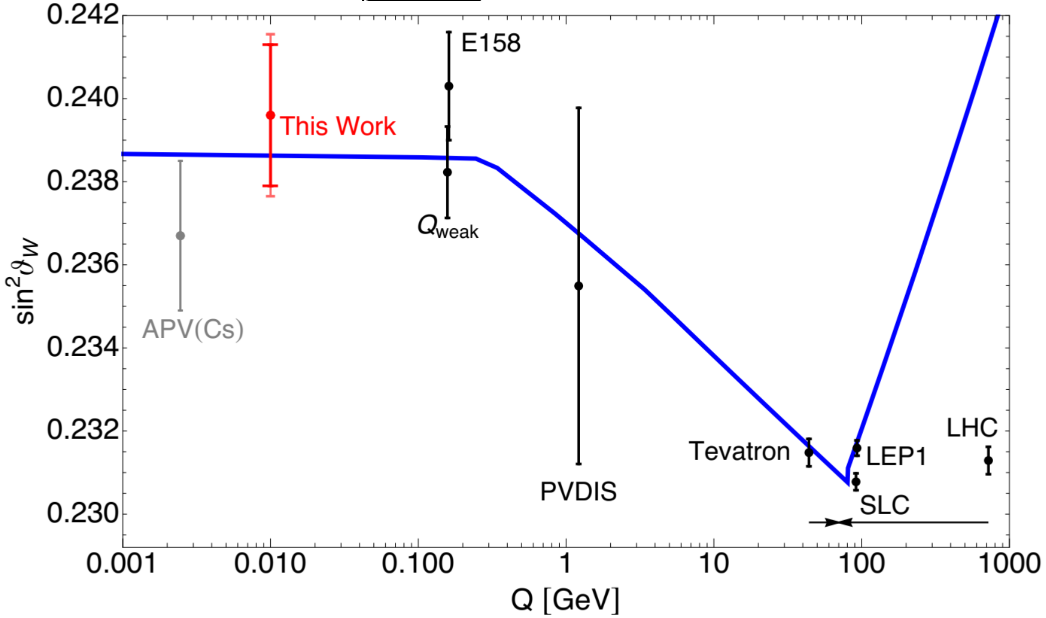

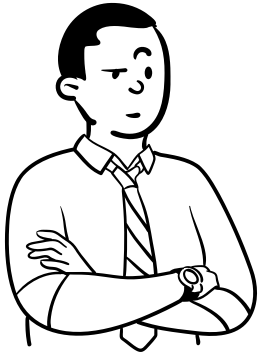

Value of ImE_{PNC} used by PDG (V. Dzuba *et al.*, PRL 109, 203003 (2012))

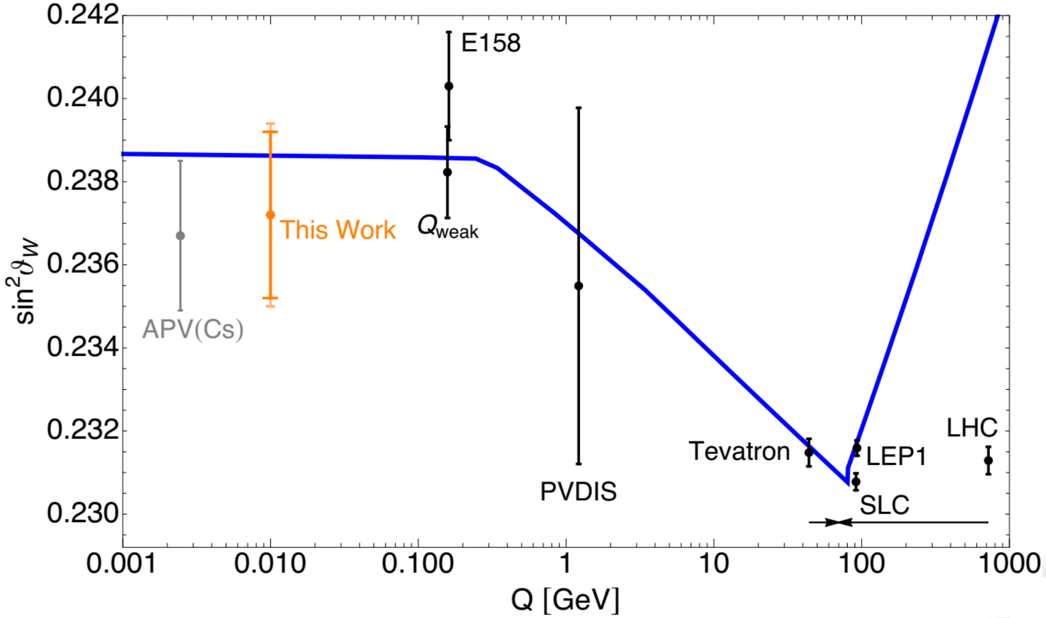

In both cases the «STANDARD MODEL RULEZ!»

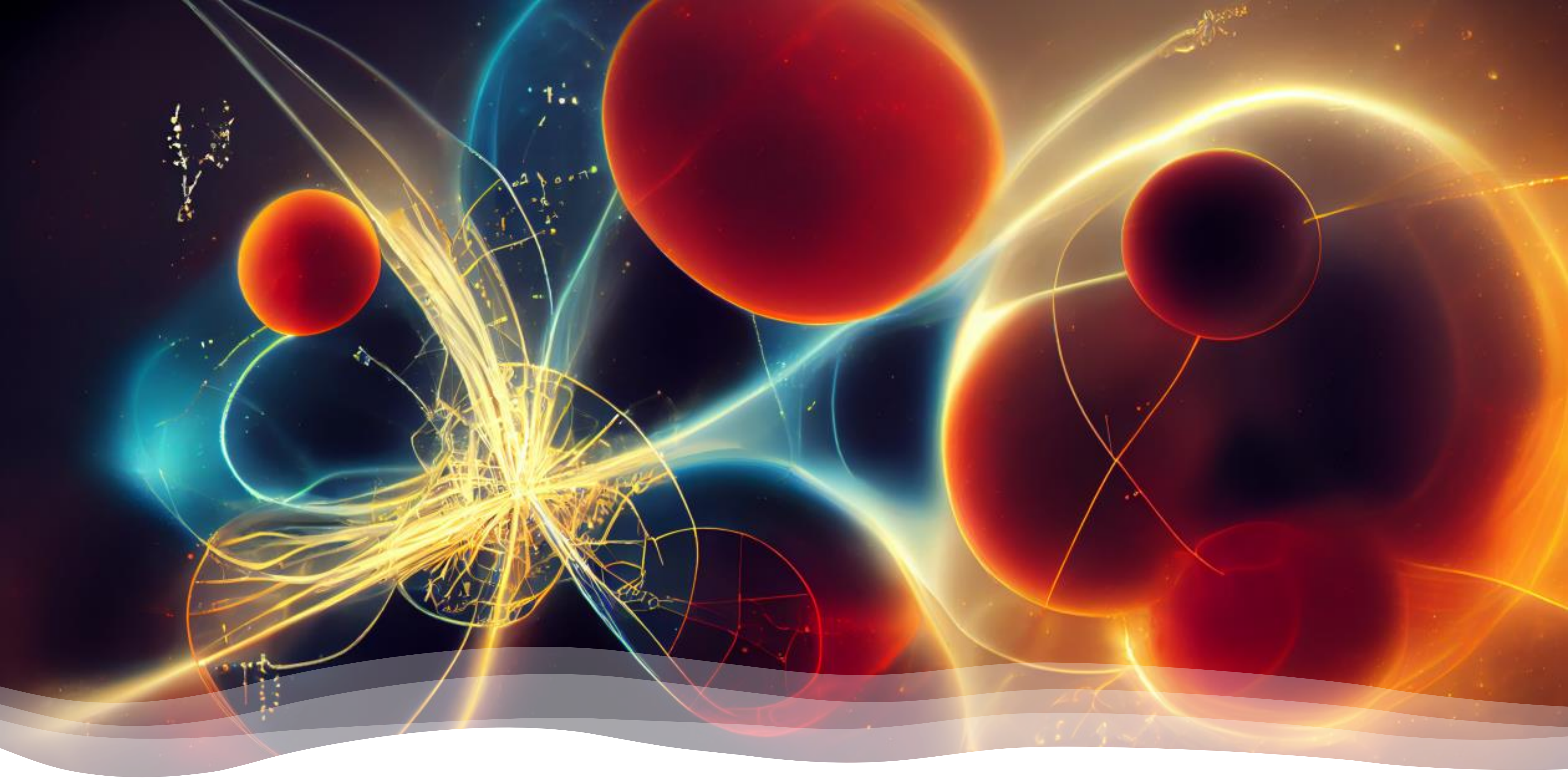

Thanks for your attention!

BACKUP

Global fit

M. Atzori Corona et al. arXiv:2405.09416

Since we "approved" the use of hadronic probes for the measurement of R_n(Cs), why not exploiting also the hadronic measurements of R_n(Pb)?

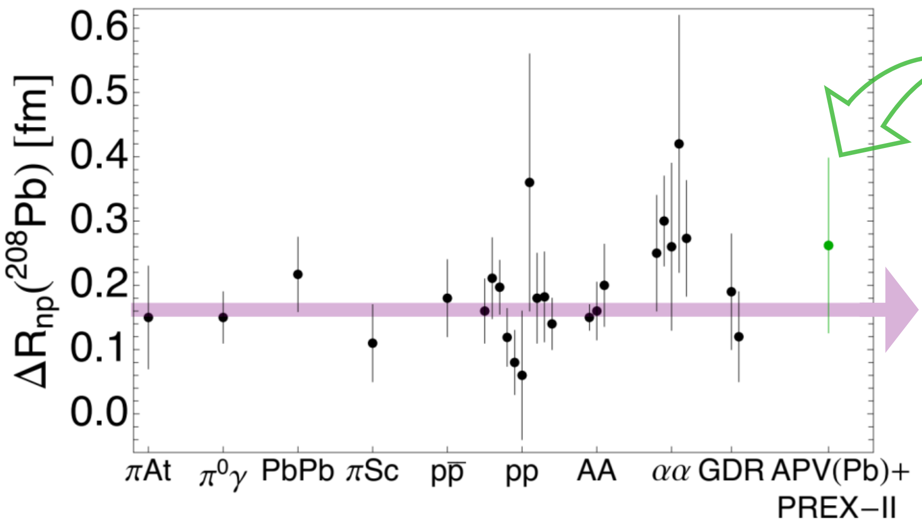

Consistent with APV(Pb)+PREX-II determination

$\Delta R_{np}^{\mathrm{non-EW}} = 0.16 \pm 0.01$ fm

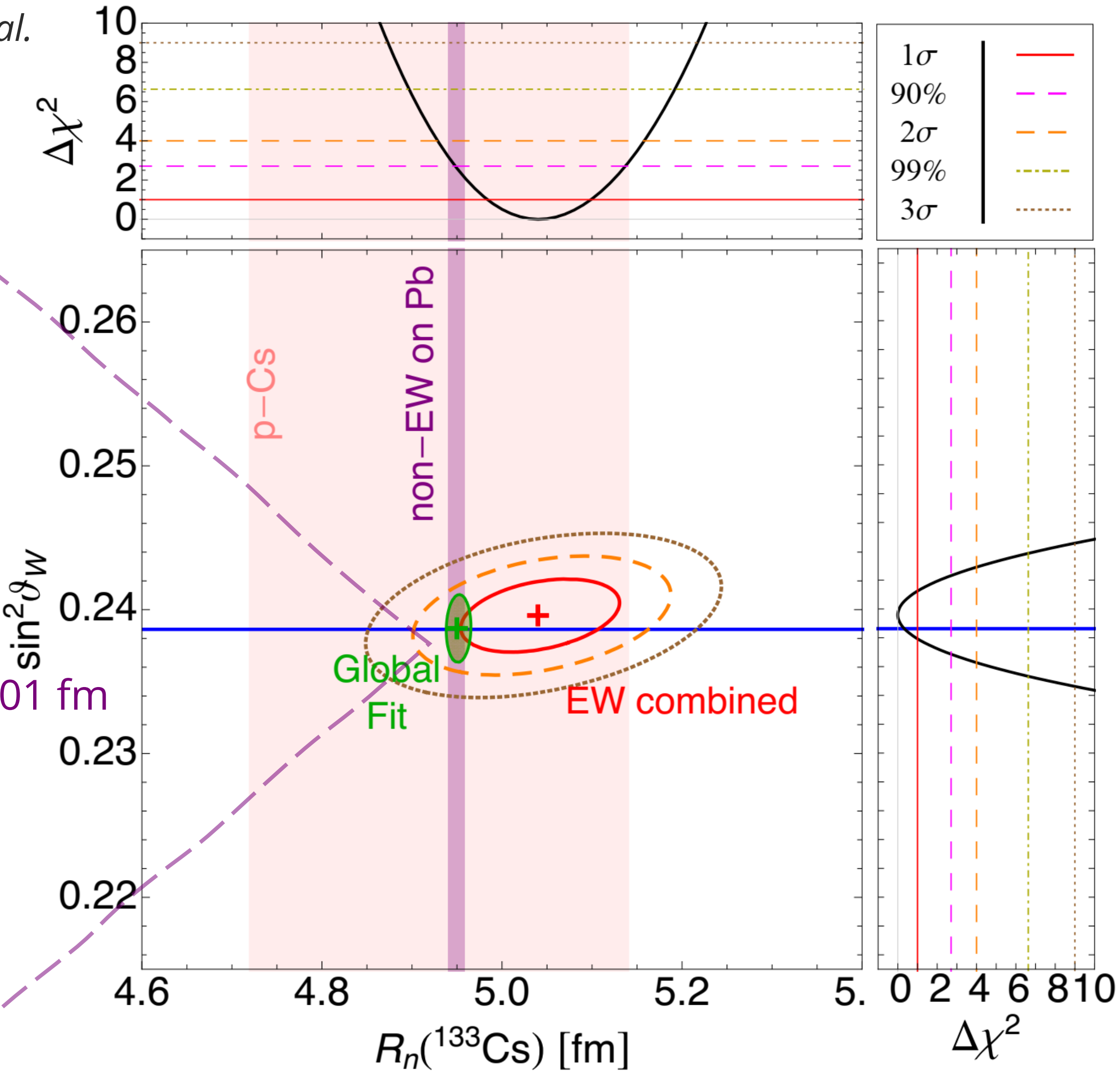

	$\sin^2\vartheta_W$	$R_n(^{133}\mathrm{Cs})$[fm]
APV(Cs)+COH+CSRe	$0.2396^{+0.0020}_{-0.0019}$	5.04 ± 0.19
EW combined	0.2396 ± 0.0017	5.04 ± 0.06
Global fit	0.2387 ± 0.0016	4.952 ± 0.009

In the global fit we don't gain much and the assumptions are too «aggressive»!

Global 1sigma with APV(21)

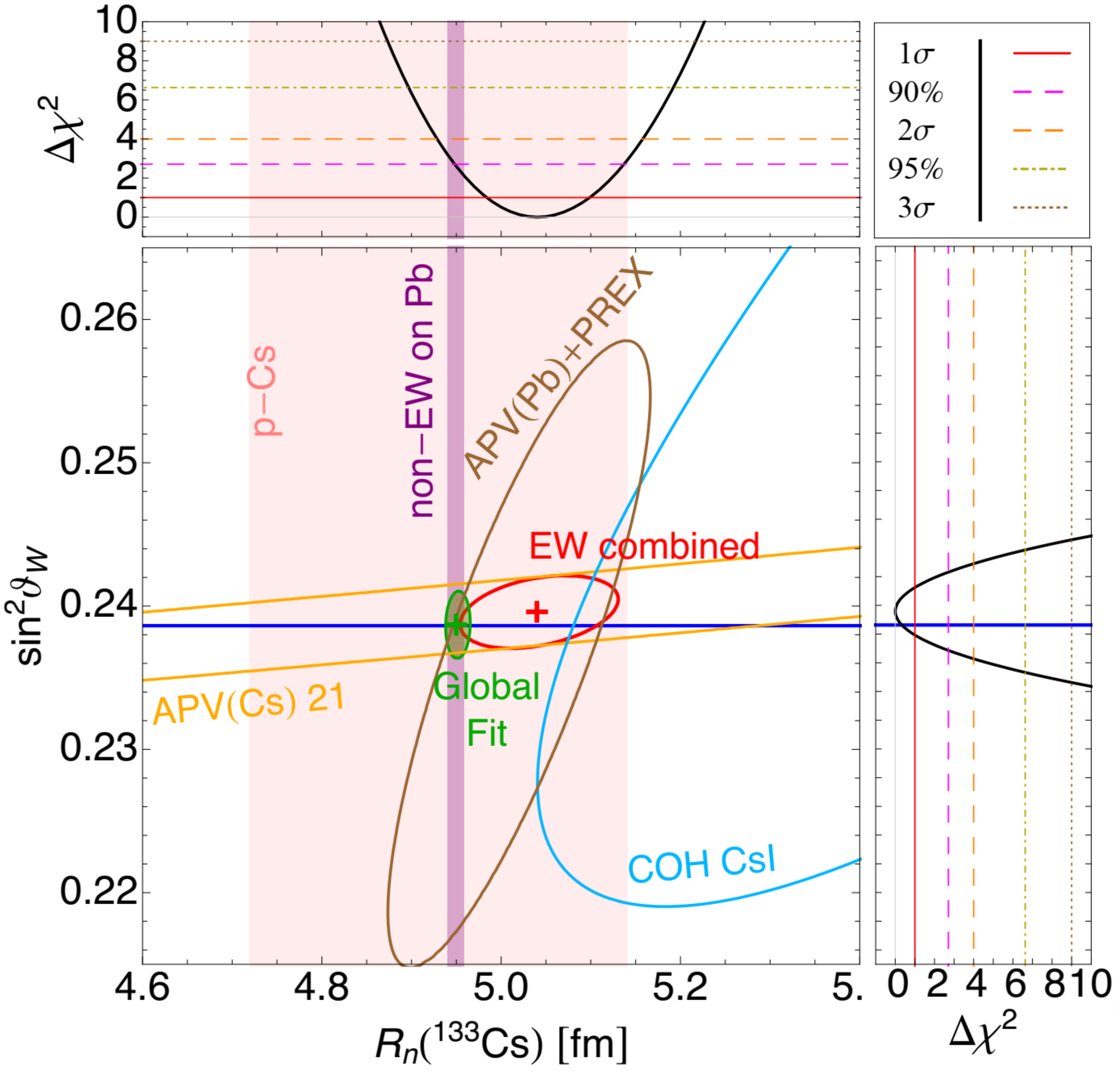

Using ImE$_{PNC}$ PDG

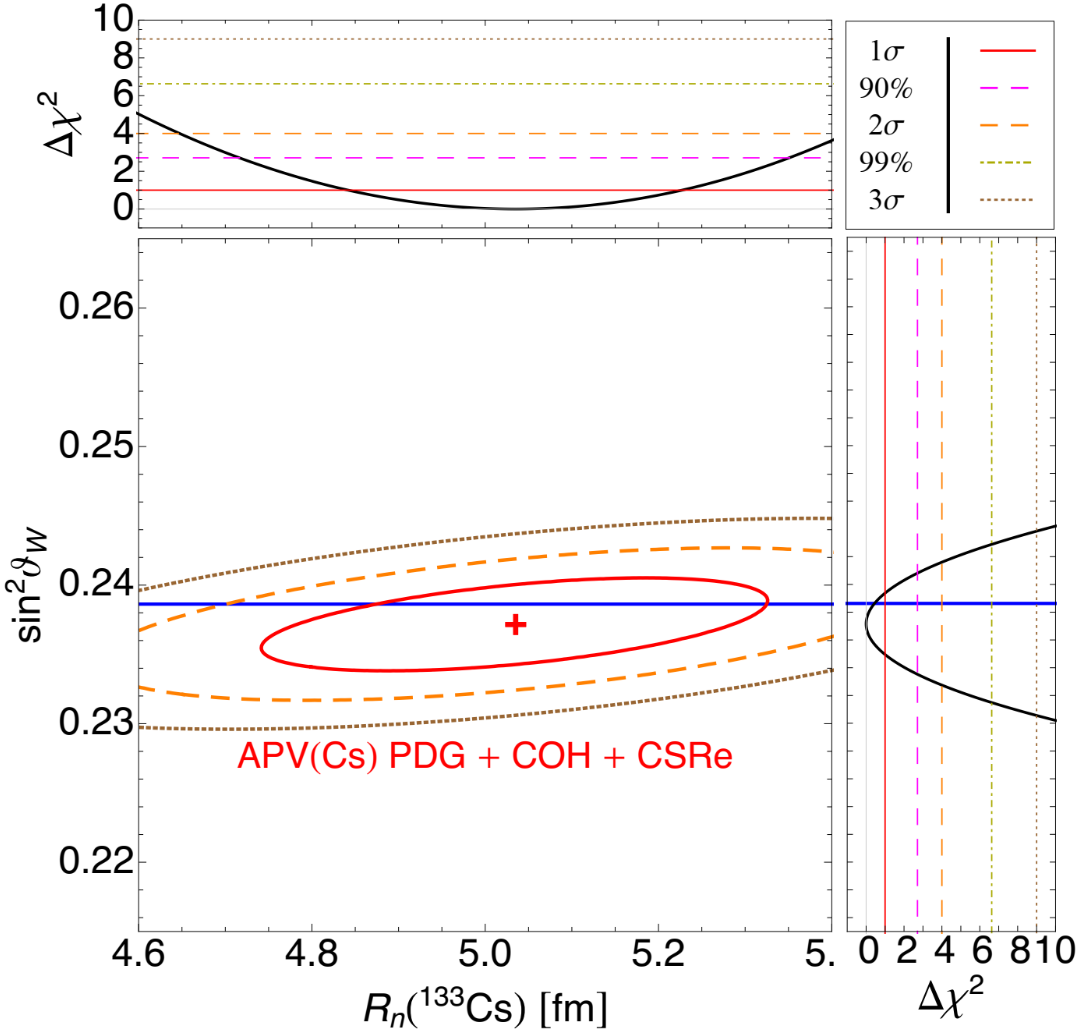

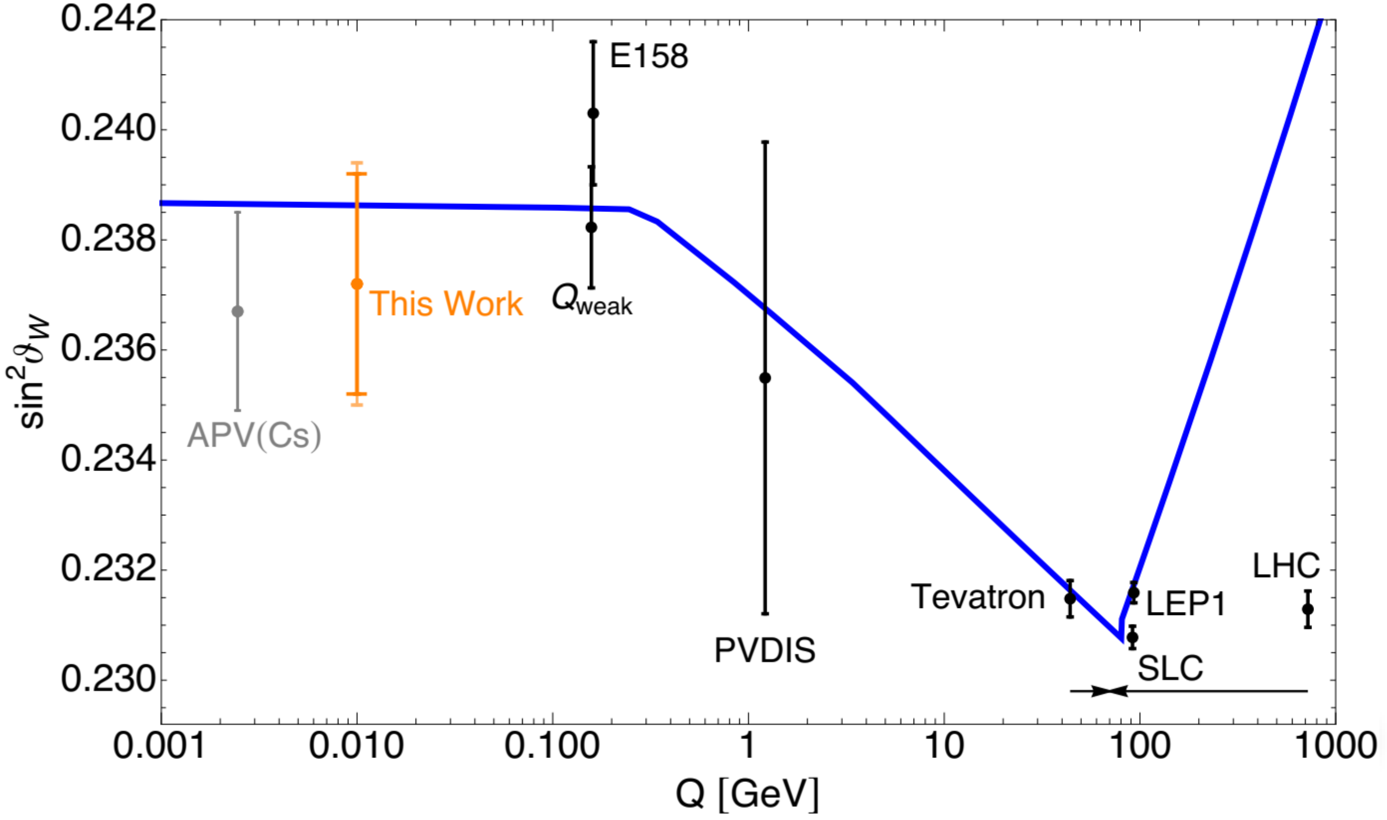

Using ImE$_{PNC}$ PDG

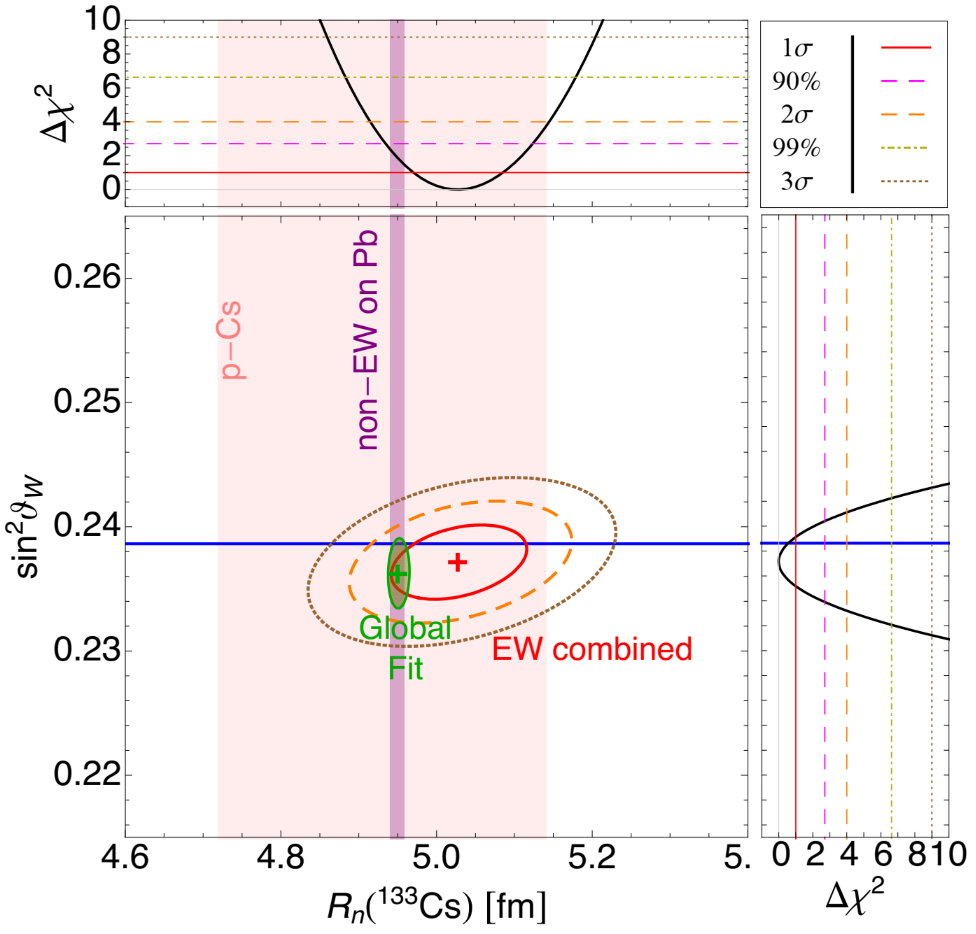

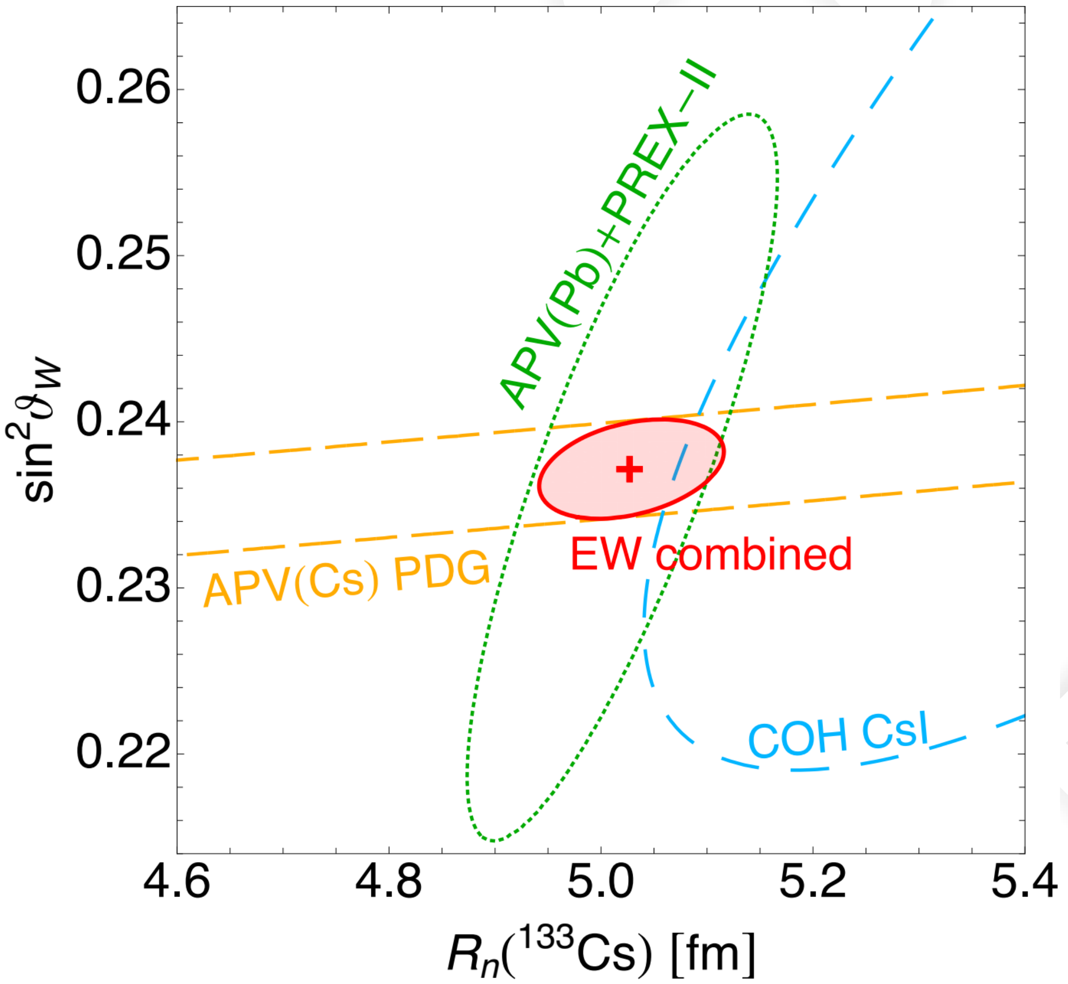

Global using ImE_{PNC} PDG

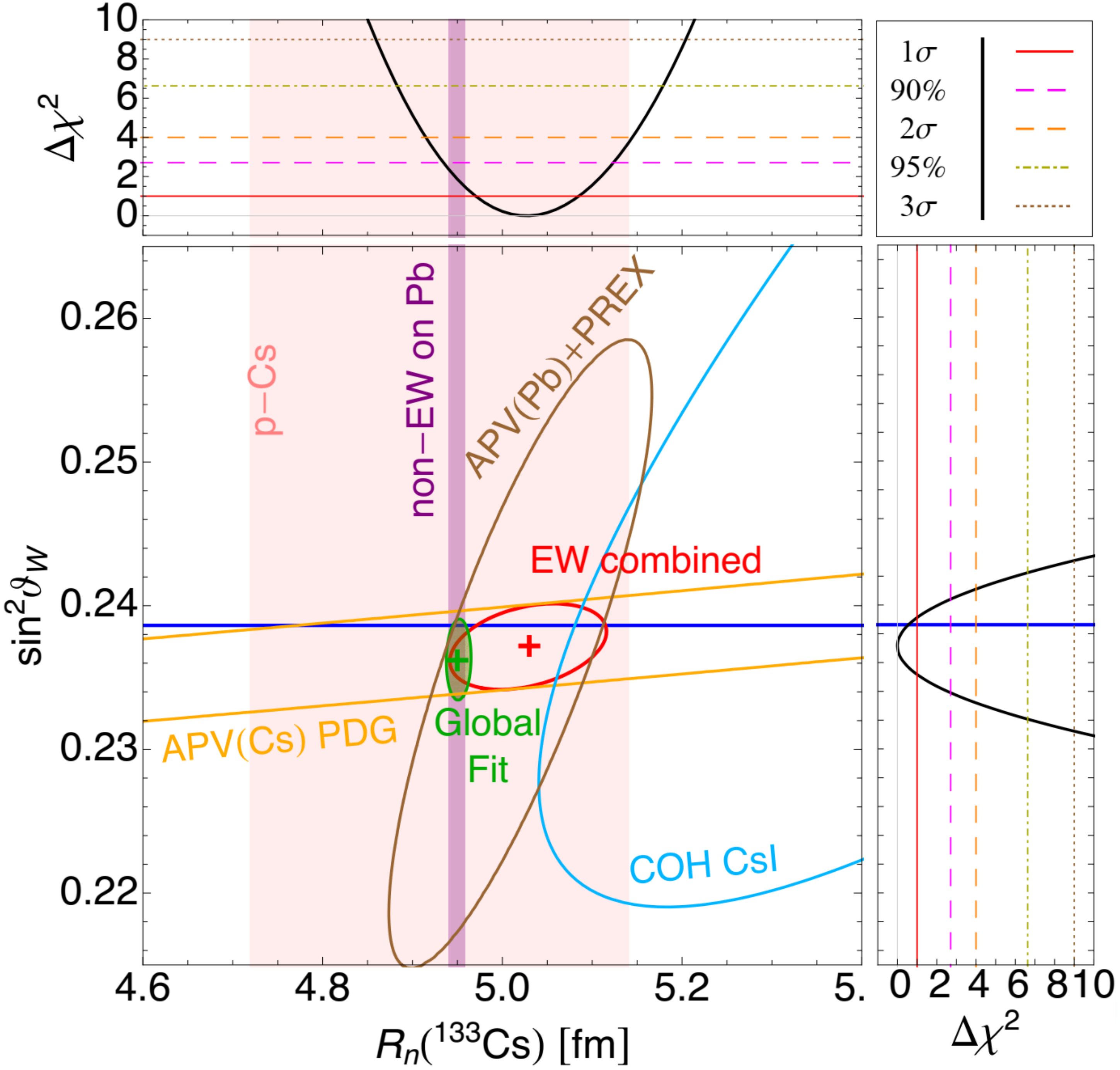

Atomic Parity Violation in cesium APV(Cs)

M. Cadeddu and F. Dordei, PRD 99, 033010 (2019), arXiv:1808.10202

+ Parity violation in an atomic system can be observed as an **electric dipole transition amplitude between two atomic states with the same parity**, such as the $6S$ and $7S$ states in cesium.

  ➢ Indeed, a transition between two atomic states with same parity is forbidden by the parity selection rule and cannot happen with the exchange of a photon.

  ✓ However, an electric dipole transition amplitude can be induced by a Z boson exchange between atomic electrons and nucleons → Atomic Parity Violation (APV) or Parity Non Conserving (PNC).

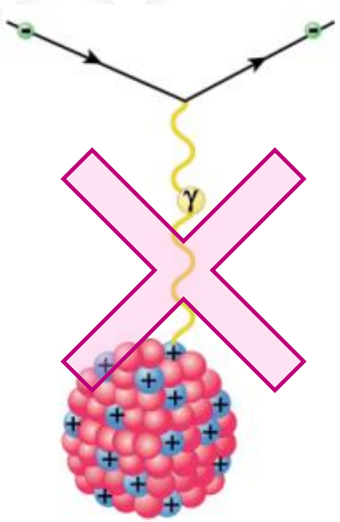

Interaction mediated by the photon and so mostly sensitive to the charge (proton) distribution

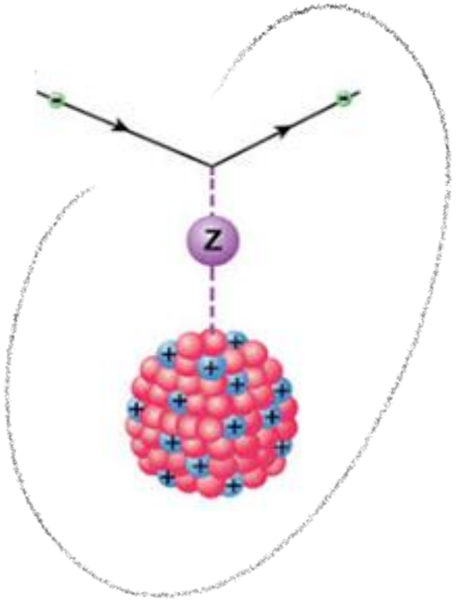

Interaction mediated by the Z boson and so mostly sensitive to the weak (neutron) distribution.

+ The quantity that is measured is the usual **weak charge**

$$Q_W^{SM} \approx Z\left(1 - 4\sin^2\theta_W^{SM}\right) - N$$

Extracting the weak charge from APV

$$Q_W = N\left(\frac{\mathrm{Im}\,E_{\mathrm{PNC}}}{\beta}\right)_{\mathrm{exp.}}\left(\frac{Q_W}{N\,\mathrm{Im}\,E_{\mathrm{PNC}}}\right)_{\mathrm{th.}}\beta_{\mathrm{exp.+th.}}$$

+ Experimental value of electric dipole transition amplitude between 6S and 7S states in Cs

C. S. Wood et al., Science **275**, 1759 (1997)

J. Guena, et al., PRA **71**, 042108 (2005)

PDG2020 average

$$\mathrm{Im}\left(\frac{E_{\mathrm{PNC}}}{\beta}\right) = -1.5924(55)\ \mathrm{mV/cm}$$

✓ Theoretical amplitude of the <u>electric dipole transition</u>

$$E_{\mathrm{PNC}} = \sum_n \left[\frac{\langle 6s|H_{\mathrm{PNC}}|np_{1/2}\rangle\langle np_{1/2}|\boldsymbol{d}|7s\rangle}{E_{6s}-E_{np_{1/2}}} + \frac{\langle 6s|\boldsymbol{d}|np_{1/2}\rangle\langle np_{1/2}|H_{\mathrm{PNC}}|7s\rangle}{E_{7s}-E_{np_{1/2}}}\right],$$

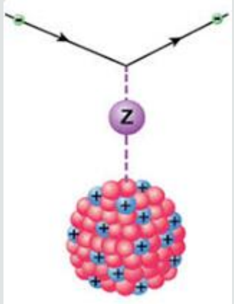

- where ***d*** is the electric dipole operator, and

$$H_{\mathrm{PNC}} = -\frac{G_F}{2\sqrt{2}}Q_W\gamma_5\rho(\boldsymbol{r})$$

Value of ImE_{PNC} used by PDG (V. Dzuba *et al.*, PRL 109, 203003 (2012))

$$\mathrm{Im}\,E_{\mathrm{PNC}} = (0.8977 \pm 0.0040)\times 10^{-11}|e|\,a_B\,Q_W/N$$ **see also**

nuclear Hamiltonian describing the **electron-nucleus weak interaction**

$\rho(\boldsymbol{r}) = \rho_p(\boldsymbol{r}) = \rho_n(\boldsymbol{r}) \rightarrow$ **neutron skin correction** needed

β: tensor transition polarizability

It characterizes the size of the Stark mixing induced electric dipole amplitude (external electric field)

Bennet & Wieman, PRL 82, 2484 (1999)
Dzuba & Flambaum, PRA 62 052101 (2000)

PDG2020 average
β = 27.064 (33) a_B^3

NEW result on ImE_{PNC} !

- I will refer with APV2021 when usign Im E_{PNC} from B. K. Sahoo et al. PRD 103, L111303 (2021)

Atomic Parity Violation for weak mixing angle measurements

✓ Weak charge in the SM including radiative corrections

Using SM prediction at low energy
$\sin^2\hat{\theta}_W(0) = 0.23857(5)$

$$Q_W^{SM+\text{r.c.}} \equiv -2\left[Z\left(g_{AV}^{ep} + 0.00005\right) + N\left(g_{AV}^{en} + 0.00006\right)\right]\left(1 - \frac{\alpha}{2\pi}\right) \approx Z\left(1 - 4\sin^2\theta_W^{SM}\right) - N$$

Theoretically

$$Q_W^{SM\ \text{th}}\left({}^{133}_{55}Cs\right) = -73.23(1)$$

1σ difference

Experimentally

$$Q_W^{\text{exp.}}\left({}^{133}_{55}Cs\right) = -72.82(42)$$

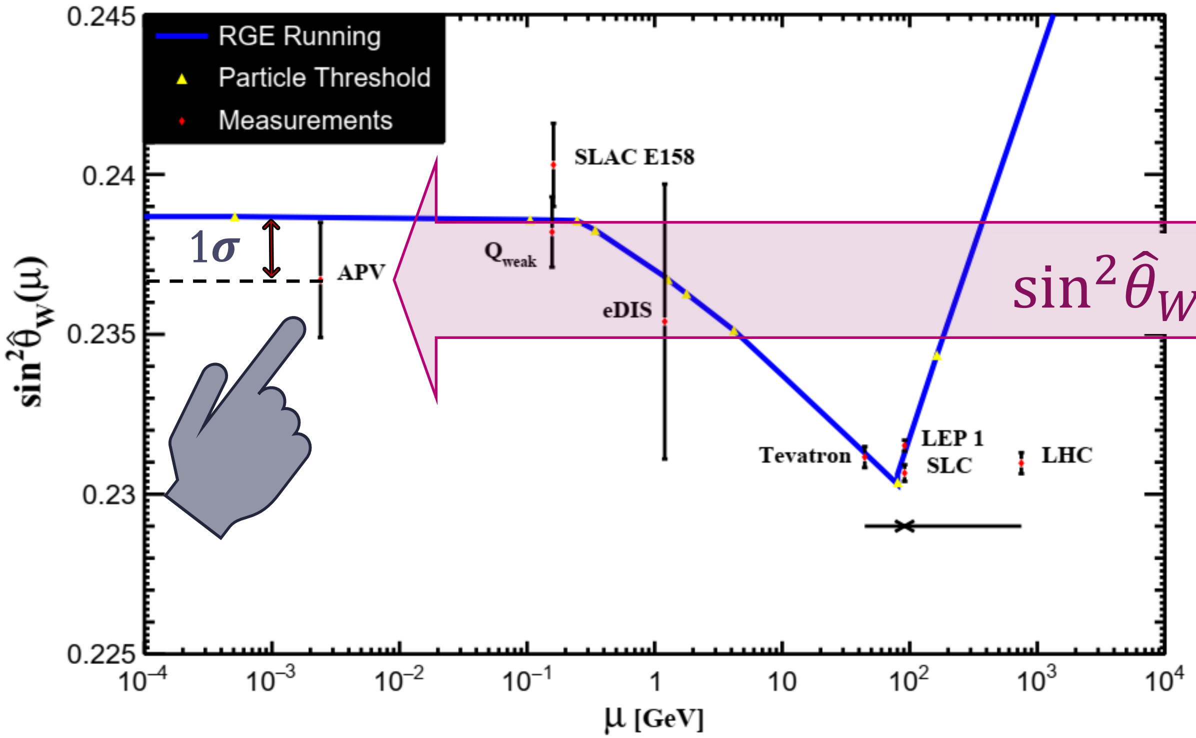

$\sin^2\hat{\theta}_W(2.4\ \text{MeV})$=0.2367±0.0018

But which Cs neutron skin correction is used?

R. L. Workman et al. (Particle Data Group), "Review of Particle Physics," PTEP **2022**, 083C01 (2022).

Extrapolated value of ΔR_{np}^{Cs}

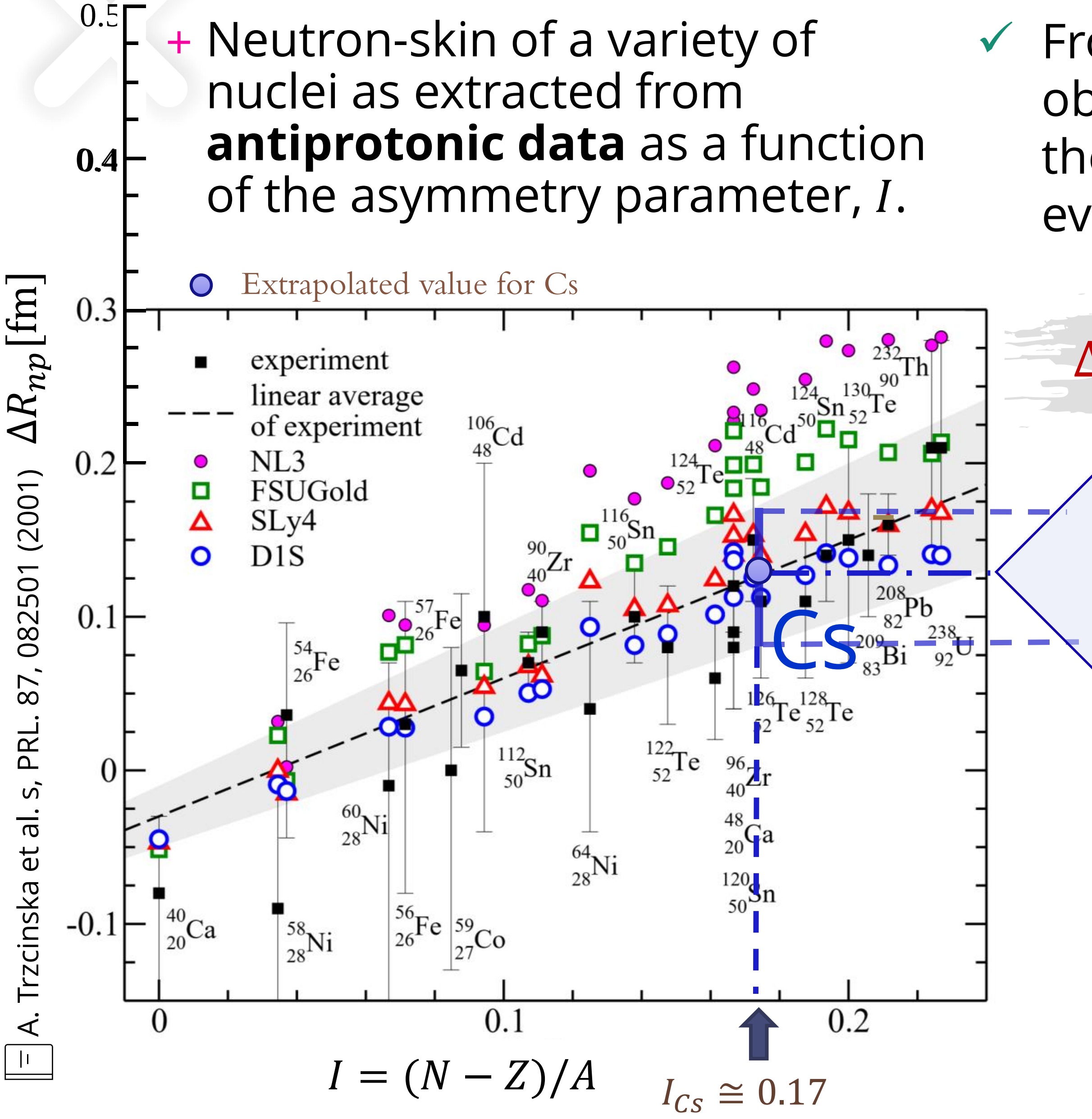

- + Neutron-skin of a variety of nuclei as extracted from **antiprotonic data** as a function of the asymmetry parameter, I.

- ✓ From this **linear fit** one obtains the relation for the neutron skin for every nuclei

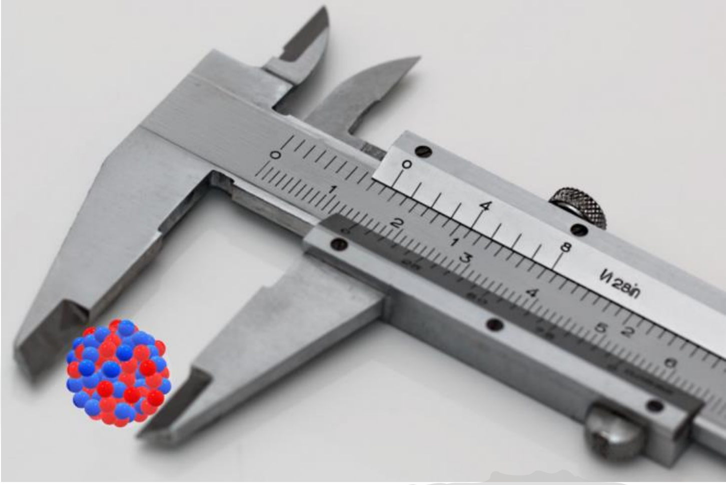

$$\Delta R_{np}[\text{fm}] = -(0.04 \pm 0.03) + (1.01 \pm 0.15)\frac{N-Z}{A}$$

For cesium it gives

$$\Delta R_{np}^{Cs}(\text{extrap}) \cong 0.13 \pm 0.04 \text{ fm}$$

Extrapolated (not measured) value for cesium!

Antiprotonic data: radiochemical and the other based on x-ray data constraining the neutron distribution at the nuclear periphery

M. Thiel et al., Journal of Physics G, 46, 9 (2019), arXiv:1904.12269v1

Extrapolated value of ΔR_{np}^{Cs}

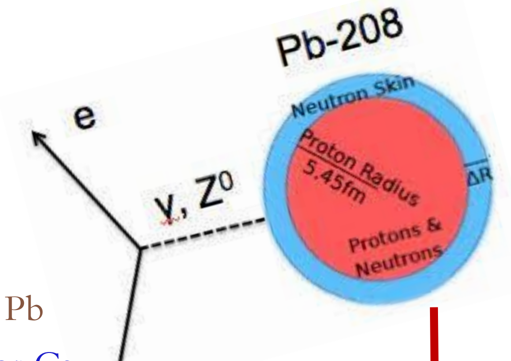

PREX-I & PREX-II

$\Delta R_{np}^{Pb} = 0.283 \pm 0.071$ fm

D. Adhikari *et al.* PRL 126, 172502 (2021)

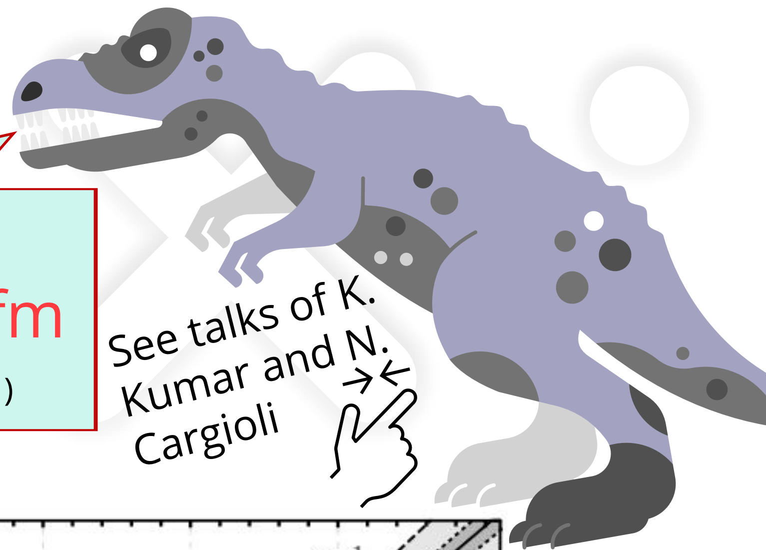

See talks of K. Kumar and N. Cargioli

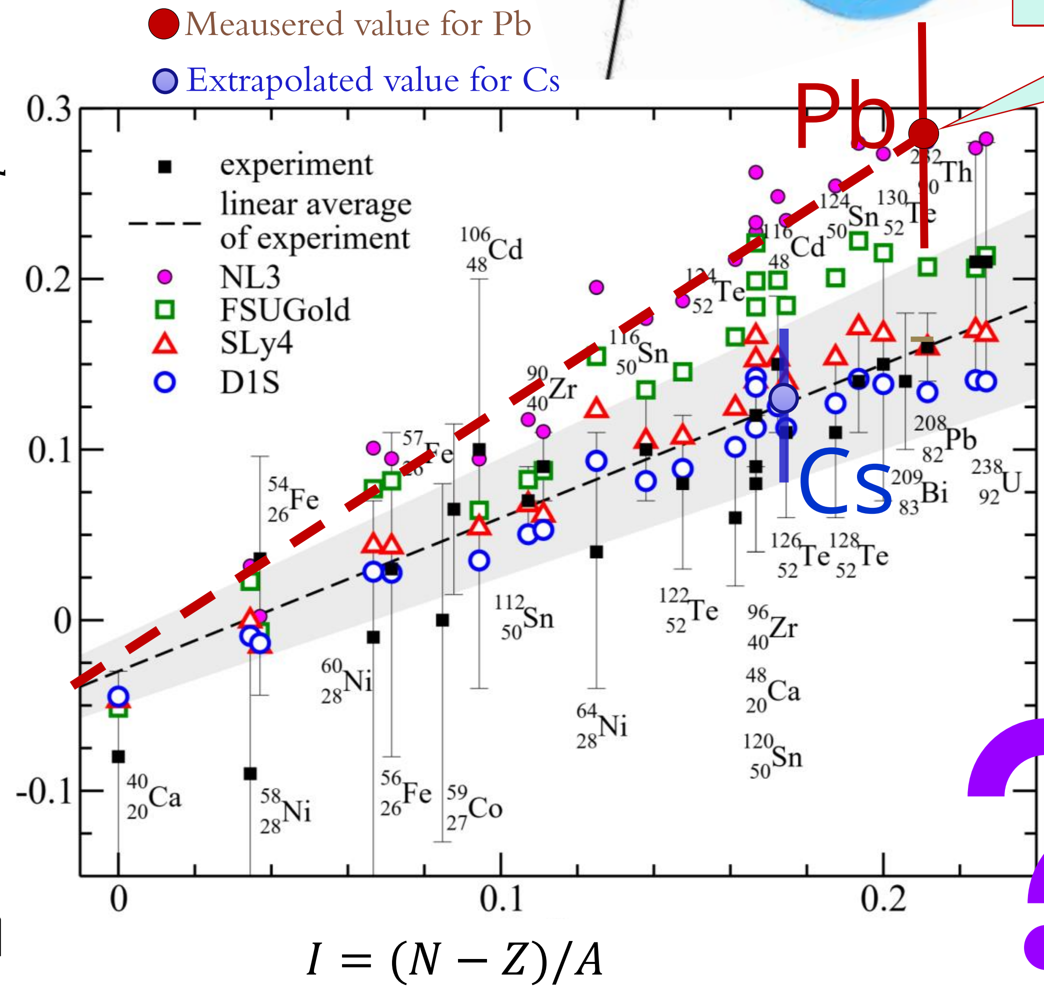

A. Trzcinska et al. s, PRL. 87, 082501 (2001

?

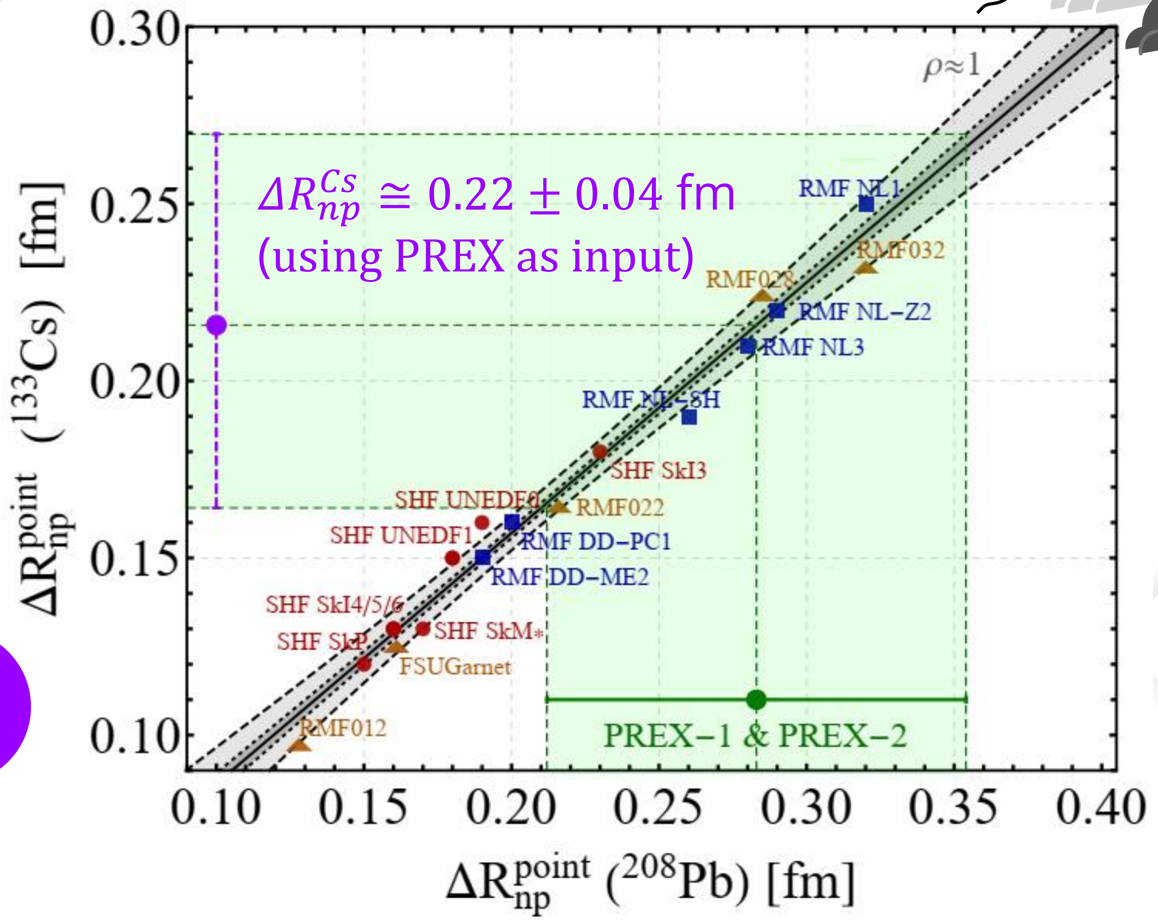

M. Cadeddu et al. PRD 104, L011701 (2021), arXiv:2104.03280

2nd advantage: extract both R_n(CsI) & $\sin^2\vartheta_W$ from data

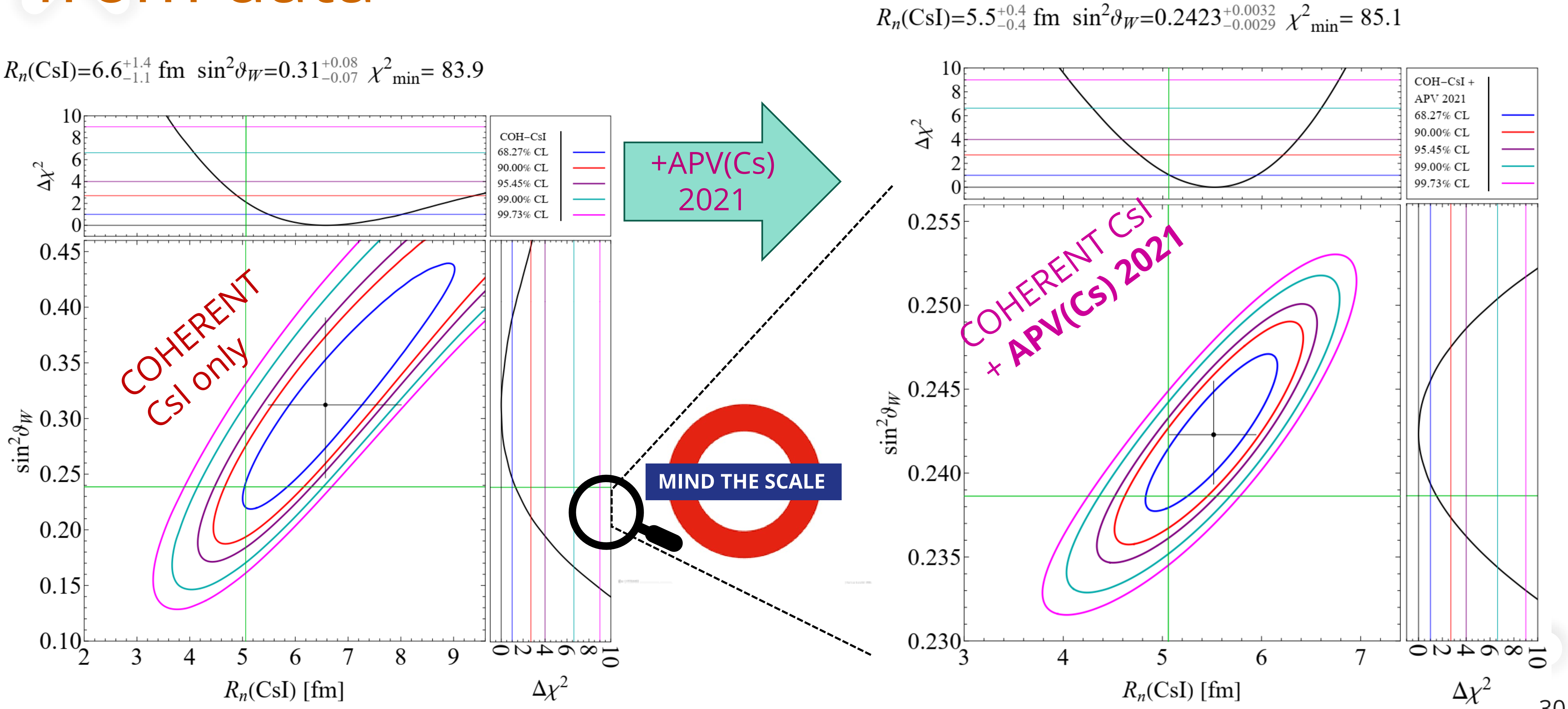

2nd advantage: extract both R_n(CsI) and $\sin^2\vartheta_W$ from data

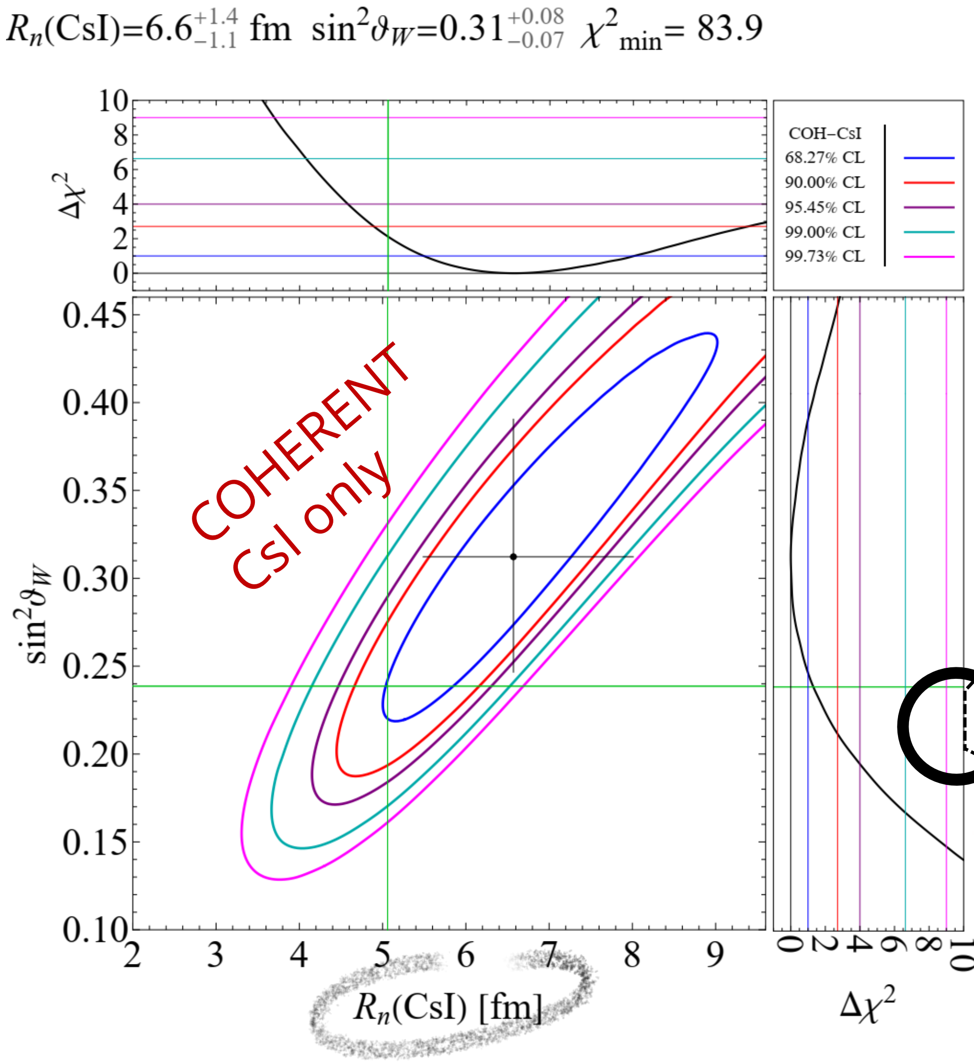

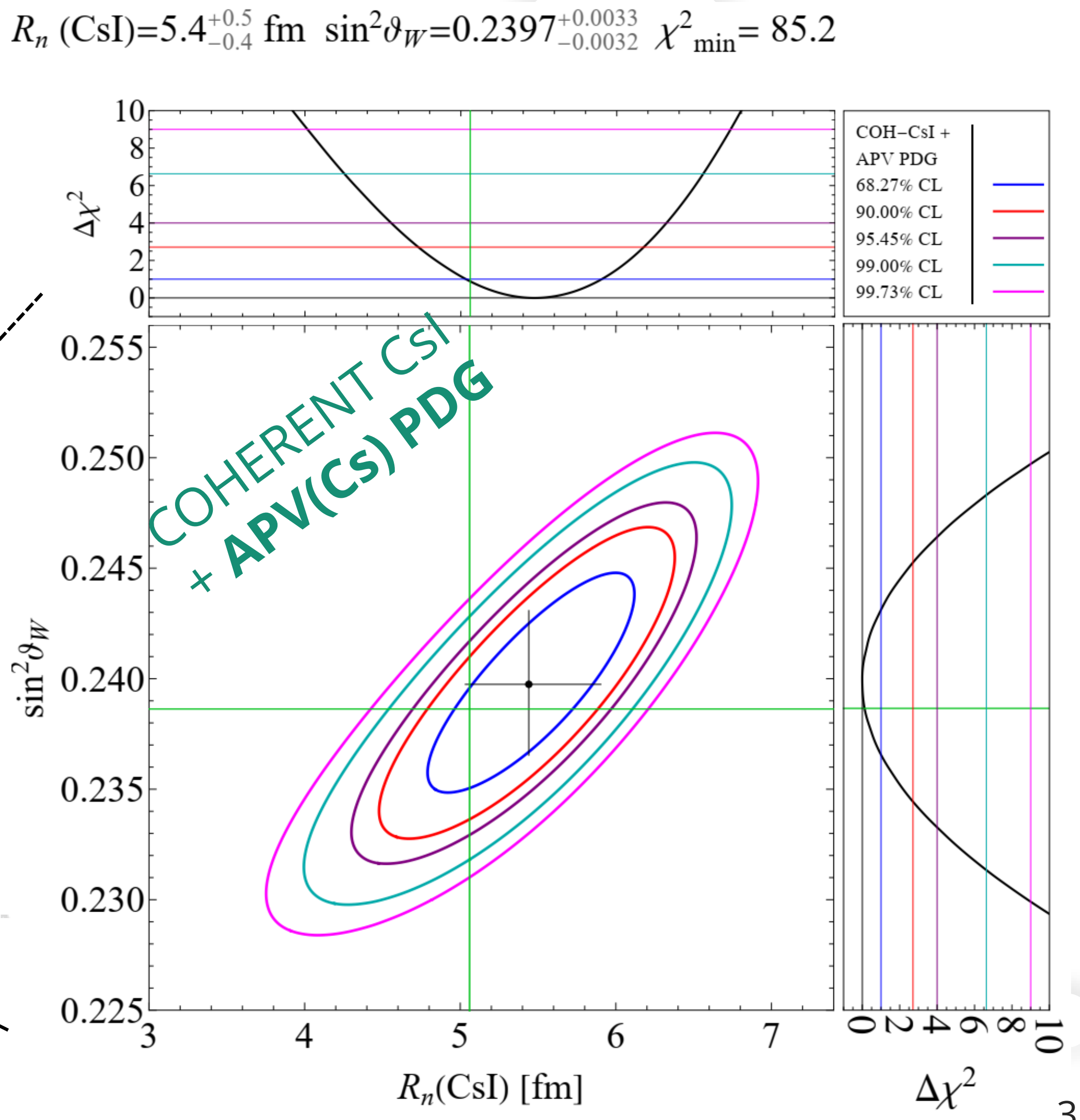

Weak mixing angle determination from APV without any assumption on R_n(Cs)

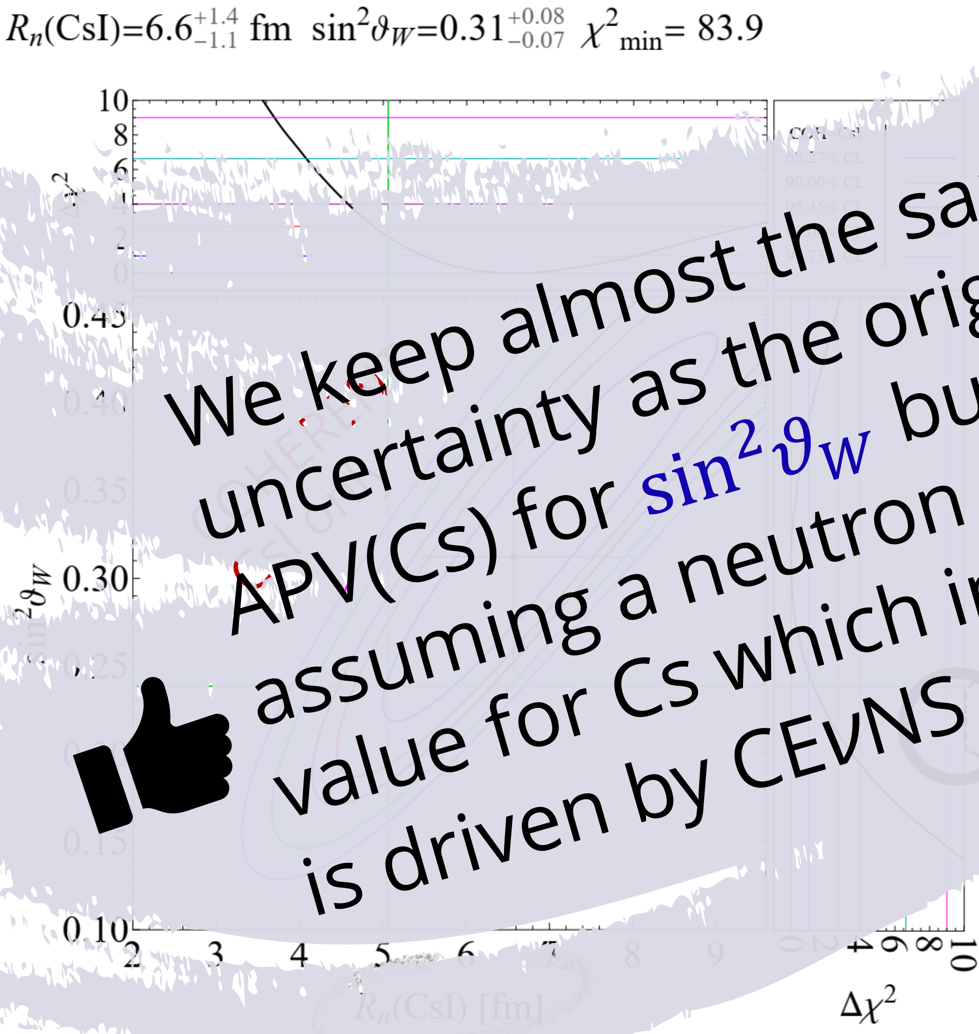

We keep almost the same uncertainty as the original APV(Cs) for $\sin^2\vartheta_W$ but not assuming a neutron skin value for Cs which instead is driven by CEνNS

No assumptions on ΔR_{np}^{Cs} are made. The skin is taken directly from CEνNS experimental data

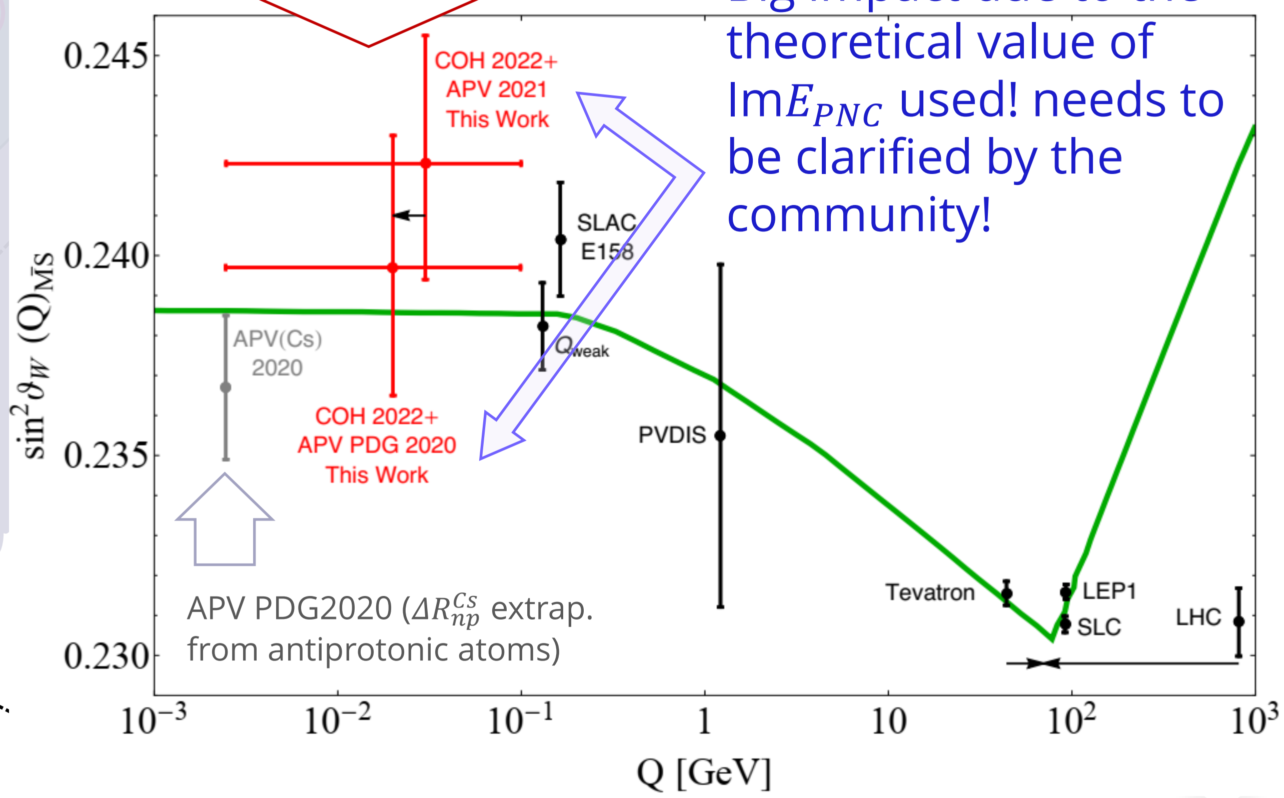

APV PDG2020 (ΔR_{np}^{Cs} extrap. from antiprotonic atoms)

Big impact due to the theoretical value of ImE_{PNC} used! needs to be clarified by the community!

Combined 2D fit with COHERENT and APV(Cs)

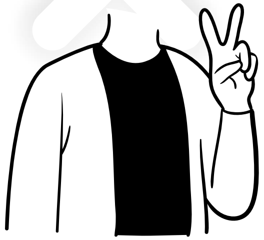

No assumptions on Cs neutron skin are made. The neutron skin is taken directly from CEνNS experimental data

Measuring the WMA at low energies could reveal the presence of light dark Z bosons that would appear as a deviation of the SM prediction of the running depending on the value of the new mediator mass and kinetic mixing.

M. Cadeddu, F. Dordei and C. Giunti, EPL 143 34001 (2023), arXiv:2307.08842

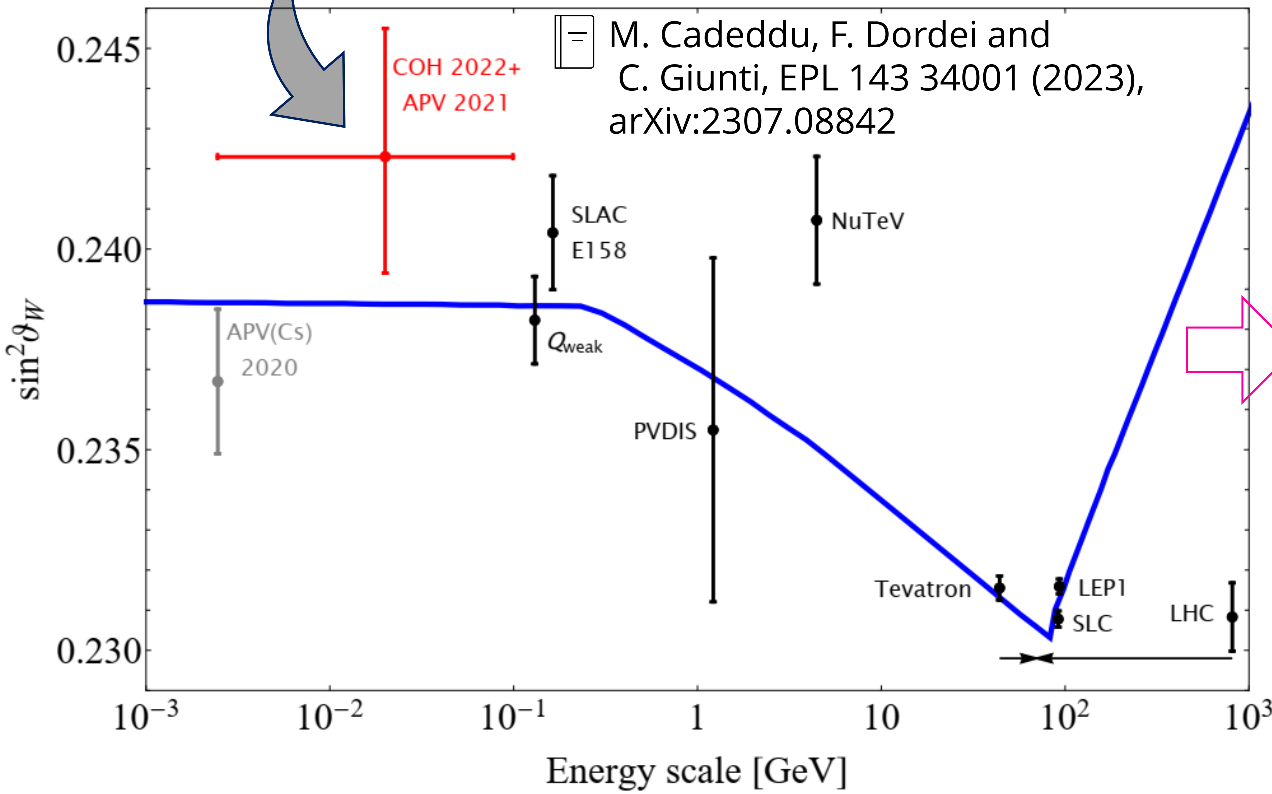

M. Cadeddu, N. Cargioli, F. Dordei, C. Giunti, E Picciau PRD 104, 011701 (2021), Arxiv:2104.03280

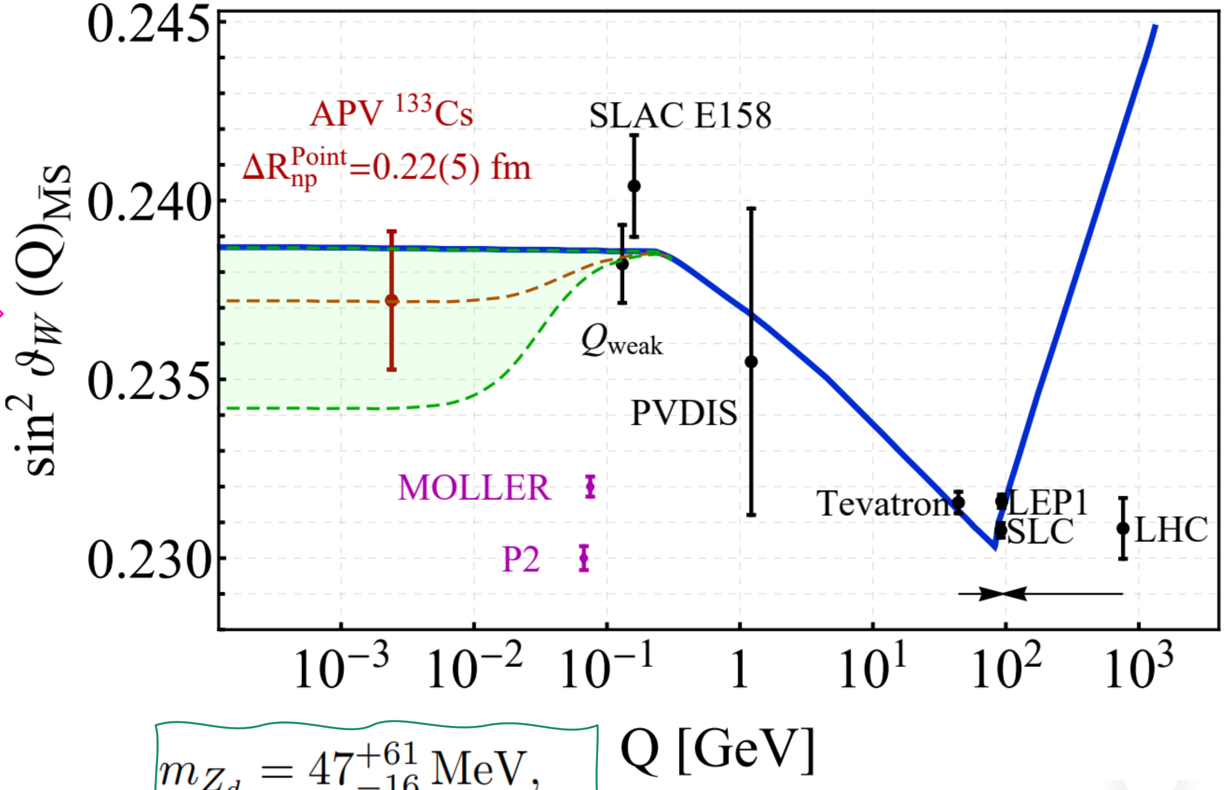

$$m_{Z_d} = 47^{+61}_{-16}\,\text{MeV}, \quad \varepsilon = 2.3^{+1.1}_{-0.4} \times 10^{-3}$$

Weak mixing angle

M. Atzori Corona et al., EPJC 83 (2023) 7, 683, arXiv:2303:09360

The Weinberg angle, θ_W is a fundamental parameter of the EW theory of the SM. It determines the relative strength of the weak NC vs. the electromagnetic interaction. There are many ways to define it, one of those is the **minimal subtraction scheme** ($\overline{MS}$).

- $\sin^2\hat{\theta}_W(M_Z) \equiv \hat{s}_Z^2 = 0.23122 \pm 0.00004\ (\overline{MS})$

The value of $\sin^2\hat{\theta}_W$ runs as a function of the momentum transfer or the energy scale. For low energies it assumes the value $\hat{s}_0^2(0) = 0.23863 \pm 0.00005\ (\overline{MS})$

	$\sin^2\vartheta_W$ best-fit$^{+1\sigma+90\%\text{CL}+2\sigma}_{-1\sigma-90\%\text{CL}-2\sigma}$	$\chi^2_{\min}$
COH-CsI	$0.231^{+0.027+0.046+0.058}_{-0.024-0.039-0.047}$	86.0
APV PDG	$0.2375^{+0.0019+0.0031+0.0038}_{-0.0019-0.0031-0.0038}$	-
APV 2021	$0.2399^{+0.0016+0.0026+0.0032}_{-0.0016-0.0026-0.0032}$	-
APV PDG + CsI	$0.2374^{+0.0020+0.0032+0.0039}_{-0.0018-0.0031-0.0037}$	86.0
APV 2021 + CsI	$0.2398^{+0.0016+0.0026+0.0032}_{-0.0015-0.0026-0.0031}$	86.0

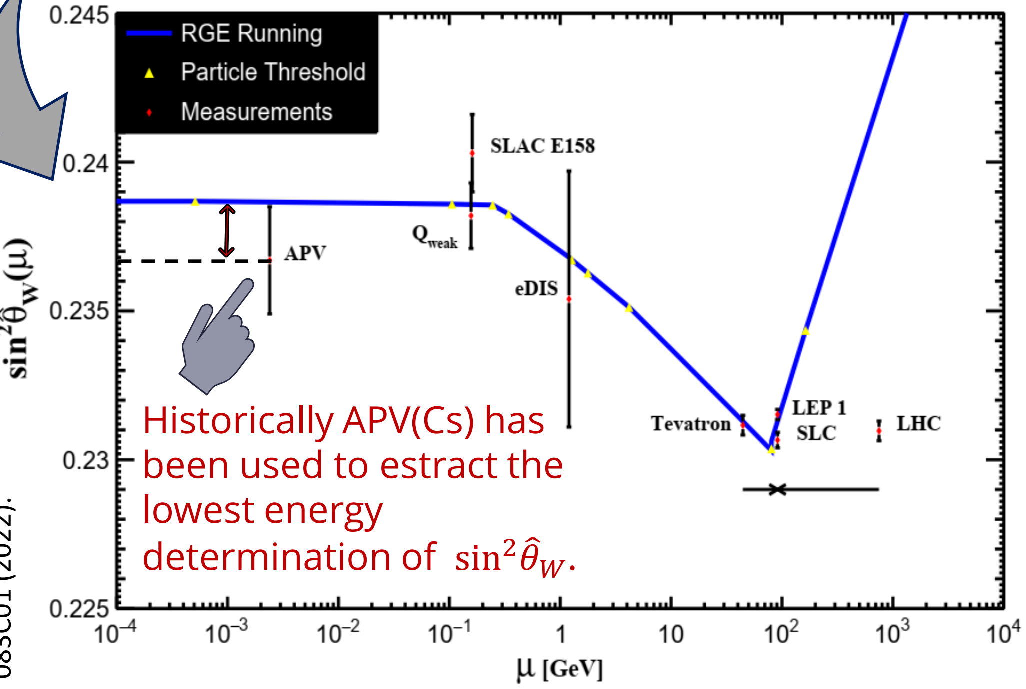

Historically APV(Cs) has been used to estract the lowest energy determination of $\sin^2\hat{\theta}_W$.

R. L. Workman et al. (Particle Data Group), "Review of Particle Physics," PTEP **2022**, 083C01 (2022).

However R_n(Cs) (or the neutron skin) has been taken from **indirect measurements** using antiprotonic atoms, which are known to be affected by considerable model dependencies

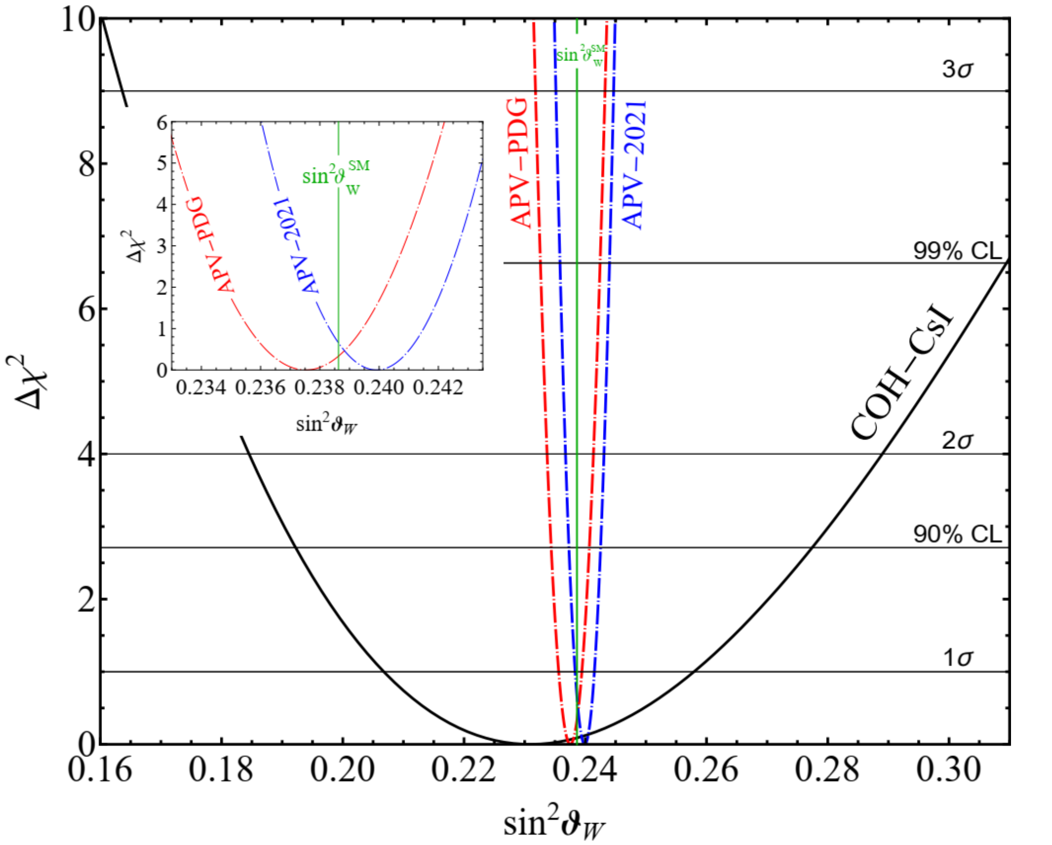

The CsI neutron skin

First result Cadeddu et al. Phys. Rev. Lett. 120, 072501 (2018), arXiv:1710.02730

M. Atzori Corona et al., EPJC 83 (2023) 7, 683 arXiv:2303.09360

R_n (CsI) $= 5.47 \pm 0.38$ fm

~7% precision

Average proton rms radius for CsI from muonic X-rays data

R_p (CsI) ≈ 4.78 fm

G. Fricke et al., Atom. Data Nucl. Data Tabl. **60**, 177 (1995)

Neutron skin: R_n (CsI)- R_p (CsI)

$\Delta R_{np}(\text{CsI}) = 0.69 \pm 0.38$ fm

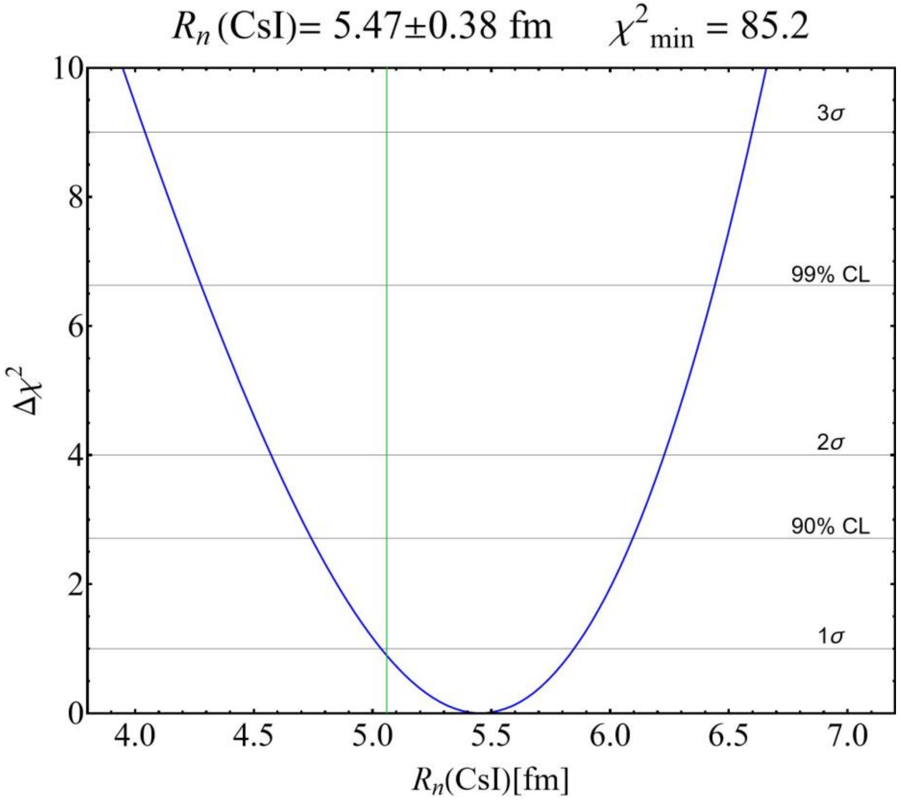

$$R_n(\text{COH}-\text{CsI}) = 5.47^{+0.38}_{-0.38}(1\sigma)^{+0.63}_{-0.72}(90\%\text{CL})^{+0.76}_{-0.89}(2\sigma)\ \text{fm},$$

Theoretical values of the neutron skin of Cs and I obtained with nuclear mean field models. The value is compatible with all the models...

$0.12 < \Delta R_{np}^{CsI} < 0.24$ fm

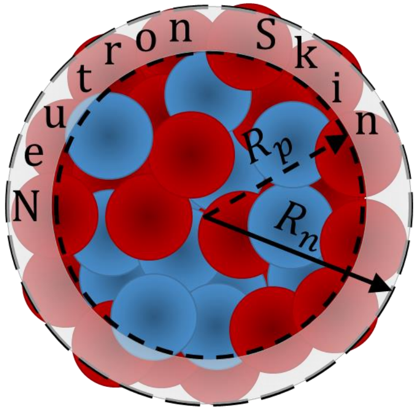

Model	^{127}I						^{133}Cs					
	R_p^{point}	R_p	R_n^{point}	R_n	$\Delta R_{np}^{\text{point}}$	ΔR_{np}	R_p^{point}	R_p	R_n^{point}	R_n	$\Delta R_{np}^{\text{point}}$	ΔR_{np}
SHF SkI3 [81]	4.68	4.75	4.85	4.92	0.17	0.17	4.74	4.81	4.91	4.98	0.18	0.18
SHF SkI4 [81]	4.67	4.74	4.81	4.88	0.14	0.14	4.73	4.80	4.88	4.95	0.15	0.14
SHF Sly4 [82]	4.71	4.78	4.84	4.91	0.13	0.13	4.78	4.85	4.90	4.98	0.13	0.13
SHF Sly5 [82]	4.70	4.77	4.83	4.90	0.13	0.13	4.77	4.84	4.90	4.97	0.13	0.13
SHF Sly6 [82]	4.70	4.77	4.83	4.90	0.13	0.13	4.77	4.84	4.89	4.97	0.13	0.13
SHF Sly4d [83]	4.71	4.79	4.84	4.91	0.13	0.12	4.78	4.85	4.90	4.97	0.12	0.12
SHF SV-bas [84]	4.68	4.76	4.80	4.88	0.12	0.12	4.74	4.82	4.87	4.94	0.13	0.12
SHF UNEDF0 [85]	4.69	4.76	4.83	4.91	0.14	0.14	4.76	4.83	4.92	4.99	0.16	0.15
SHF UNEDF1 [86]	4.68	4.76	4.83	4.91	0.15	0.15	4.76	4.83	4.90	4.98	0.15	0.15
SHF SkM* [87]	4.71	4.78	4.84	4.91	0.13	0.13	4.76	4.84	4.90	4.97	0.13	0.13
SHF SkP [88]	4.72	4.80	4.84	4.91	0.12	0.12	4.79	4.86	4.91	4.98	0.12	0.12
RMF DD-ME2 [89]	4.67	4.75	4.82	4.89	0.15	0.15	4.74	4.81	4.89	4.96	0.15	0.15
RMF DD-PC1 [90]	4.68	4.75	4.83	4.90	0.15	0.15	4.74	4.82	4.90	4.97	0.16	0.15
RMF NL1 [91]	4.70	4.78	4.94	5.01	0.23	0.23	4.76	4.84	5.01	5.08	0.25	0.24
RMF NL3 [92]	4.69	4.77	4.89	4.96	0.20	0.19	4.75	4.82	4.95	5.03	0.21	0.20
RMF NL-Z2 [93]	4.73	4.80	4.94	5.01	0.21	0.21	4.79	4.86	5.01	5.08	0.22	0.22
RMF NL-SH [94]	4.68	4.75	4.86	4.94	0.19	0.18	4.74	4.81	4.93	5.00	0.19	0.19

CEνNS players

$$\pi^+ \rightarrow \mu^+ + \nu_\mu$$ Prompt component

$$\mu^+ \rightarrow e^+ + \bar{\nu}_\mu + \nu_e$$ Delayed component

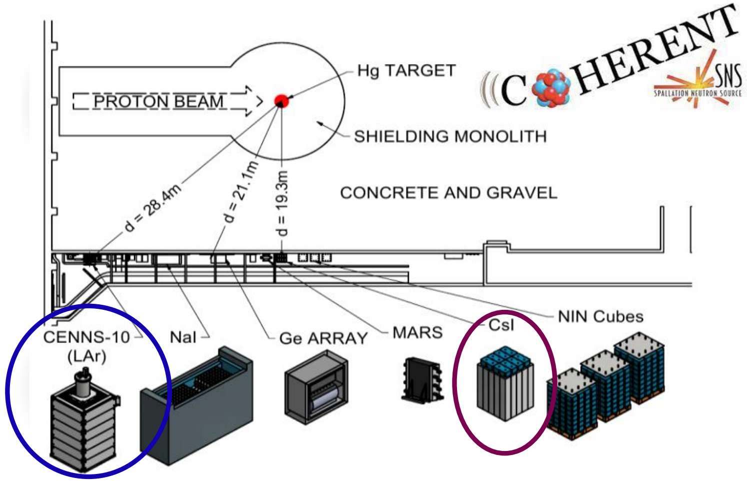

COHERENT CsI

D. Akimov et al. **Science** 357.6356 (2017)

+ Updated in Akimov et al., PRL 129, 081801 (2022)

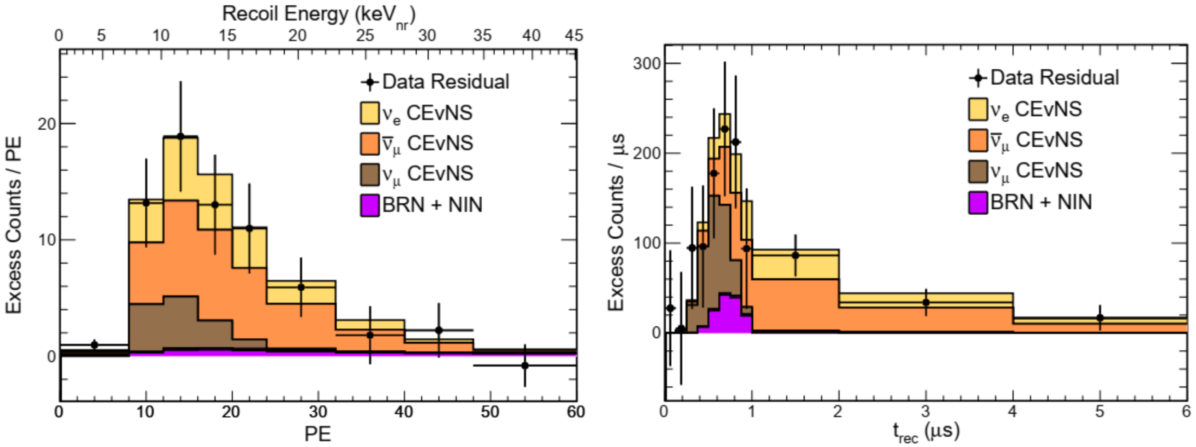

	Prior Prediction	Best-Fit Total
Steady-state background	1286 ± 27	1273 ± 24
BRN	18.4 ± 4.6	17.3 ± 4.5
NIN	5.6 ± 2.0	5.5 ± 2.0
CEvNS	–	306 ± 20

Table I. A summary of prior prediction and best-fit event rates and statistical uncertainties for CEvNS and each background type. The standard-model expectation for CEvNS is $341 \pm 11 \pm 42$.

COHERENT Ar

Akimov et al., COHERENT Coll. PRL 126, 01002 (2021)

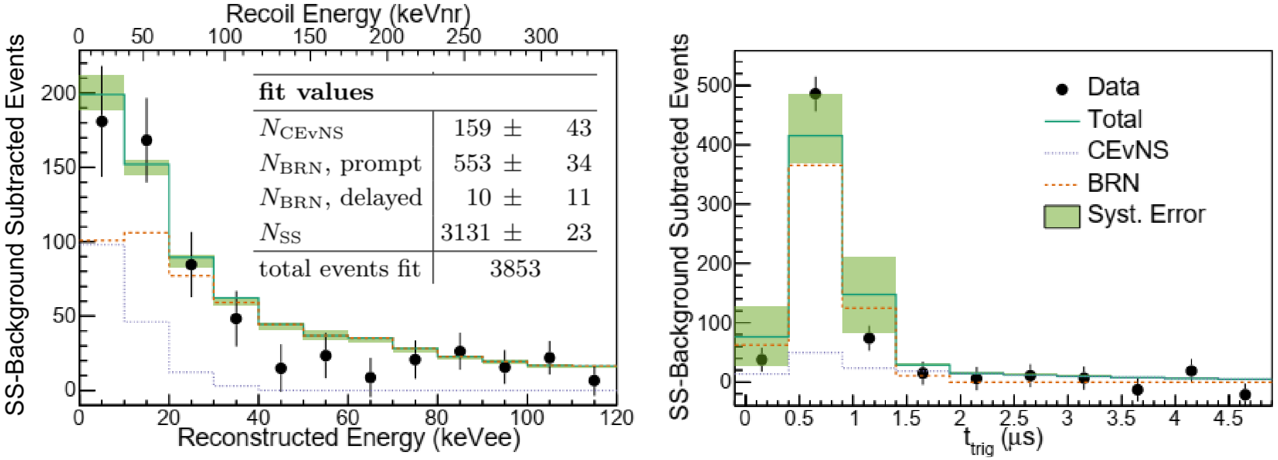

2022 New player:

NCC- 1701 (Dresden-II)

+ 3 kg ultra-low noise germanium detector.

A strong preference for the presence of CEνNS is found.

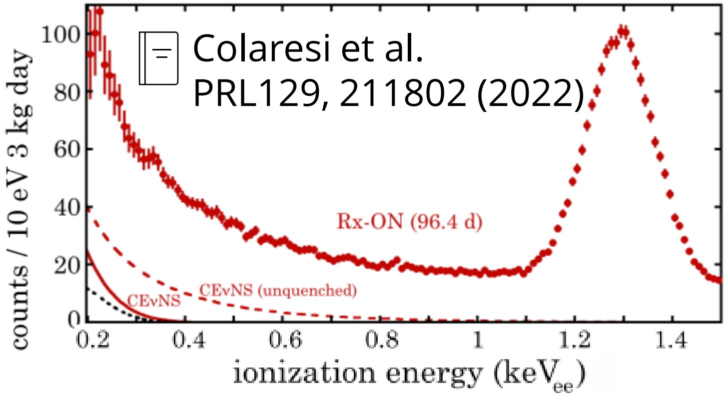

Colaresi et al. PRL129, 211802 (2022)

The past, present and future of R_n measurements with CEνNS and PVES

See details in **D. Akimov et al., arXiv:2204.04575 (2022)**

- **COH-CryoCsI-I**: 10 kg, cryogenic temperature ($\sim 40K$), twice the light yield of present CsI crystal at 300K
- **COH-CryoCsI-II**: 700 kg undoped CsI detector. Both lower energy threshold of 1.4 keVnr while keeping the shape of the energy efficiency of the present COHERENT CsI.

COHERENT future argon: "COH-LAr-750"
LAr based detector for precision CEνNS

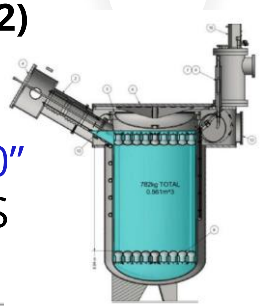

Single phase, scintillation only, 750 kg total (610 kg fiducial)
- ✓ 3000 CEνNS/year

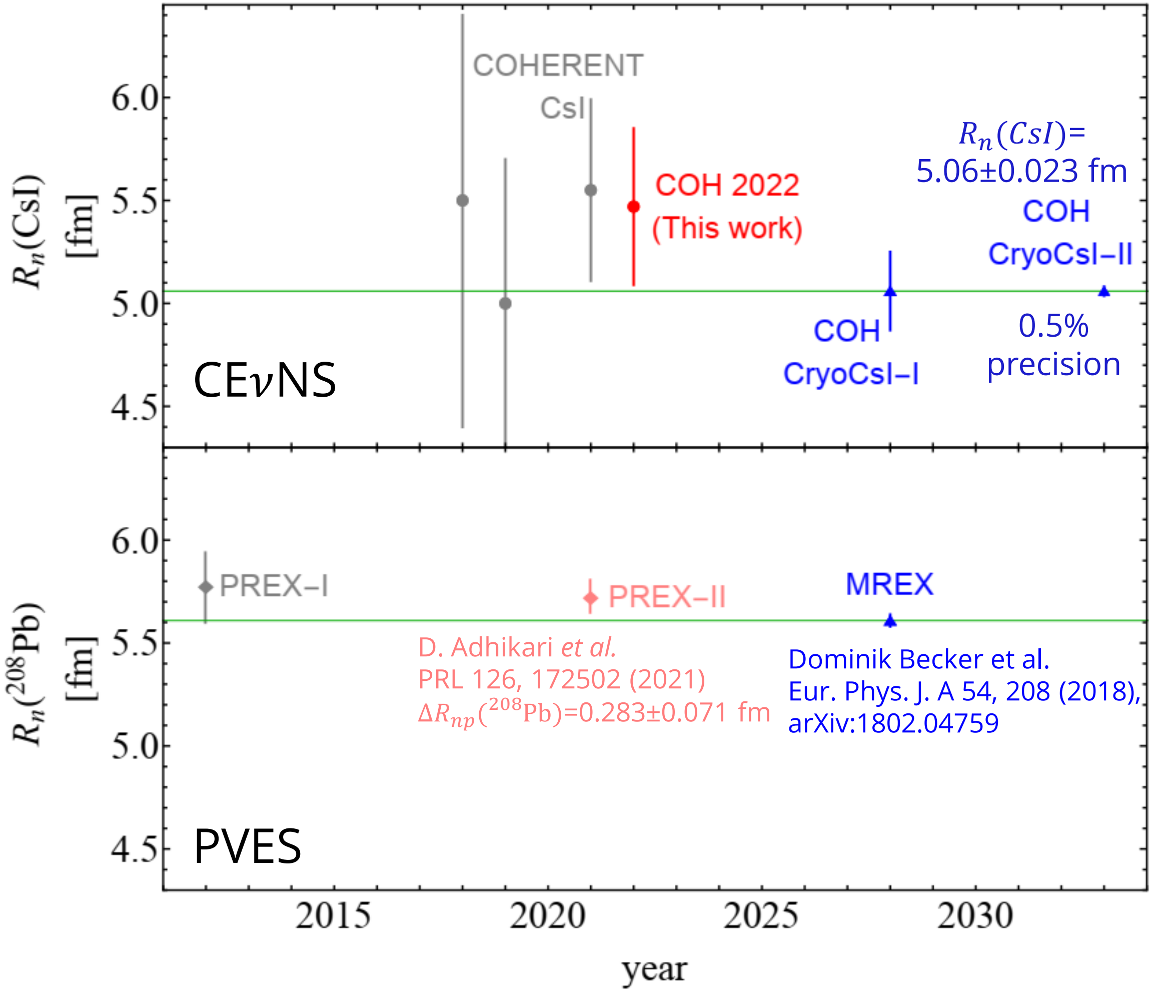

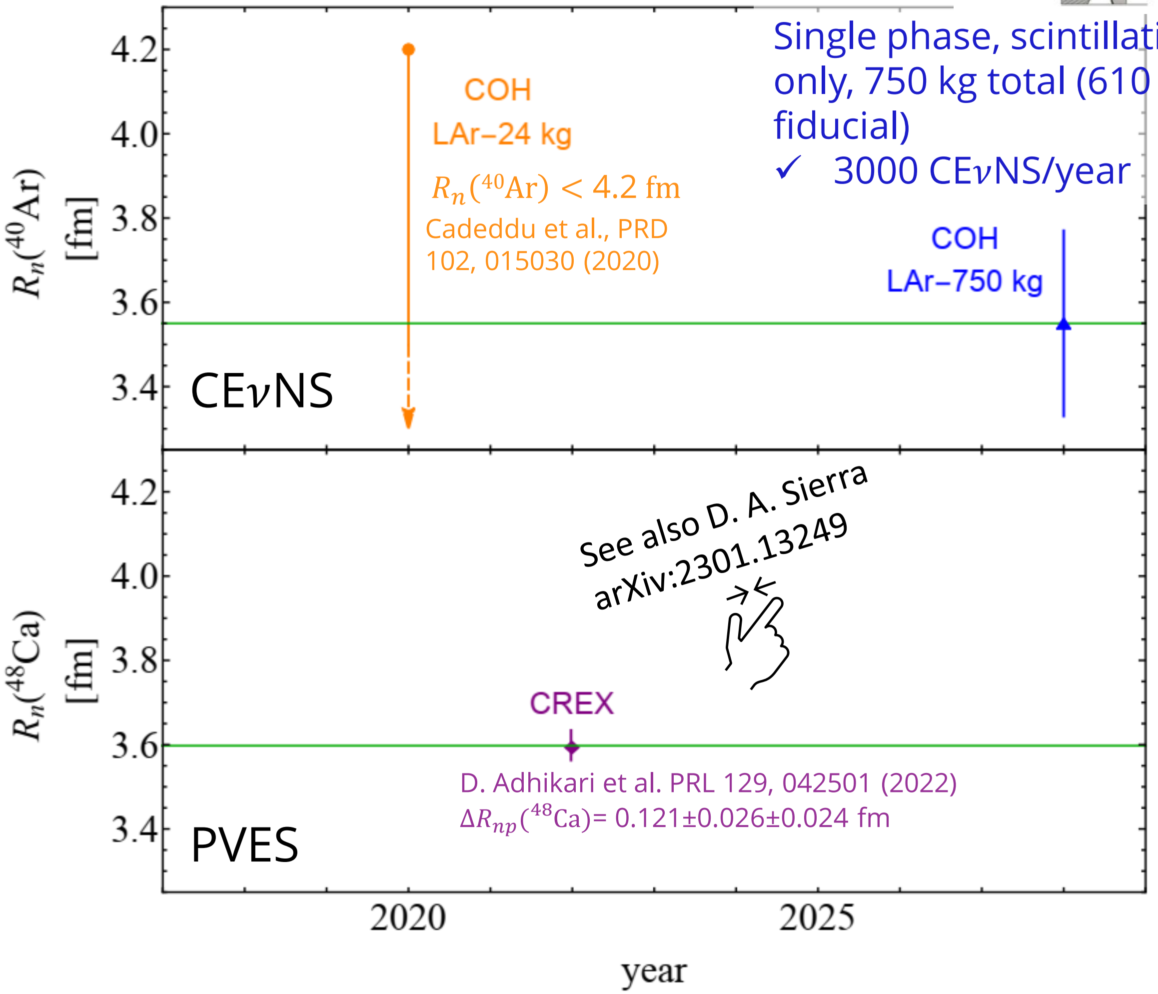

The past, present and future of $\sin^2\vartheta_W$ with CEνNS and APV

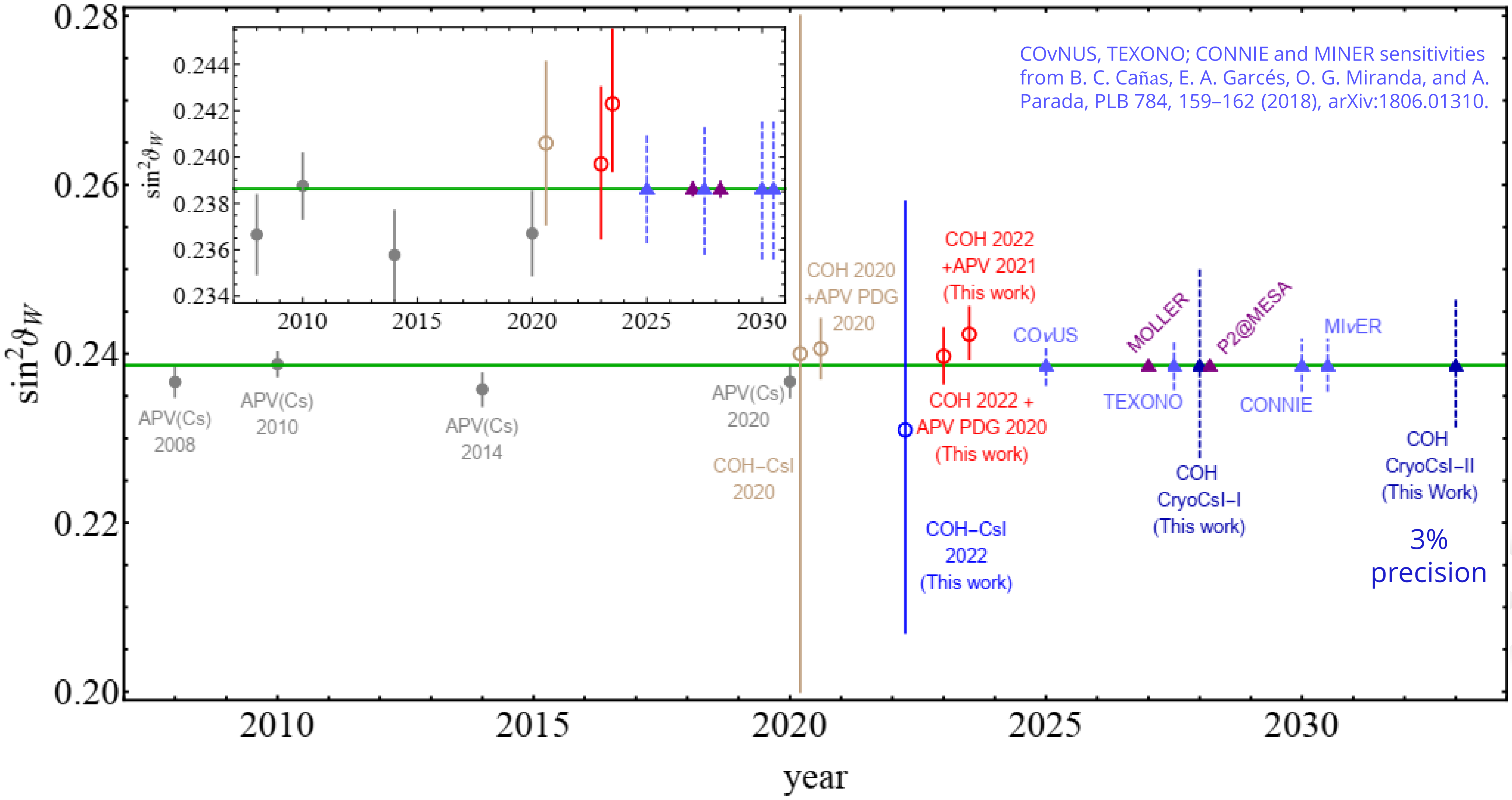

Neutron nuclear radius in argon

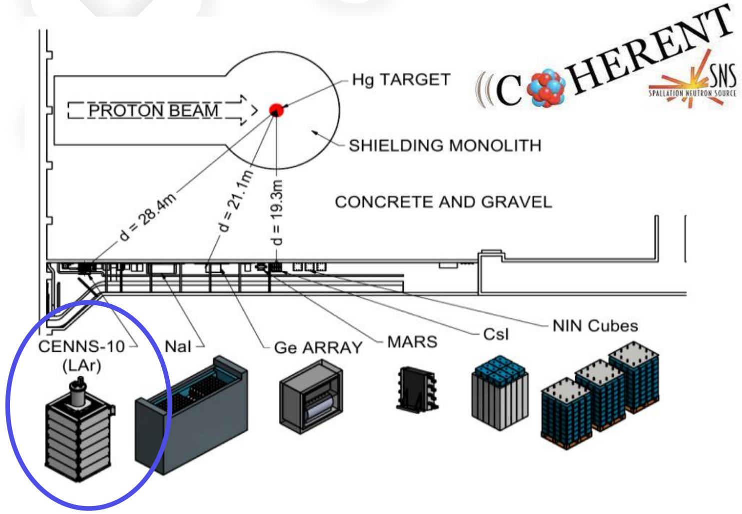

Combined fit in (time, energy, PSP) space suggest >3σ CEvNS detection significance

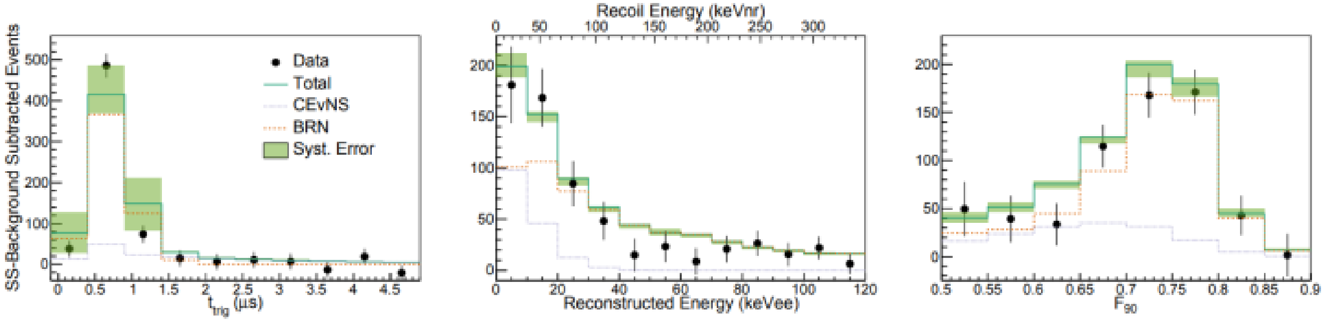

Dominant backgrounds:

1. ^{39}Ar beta decay
2. Beam related neutrons

Akimov et al, COHERENT Coll. PRL 126, 01002 (2021)

Cadeddu et al., PRD 102, 015030 (2020)

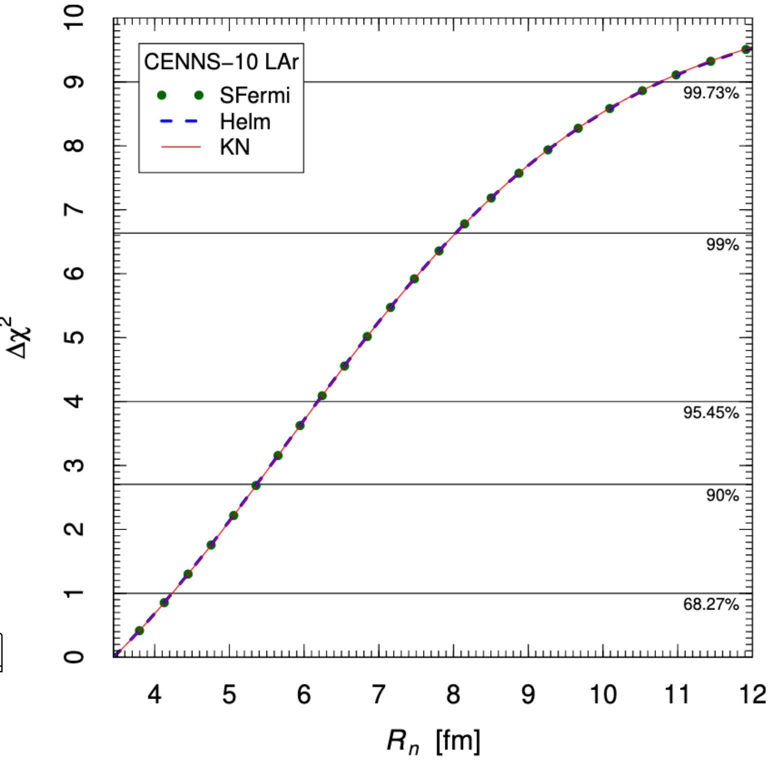

COHERENT Argon

$$R_n(^{40}\mathrm{Ar}) < 4.2\ \mathrm{fm}$$

More statistics needed.

Theoretical values

Interaction		R_p^{point}	R_n^{point}
Sky3D			
SkI3	[37]	3.33	3.43
SkI4	[37]	3.31	3.41
Sly4	[38]	3.38	3.46
Sly5	[38]	3.37	3.45
Sly6	[38]	3.36	3.44
Sly4d	[39]	3.35	3.44
SV-bas	[40]	3.33	3.42
UNEDF0	[41]	3.37	3.47
UNEDF1	[42]	3.33	3.43
SkM*	[43]	3.37	3.45
SkP	[44]	3.40	3.48

See also:
Payne et al.,
PRC 100, 061304 (2019)

See also:
Miranda et al.,
JHEP 05 (2020) 130

COHERENT future argon: "COH-Ar-750"
LAr based detector for precision CEνNS

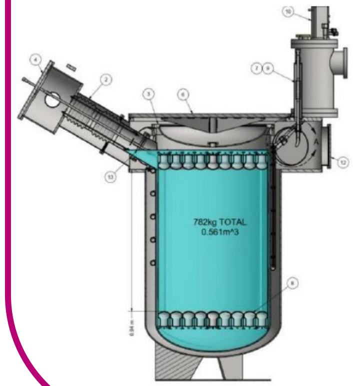

- Single phase, scintillation only, 750 kg total (610 kg fiducial)
- 3000 CEνNS/year

Improvements with the latest CsI dataset

+ New quenching factor

$$E_{ee} = f(E_{nr}) = aE_{nr} + bE_{nr}^2 + cE_{nr}^3 + dE_{nr}^4.$$

a=0.05546, b=4.307, c= -111.7, d=840.4

Akimov et al. (COHERENT Coll), arXiv:2111.02477, JINST 17 P10034 (2022)

+ 2D fit, arrival time information included

$$N_{ij}^{\mathrm{CE}\nu\mathrm{NS}} = (N_i^{\mathrm{CE}\nu\mathrm{NS}})_{\nu_\mu} P_j^{(\nu_\mu)} + (N_i^{\mathrm{CE}\nu\mathrm{NS}})_{\nu_e,\bar{\nu}_\mu} P_j^{(\nu_e,\bar{\nu}_\mu)}$$

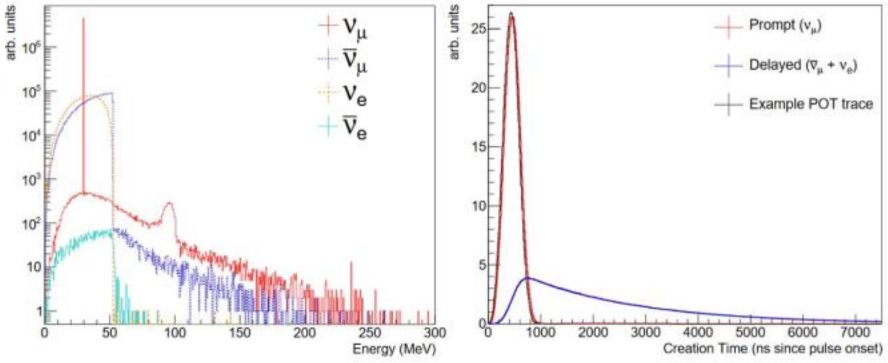

+ Doubled the statistics and reduced syst. uncertainties

$$\sigma_{\mathrm{CE}\nu\mathrm{NS}} = 13\%, \sigma_{\mathrm{BRN}} = 0.9\%,$$
$$\text{and } \sigma_{\mathrm{SS}} = 3\%$$

➢ Theoretical number of CEvNS events

$$\boxed{N_i^{\mathrm{CE}\nu\mathrm{NS}} = N(\mathrm{CsI}) \int_{T_{\mathrm{nr}}^i}^{T_{\mathrm{nr}}^{i+1}} dT_{\mathrm{nr}}\, A(T_{\mathrm{nr}}) \int_0^{T'^{\max}_{\mathrm{nr}}} dT'_{\mathrm{nr}}\, R(T_{\mathrm{nr}}, T'_{\mathrm{nr}}) \int_{E_{\min}(T'_{\mathrm{nr}})}^{E_{\max}} dE \times \sum_{\nu=\nu_e,\nu_\mu,\bar{\nu}_\mu} \frac{dN_\nu}{dE}(E) \frac{d\sigma_{\nu\text{-CsI}}}{dT'_{\mathrm{nr}}}(E, T'_{\mathrm{nr}}),}$$

➢ With the inclusion of energy resolution

$$\boxed{R(N_{\mathrm{PE}}, N'_{\mathrm{PE}}) = \frac{[a_R(1+b_R)]^{1+b_R}}{\Gamma(1+b_R)} N_{\mathrm{PE}}^{b_R}\, e^{-a_R(1+b_R)N_{\mathrm{PE}}}}$$

✓ Analysis with a Gaussian least-square function

$$\boxed{\chi_C^2 = \sum_{i=2}^{9} \sum_{j=1}^{11} \left(\frac{N_{ij}^{\exp} - \sum_{z=1}^{3}(1+\eta_z) N_{ij}^z}{\sigma_{ij}} \right)^2 + \sum_{z=1}^{3} \left(\frac{\eta_z}{\sigma_z} \right)^2,}$$

Cadeddu et al., PRC 104, 065502 (2021), arXiv:2102.06153

Analysis updated in this talk using a Poissonian least-square function after the COHERENT data release!

arXiv:2303.09360

$R_n(\mathrm{Cs})=5.3^{+1.3}_{-1.2}$ fm $R_n(\mathrm{I})=5.6^{+1.6}_{-1.2}$ fm $\chi^2{}_{\mathrm{min}}= 85.2$

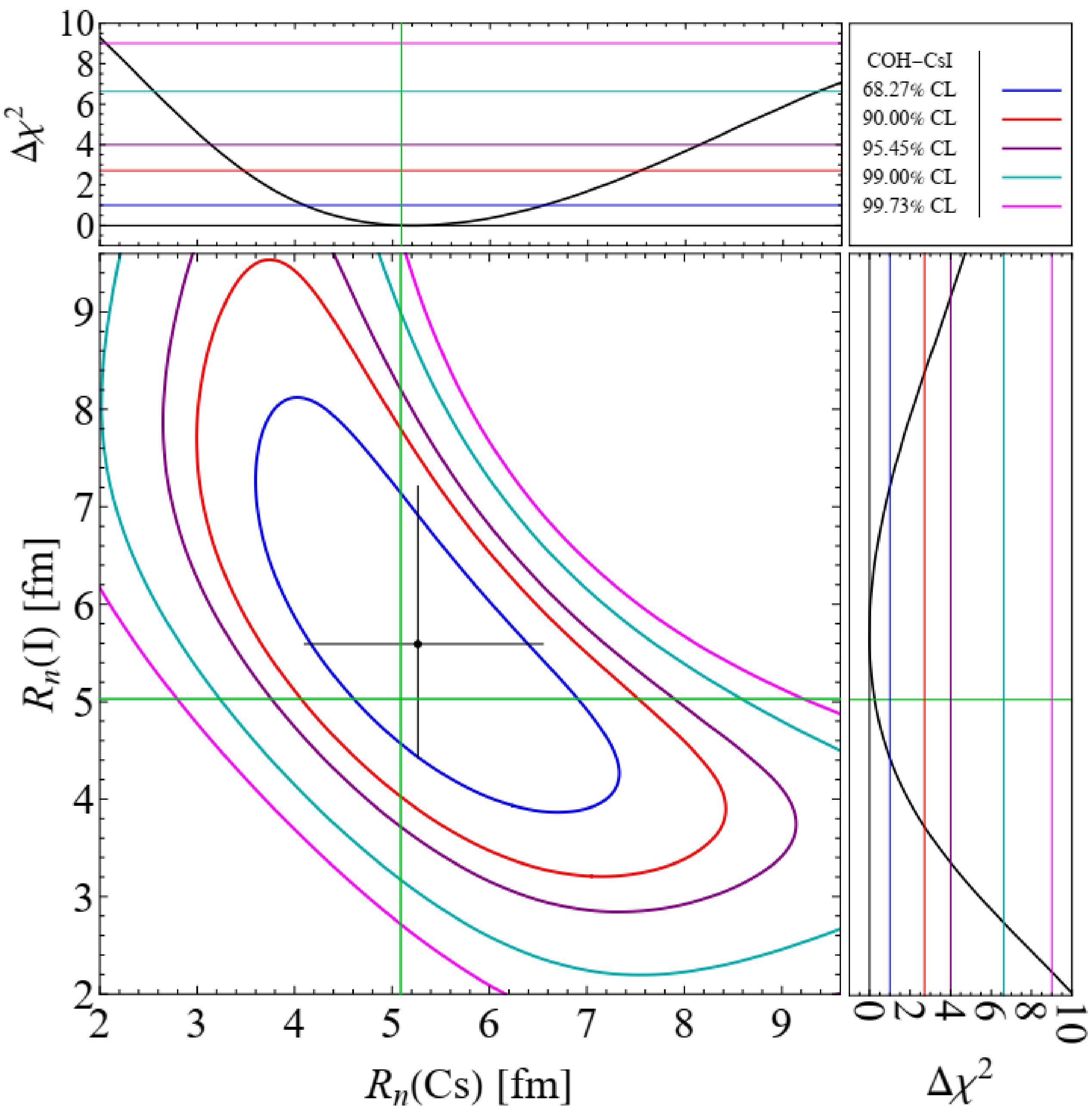

COHERENT CsI χ^2

+ Poissonian least-square function:

+ Since in some energy-time bins the number of events is zero, we used the Poissonian least-squares function

$$\chi^2_{\mathrm{CsI}} = 2\sum_{i=1}^{9}\sum_{j=1}^{11}\left[\sum_{z=1}^{4}(1+\eta_z)N_{ij}^{z} - N_{ij}^{\mathrm{exp}} + N_{ij}^{\mathrm{exp}}\ln\left(\frac{N_{ij}^{\mathrm{exp}}}{\sum_{z=1}^{4}(1+\eta_z)N_{ij}^{z}}\right)\right] + \sum_{z=1}^{4}\left(\frac{\eta_z}{\sigma_z}\right)^2, \qquad (10)$$

where the indices i, j represent the nuclear-recoil energy and arrival time bin, respectively, while the indices $z = 1, 2, 3, 4$ for N_{ij}^{z} stand, respectively, for CEνNS, ($N_{ij}^{1} = N_{ij}^{\mathrm{CE}\nu\mathrm{NS}}$), beam-related neutron ($N_{ij}^{2} = N_{ij}^{\mathrm{BRN}}$), neutrino-induced neutron ($N_{ij}^{3} = N_{ij}^{\mathrm{NIN}}$) and steady-state ($N_{ij}^{4} = N_{ij}^{\mathrm{SS}}$) backgrounds obtained from the anti-coincidence data. In our notation, N_{ij}^{exp} is the experimental event number obtained from coincidence data and $N_{ij}^{\mathrm{CE}\nu\mathrm{NS}}$ is the predicted number of CEνNS events that depends on the physics model under consideration, according to the cross-section in Eq. (1), as well as on the neutrino flux, energy resolution, detector efficiency, number of target atoms and the CsI quenching factor [16]. We take into account the systematic uncertainties with the nuisance parameters η_z and the corresponding uncertainties $\sigma_{\mathrm{CE}\nu\mathrm{NS}} = 0.12$, $\sigma_{\mathrm{BRN}} = 0.25$, $\sigma_{\mathrm{NIN}} = 0.35$ and $\sigma_{\mathrm{SS}} = 0.021$ as explained in Refs. [6, 16].

Dresden-II weak mixing angle results

M. Atzori Corona et al., JHEP **09**, 164 (2022), arXiv:2205.09484

+ Insensitive to $R_n(\mathrm{Ge})$
+ Insensitive to the antineutrino flux parametrization

+ Very sensitive to the Ge quenching factor parametrization

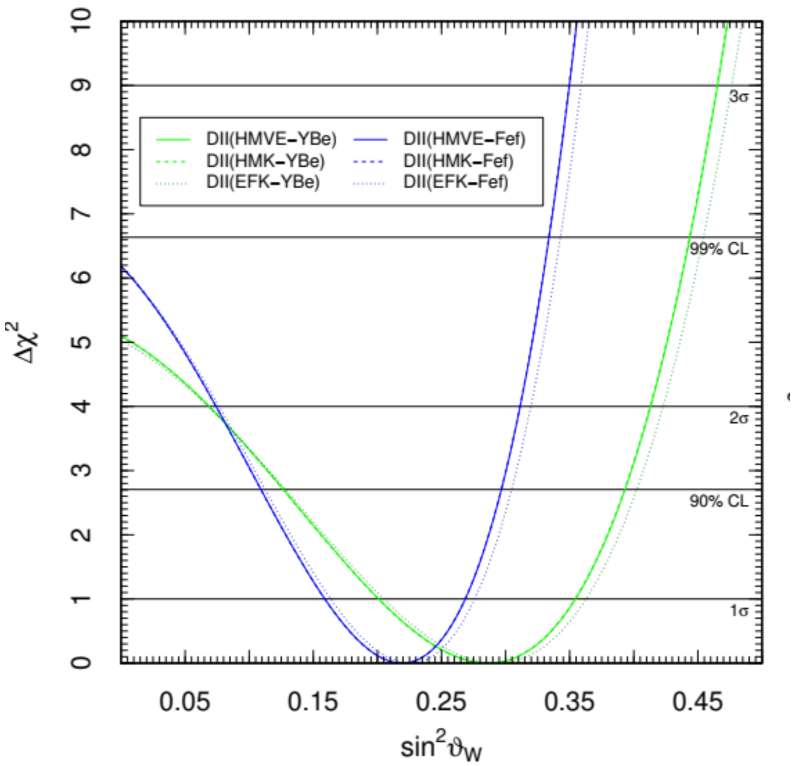

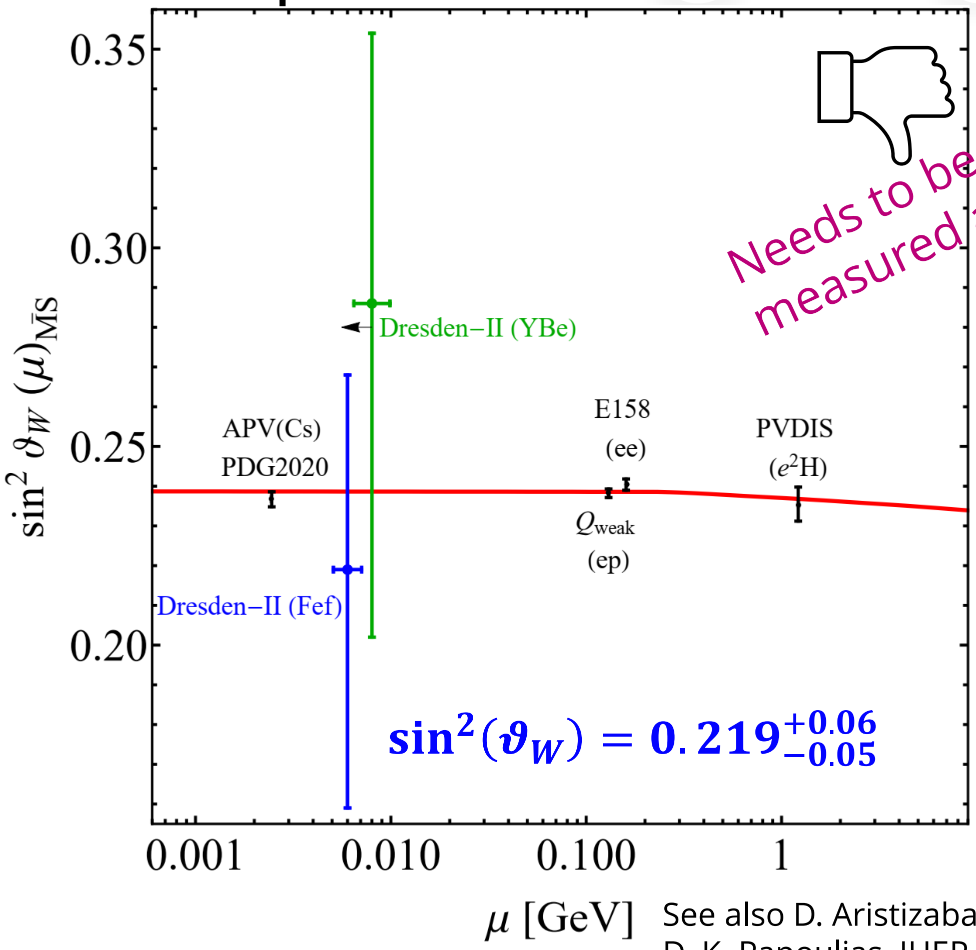

$$\sin^2(\vartheta_W) = 0.219^{+0.06}_{-0.05}$$

Needs to be accurately measured at low energies

See also D. Aristizabal Sierra, V. De Romeri, and D. K. Papoulias, JHEP **09**, 076 (2022)

THE NUCLEAR FORM FACTOR

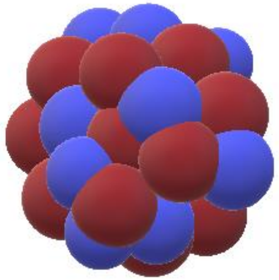

- The nuclear form factor, F(q), is taken to be the **Fourier transform** of a spherically symmetric ground state **mass distribution (both proton and neutrons)** normalized so that **F(0) = 1**:

Helm R. Phys. Rev. **104**, 1466 (1956)

For a weak interaction like for CEvNS you deal with the **weak form factor**: the Fourier transform of the weak charge distribution (neutron + proton distribution weighted by the weak mixing angle)

It is convenient to have an analytic expression like the **Helm form factor**

$$\boxed{F_N^{\mathrm{Helm}}(q^2) = 3\,\frac{j_1(qR_0)}{qR_0}\,e^{-q^2 s^2/2}}$$

$$\frac{d\sigma}{dE_r} \cong \frac{G_F^2\, m_N}{4\pi}\left(1 - \frac{m_N E_r}{2E_\nu^2}\right) Q_w^2 \times |F_{weak}(E_r)|^2$$

Weak charge × weak form factor

$$\left[g_V^p Z F_Z(E_r, R_p) + g_V^n N F_N(E_r, R_n)\right]^2$$

Proton + Neutron from factor

Extensively studied
Huge bibliography

Poorly known…

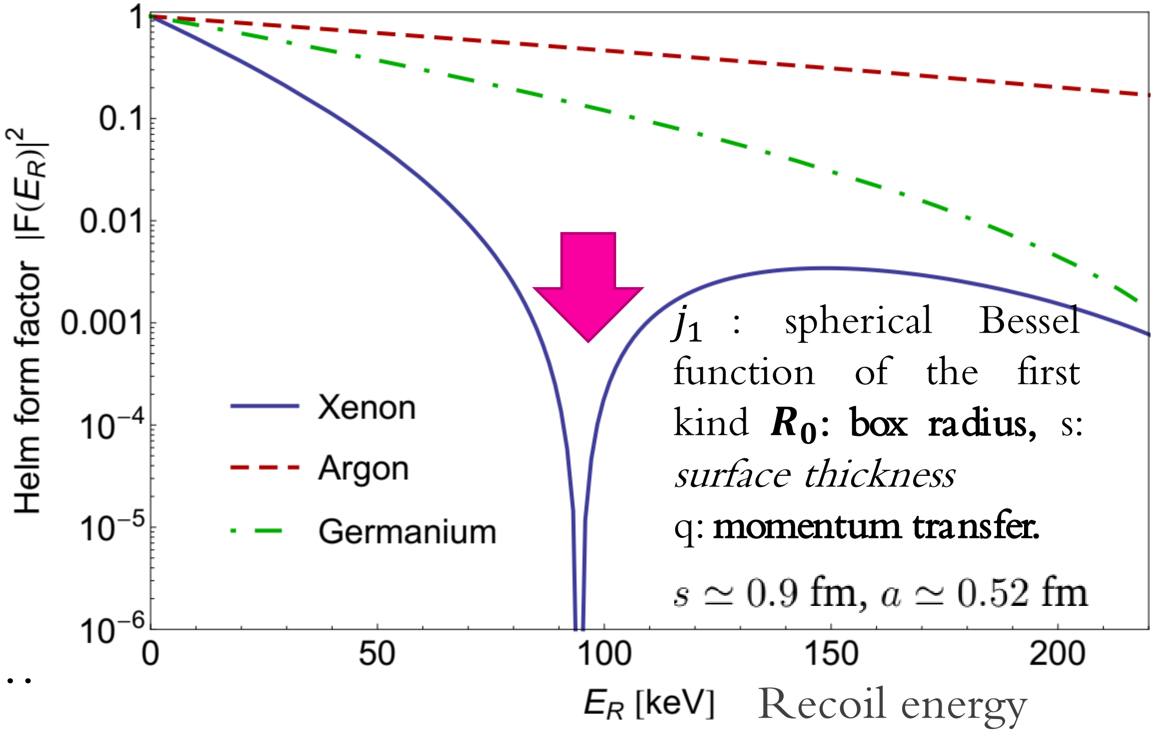

j_1 : spherical Bessel function of the first kind **R_0: box radius,** s: *surface thickness*
q: **momentum transfer.**
$s \simeq 0.9$ fm, $a \simeq 0.52$ fm

Recoil energy

FITTING THE COHERENT CsI DATA FOR THE NEUTRON RADIUS

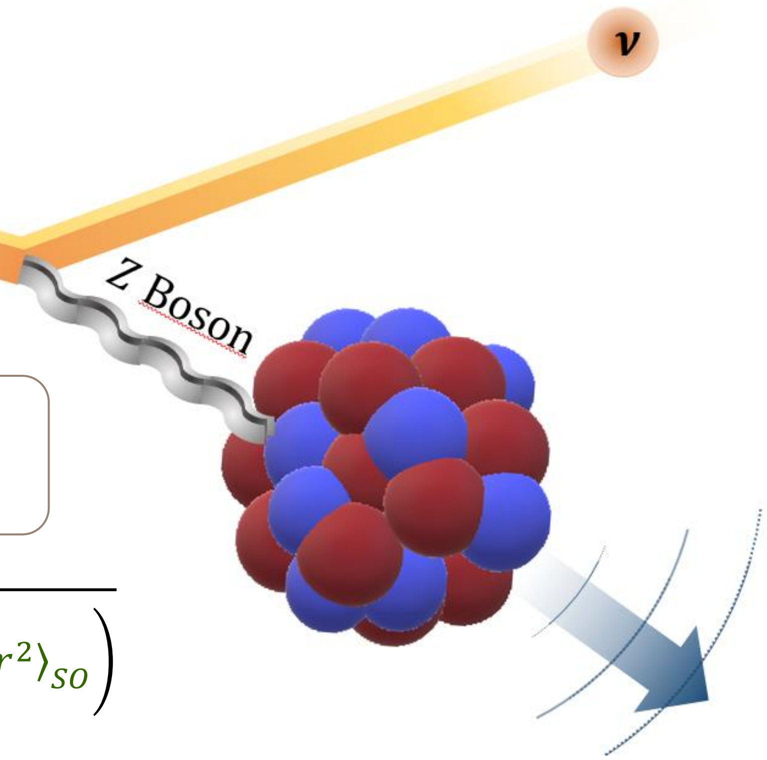

G. Fricke et al., Atom. Data Nucl. Data Tabl. **60**, 177 (1995)

✓ From muonic X-rays data we have

(For fixed $t = 2.3$ fm)

$R_{ch}^{Cs} = 4.804$ fm (Cesium charge rms radius)

$R_{ch}^{I} = 4.749$ fm (Iodine charge rms radius)

$$R_p^{\mathrm{rms}} = \sqrt{R_{\mathrm{ch}}^2 - \left(\frac{N}{Z}\langle r_{\mathrm{n}}^2\rangle + \frac{3}{4M^2} + \langle r^2\rangle_{SO}\right)}$$

$R_p^{Cs} = 4.821 \pm 0.005$ fm (Cesium rms proton radius)

$R_p^{I} = 4.766 \pm 0.008$ fm (Iodine rms-proton radius)

$$\frac{d\sigma}{dE_r} \cong \frac{G_F^2\, m_N}{4\pi}\left(1 - \frac{m_N E_r}{2E_\nu^2}\right)\left[g_V^p Z F_Z\left(E_r, R_p^{Cs/I}\right) + g_V^n N F_N\left(E_r, R_n^{CsI}\right)\right]^2$$

R_n^{Cs} & R_n^{I} very well known so we fitted COHERENT CsI data looking for R_n^{CsI} …

FROM THE CHARGE TO THE PROTON RADIUS

One need to take into account finite size of both protons and neutrons plus other corrections

$$R_{ch}^2 = R_{\text{point}}^2 + \langle r_{\text{p}}^2 \rangle + \frac{N}{Z} \langle r_{\text{n}}^2 \rangle + \frac{3}{4M^2} + \langle r^2 \rangle_{SO}$$

Charge radius

Point-proton radius

Mean squared charge radius of a single proton

$\langle r_{\text{p}}^2 \rangle = 0.7071\ \text{fm}^2$

Mean squared charge radius of a single neutron

$\langle r_{\text{n}}^2 \rangle = -0.1161\ \text{fm}^2$

Relativistic Darwin-Foldy correction

$\sim 0.033\ \text{fm}^2$

Spin-orbit correction

$\sim 0.09\ \text{fm}^2$ for ^{48}Ca

$\sim 0.028\ \text{fm}^2$ for ^{208}Pb

G. Hagen et al. *Nature Physics* **12**, 186–190 (2016), Arxiv: 1509.07169

M. Cadeddu et al. PRD 102, 015030 (2020), Arxiv: 2005.01645

$$R_p^{\text{rms}} = \sqrt{R_{\text{point}}^2 + \langle r_{\text{p}}^2 \rangle} =$$

$$= \sqrt{R_{ch}^2 - \left(\frac{N}{Z} \langle r_{\text{n}}^2 \rangle + \frac{3}{4M^2} + \langle r^2 \rangle_{SO} \right)}$$

RMS proton distribution radius

The proton form factor

$$\frac{d\sigma_{\nu-CsI}}{dT} = \frac{G_F^2 M}{4\pi}\left(1 - \frac{MT}{2E_\nu^2}\right)\left[N\, \boldsymbol{F_N(T, R_n)} - \varepsilon Z\, \boldsymbol{F_Z(T, R_p)}\right]^2$$

Electron scattering and muonic spectroscopy can probes only the proton distribution

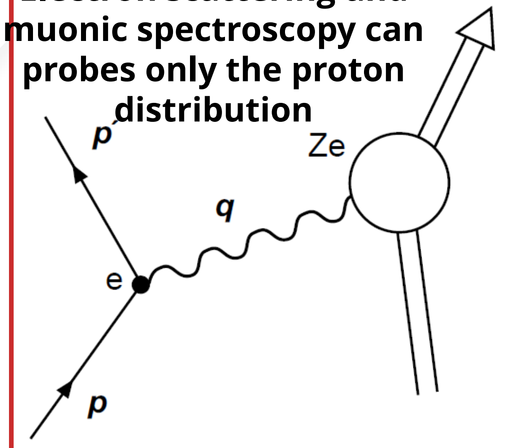

The proton structures of $^{133}_{55}Cs\ (N = 78)$ and $^{127}_{53}I\ (N = 74)$ have been studied with muonic spectroscopy and the data were fitted with **two-parameter Fermi density distributions** of the form

$$\boxed{\rho_F(r) = \frac{\rho_0}{1 + e^{(r-c)/a}}}$$

Where, the **half-density radius c** is related to the **rms radius** and the a parameter quantifies the **surface thickness** $t = 4\,a\,\ln 3$ (in the analysis fixed to 2.30 fm).

- Fitting the data they obtained

$$R_{ch}^{Cs} = 4.804 \text{ fm}$$ (Caesium proton rms radius)

$$R_{ch}^{I} = 4.749 \text{ fm}$$ (Iodine proton rms radius)

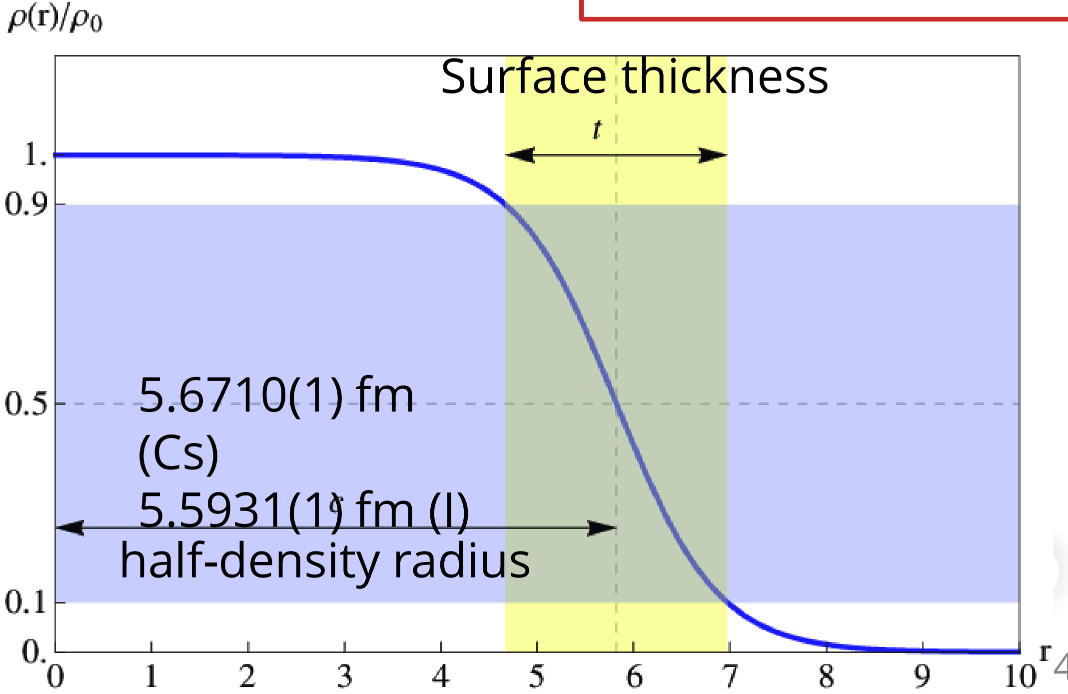

[G. Fricke et al., *Atom. Data Nucl. Data Tabl.* **60**, 177 (1995)]

Weak mixing angle (WMA)

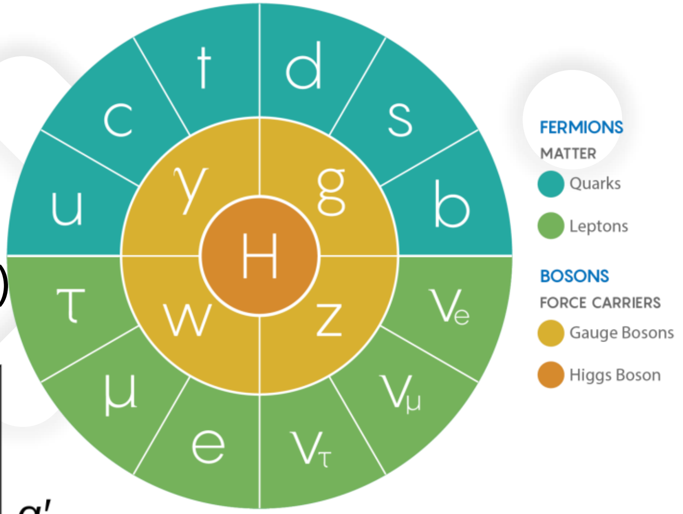

+ The Weinberg angle, θ_W is a fundamental parameter of the **electroweak** (EW) theory of the Standard Model (SM), usually expressed as $\sin^2\theta_W$
+ WMA determines the relative strength of the weak neutral current (NC) vs. electromagnetic interaction

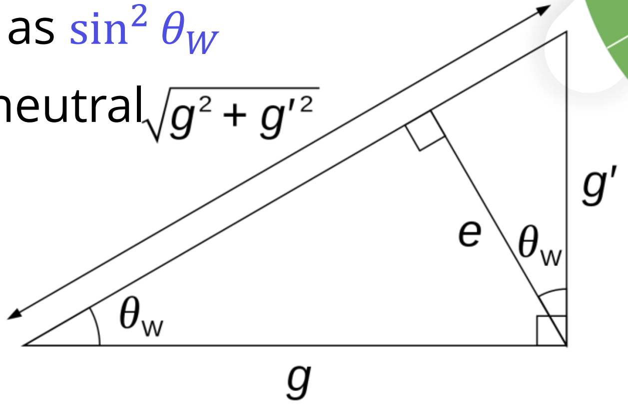

$$e = g\sin\theta_W$$
$$e = g'\cos\theta_W$$

➢ **Tree-level** $\sin^2\theta_W = 1 - \frac{M_W^2}{M_Z^2} = \frac{g'^2}{g^2+g'^2}$

+ The **on-shell scheme** promotes the tree-level formula to a definition of the renormalized $\sin^2\theta_W$ to all orders in perturbation theory (quite sensitive to the top mass)

➢ $\sin^2\theta_W \to s_W^2 \equiv 1 - \frac{M_W^2}{M_Z^2} = 0.22343 \pm 0.00007$ (on−shell)

+ **Minimal subtraction scheme** ($\overline{\mathrm{MS}}$) $\sin^2\hat{\theta}_W(\mu) = \frac{\hat{g}'^2(\mu)}{\hat{g}^2(\mu)+\hat{g}'^2(\mu)}$ where the couplings are defined in the $\overline{\mathrm{MS}}$ and the energy scale μ is conveniently chosen to be M_Z for many EW processes (less sensitive to the top mass)

➢ $\sin^2\hat{\theta}_W(M_Z) \equiv \hat{s}_Z^2 = 0.23122 \pm 0.00003$ ($\overline{\mathrm{MS}}$)

Scale dependent→ running of WMA

Scale dependence of the weak mixing angle

- The value of $\sin^2\hat{\theta}_W$ varies as a function of the momentum transfer or energy scale («running»).
- Working in the $\overline{\mathrm{MS}}$, the main idea is to relate the case of the WMA to that of the electromagnetic coupling $\hat{\alpha}$
- The vacuum polarization contributions are crucial

Allows precision tests of the Standard Model!

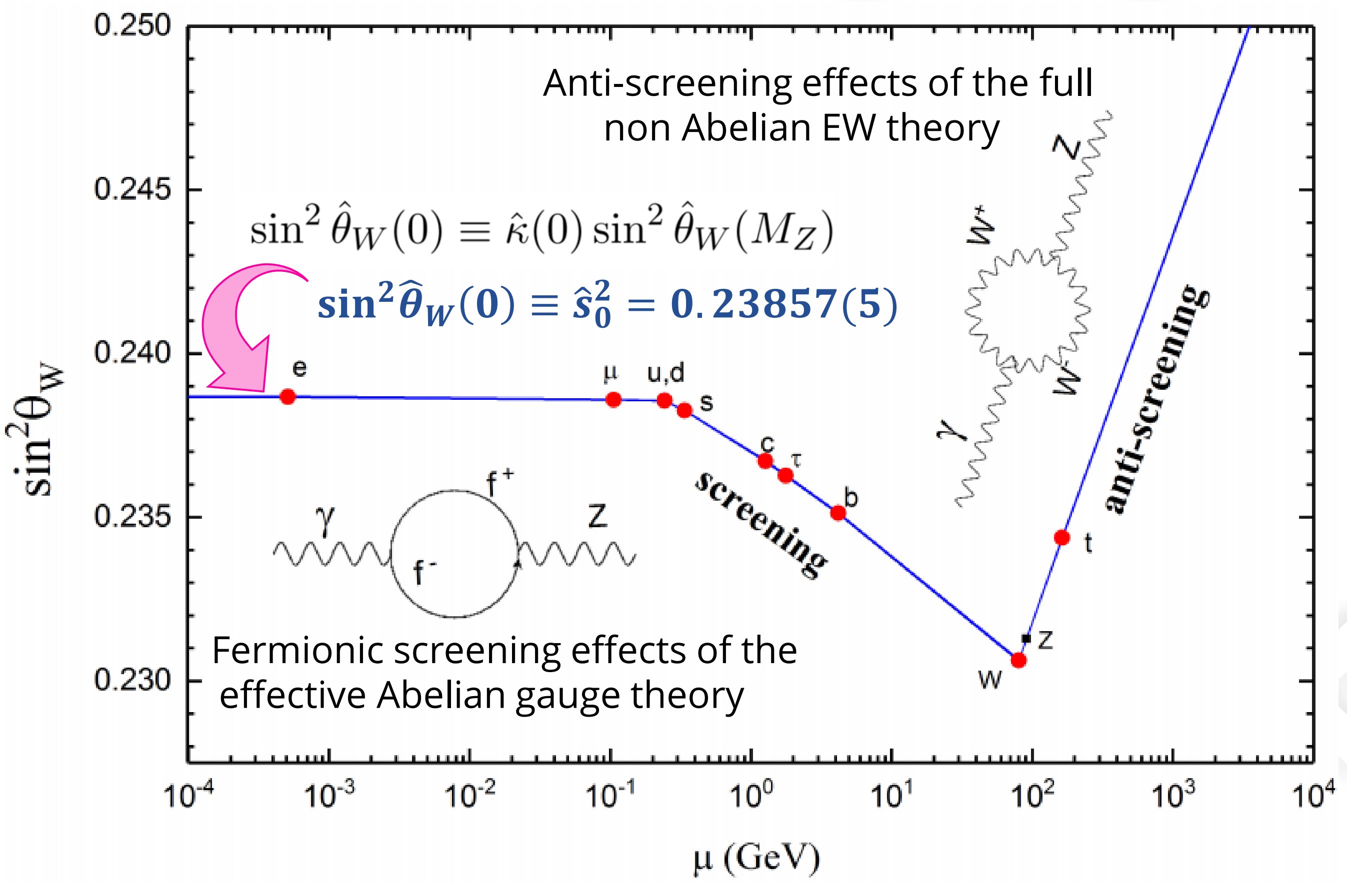

[Erler et al. JHEP 03 (2018) 196, ArXiv:1712.09146]

The «running» function changes sign at $\mu = M_W$ where the fermionic screening effects are overcompensated by the anti-screening effects

Neutron radius determination of ^{133}Cs and its impact on the interpretation of CEνNS-CsI measurement

Y. Huang[a,b], S. Y. Xia[c,d], Y. F. Li[c,d], X. L. Tu[a,*], J. T. Zhang[a], C. J. Shao[a], K. Yue[a], P. Ma[a], Y. F. Niu[e], Z. P. Li[f], Y. Kuang[f], X. Q. Liu[b], J. F. Han[b], P. Egelhof[g], Yu. A. Litvinov[g], M. Wang[a], Y. H. Zhang[a], X. H. Zhou[a], Z. Y. Sun[a]

[a] *Institute of Modern Physics, Chinese Academy of Sciences, Lanzhou 730000, China*
[b] *Key Laboratory of Radiation Physics and Technology of the Ministry of Education, Institute of Nuclear Science and Technology, Sichuan University, Chengdu 610064, China*
[c] *Institute of High Energy Physics, Chinese Academy of Sciences, Beijing 100049, China*
[d] *School of Physical Sciences, University of Chinese Academy of Sciences, Beijing 100049, China*
[e] *School of Nuclear Science and Technology, Lanzhou University, Lanzhou 730000, China*
[f] *School of Physical Science and Technology, Southwest University, Chongqing 400715, China*
[g] *GSI Helmholtzzentrum für Schwerionenforschung GmbH, D-64291 Darmstadt, Germany*

Abstract

Proton-^{133}Cs elastic scattering at low momentum transfer is performed using an in-ring reaction technique at the Cooler Storage Ring at the Heavy Ion Research Facility in Lanzhou. Recoil protons from the elastic collisions between the internal H_2-gas target and the circulating ^{133}Cs ions at 199.4 MeV/u are detected by a silicon-strip detector. The matter radius of ^{133}Cs is deduced by describing the measured differential cross sections using the Glauber model. Employing the adopted proton distribution radius, a point-neutron radius of 4.86(21) fm for ^{133}Cs is obtained. With the newly determined neutron radius, the weak mixing angle $\sin^2\theta_W$ is independently extracted to be 0.227(28) by fitting the coherent elastic neutrino-nucleus scattering data. Our work limits the $\sin^2\theta_W$ value in a range smaller than the ones proposed by the previous independent approaches, and would play an important role in searching new physics via the high precision CEνNS-CsI cross section data in the near

*Corresponding author.
Email address: tuxiaolin@impcas.ac.cn (X. L. Tu)

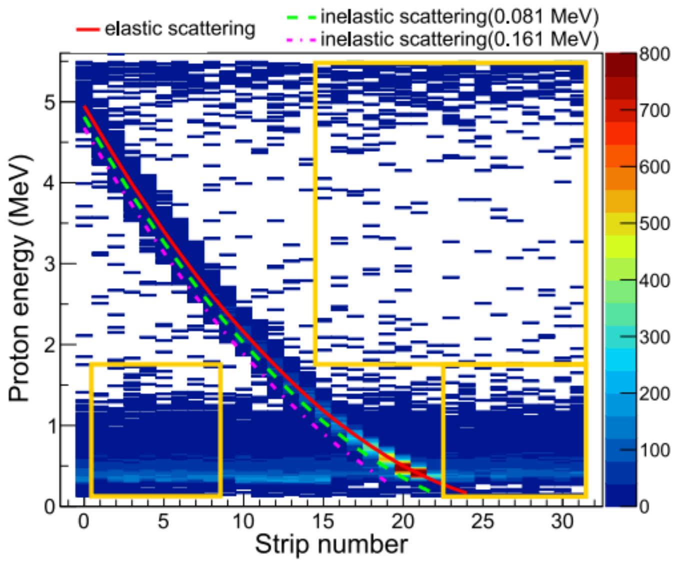

Figure 1: Scatter plot of the recoil proton energy versus the strip number of DSSD. The solid (red), dashed (green), and dash-dotted (pink) lines denote the calculated proton energies for elastic and two inelastic scattering channels, respectively. For more details see text.

Small-angle p-nucleus elastic distributions are sensitive to matter distribution radius.

present work, a well established procedure [44, 49, 50] based on the Glauber multiple-scattering theory [51] is employed to extract the matter radius of ^{133}Cs through describing the measured $\frac{d\sigma}{d\Omega}(\theta)$. The $\frac{d\sigma}{d\Omega}(\theta)$ values are expressed in the Glauber model as a function of the matter density distribution $\rho(r)$ and the proton-nucleon scattering amplitude $f_{pi}(q)$ with $i = n$ or p, see Ref. [50] for details. To reduce the model-dependent errors of matter radius, the scattering amplitude parameters were calibrated at 200 MeV [48] to be $\sigma_{pp} = 1.788(20)$ fm^2, $\sigma_{pn} = 3.099(27)$ fm^2, $\alpha_{pp} = 0.893(17)$, $\alpha_{pn} = 0.325(23)$, and $\beta_{pp} = \beta_{pn} = 0.528(41)$ fm^2, which are adopted here to calculate the $f_{pi}(q)$. These values have been adopted to fit the differential cross sections of p-^{16}O elastic scattering at 200 MeV and reproduce the well-known matter radius of ^{16}O [48].

As shown in Fig. 2, the measured ddσ Ω(θ) are well described with the Glauber model by adjusting R and L0. With the obtained R and fixed a, a root-mean-square (rms) point-matter radius Rpm for 133Cs is determined to be

$$R_{\rm pm} = \left(\frac{\int \rho(r) r^4 dr}{\int \rho(r) r^2 dr} \right)^{\frac{1}{2}} = 4.811 \pm 0.127 \text{ fm}, \tag{3}$$

where uncertainties from statistics, input parameters, and Glauber model are about 0.12 fm, 0.03 fm, and 0.03 fm, respectively. The radius uncertainties caused by statistics and input parameters are estimated by using the randomly sampled experimental $\frac{d\sigma}{d\Omega}(\theta)$ and input parameters within 2σ band [50], respectively. The model-dependent error at 200 MeV is estimated by comparing the well-known proton radii with the matter radii of ^{12}C, ^{16}O, and ^{28}Si determined with the similar method, where similar proton and matter radii are expected for the $N = Z$ nuclei. To check the effects of background, only recoil protons with energies > 1 MeV were analyzed, and a consistent radius of 4.825 fm is obtained. Details and reliability considerations about radius determinations can be found in Refs. [30, 50].

With the obtained $R_{\rm pm}$, a point-neutron distribution radius $R_{\rm pn}$ of ^{133}Cs is determined to be

$$R_{\rm pn} = \sqrt{\frac{A}{N} R_{\rm pm}^2 - \frac{Z}{N} R_{\rm pp}^2} = 4.86 \pm 0.21 \text{ fm}, \tag{4}$$

where N, Z, and A are the neutron, proton, and mass number, respectively. The adopted point-proton radius $R_{\rm pp}$ of 4.740(5) fm for ^{133}Cs is deduced from charge radius [30, 54].

We extract the neutron skin of ^{133}Cs to be $R_{\rm pn} - R_{\rm pp} = 0.12(21)$ fm.

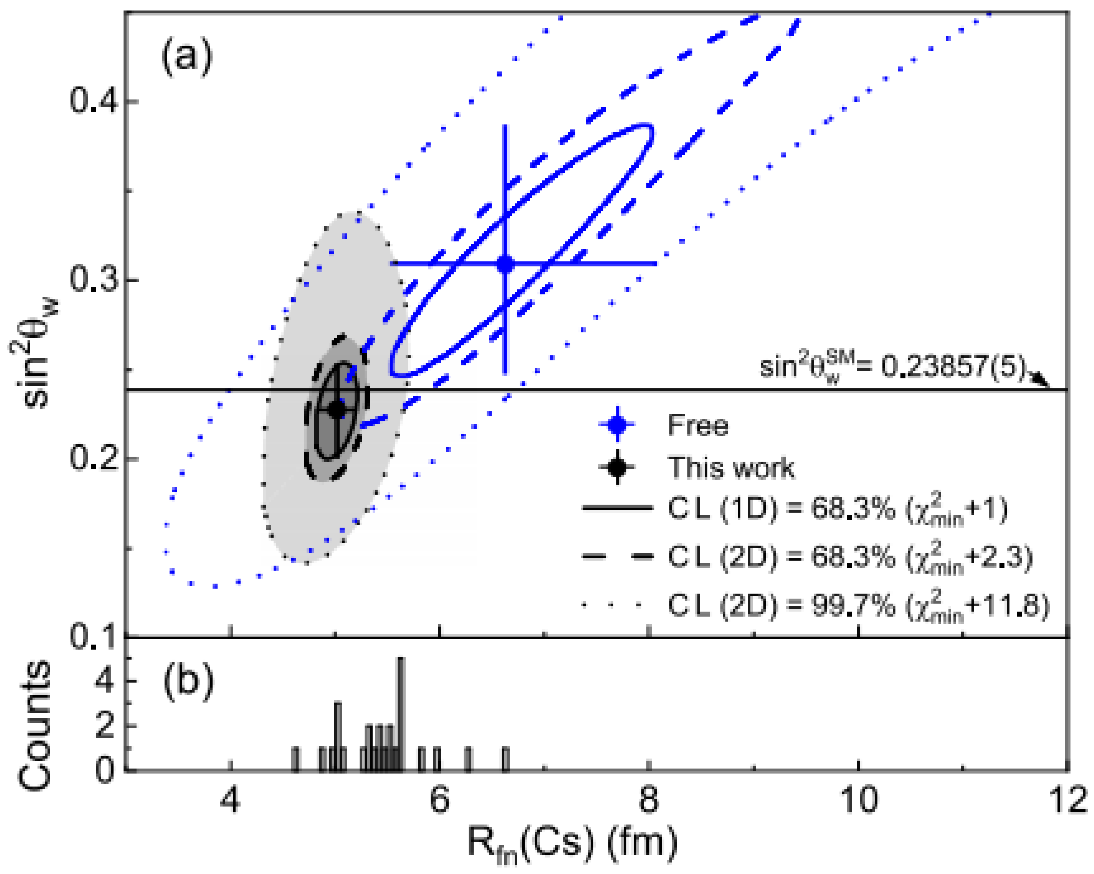

Figure 4: (a) The $\chi^2_{\rm all}$ contours in the plane of $R_{\rm fn}$ versus $\sin^2\theta_W$. The blue curves and point represent results when both $R_{\rm fn}$ and $\sin^2\theta_W$ are free variables in the CEνNS-CsI data fitting. The black curves and point add the constraint imposed by the presently deduced radius. (b) The distribution of reported neutron radii of ^{133}Cs [15, 17, 18, 20, 21, 22, 23, 24, 25, 26, 27] deduced from the CEνNS-CsI data [10, 11].

Parity Violation Electron Scattering (PVES) and APV on Lead

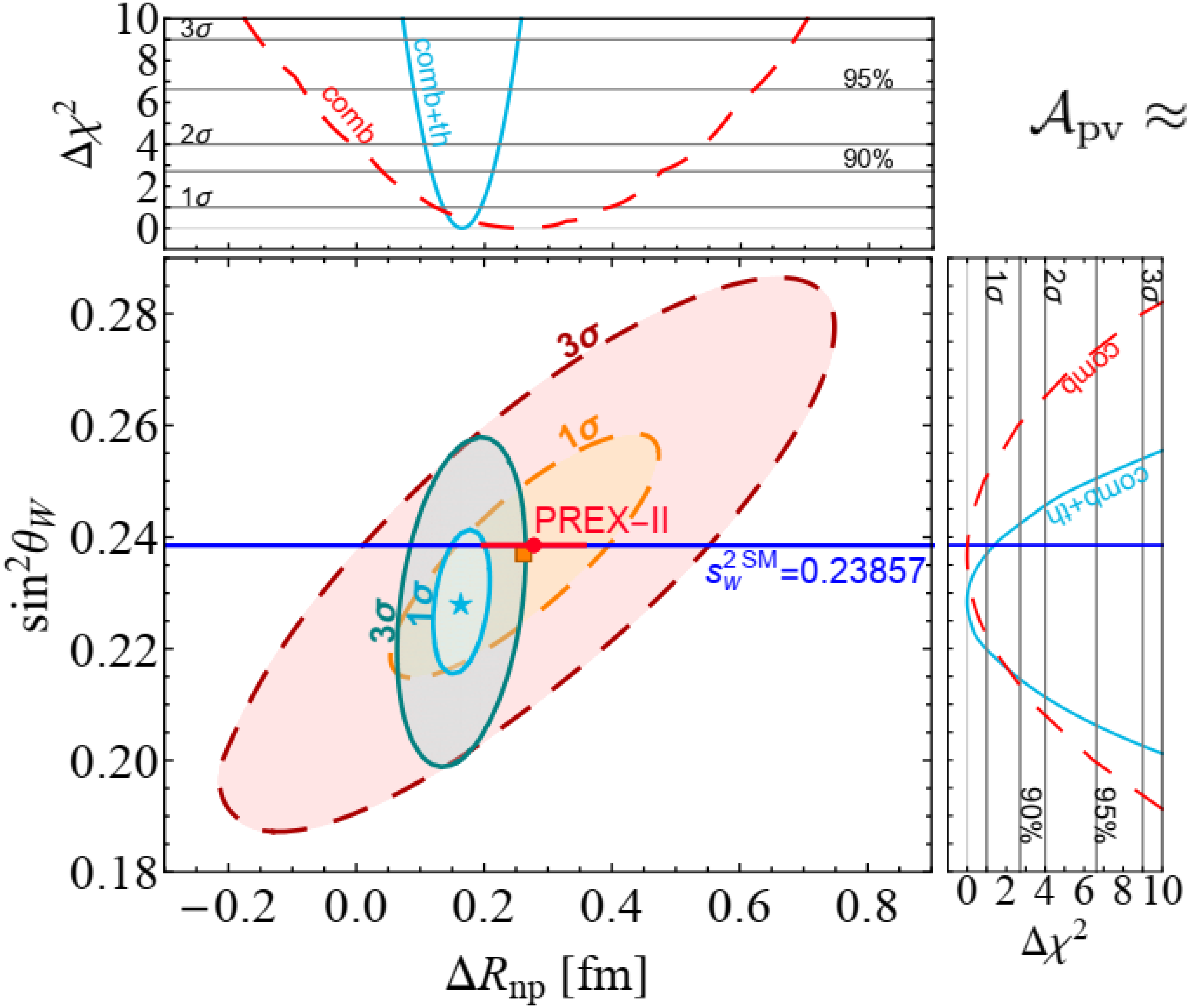

$$A_{\mathrm{pv}} \approx \frac{G_F Q^2}{4\pi\alpha\sqrt{2}} \frac{Q_W F_W(Q^2)}{Z F_{\mathrm{ch}}(Q^2)},$$

Arxiv: 2112.09717

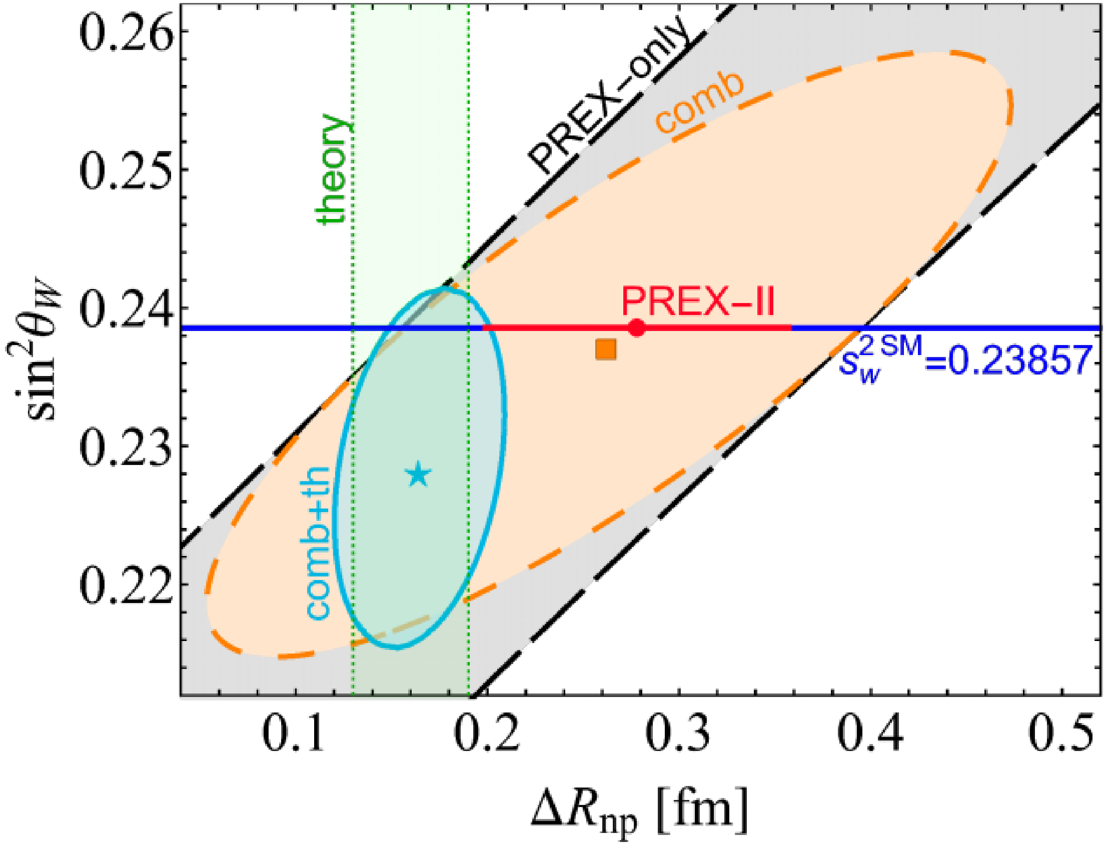

Lead neutron skin from non-EW probes…

	Experimental Δr_{np}^{exp} (fm)	Method	Evaluated Δr_{np}^{eva} (fm)	Difference $\frac{\Delta r_{np}^{eva}-\Delta r_{np}^{exp}}{\text{error}}$
^{208}Pb	0.150(20) [21,36]	AA	0.167(11)	0.9
	0.250(90) [49]	(α,α)		−0.9
	0.080(50) [56]	(p,p)		1.7
	0.160(50) [57]	(p,p)		0.1
	0.060(100) [59]	(p,p)		1.1
	0.360(200) [64]	(p,p)		−1.0
	0.180(70) [67]	(p,p)		−0.2
	0.190(90) [72]	GDR		−0.3
	0.300(70) [74]	(α,α)		−1.9
	0.211(63) [75]	(p,p)		−0.7
	0.197(42) [76]	(p,p)		−0.7
	0.260(130) [77]	(α,α)		−0.7
	0.420(200) [77]	(α,α)		−1.3
	0.273(90) [78]	(α,α)		−1.2
	0.182(70) [79]	(p,p)		−0.2
	0.140(40) [80]	(p,p)		0.7
	0.180(35) [81]	PDR		−0.4
	0.120(70) [82]	GDR		0.7
	0.160(45) [83]	AA		0.2
	0.200(64) [32]	AA		−0.5

PRC 104, 034303 (2021)

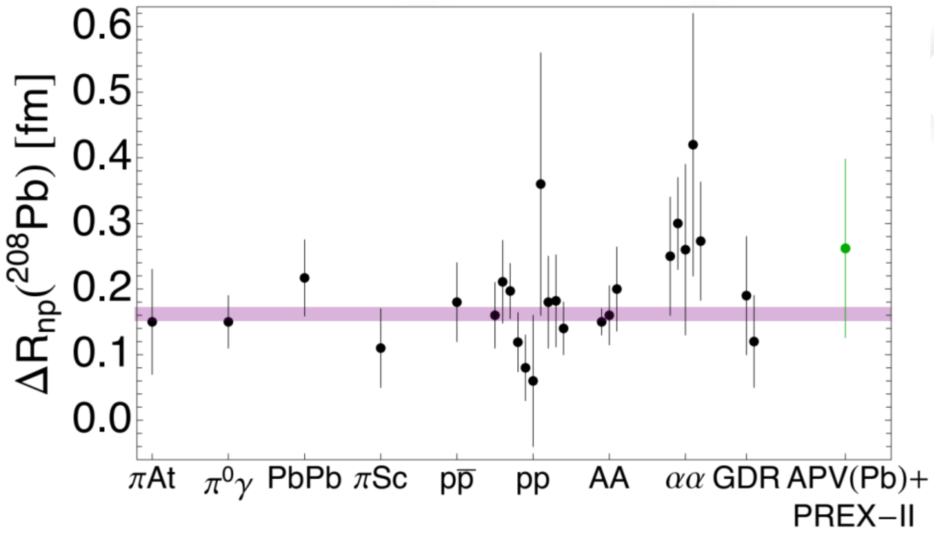

Table 4. ^{208}Pb neutron skin measurements and theoretical predictions with 1σ uncertainties

^{208}Pb Experiment	**Reference**	r_{np}^{208} (fm)
Coherent $\pi^0\gamma$ production	[77]	$0.15^{+0.03}_{-0.04}$
Pionic atoms	[73]	0.15 ± 0.08
Pion scattering	[73]	0.11 ± 0.06
$\bar{p}$ annihilation	[78,79]	0.18 ± 0.06
Elastic polarized p scattering	[70]	0.16 ± 0.05
Elastic polarized p scattering	[80]	$0.211^{+0.054}_{-0.063}$
Elastic p scattering	[81]	0.197 ± 0.042
Elastic p scattering	[72]	0.119 ± 0.045
Parity-violating e^- scattering (PREX I+II)	[17]	0.283 ± 0.071
^{208}Pb experimental weighted mean		0.166 ± 0.017
Pygmy dipole resonances	[82]	0.180 ± 0.035
r_{np}^{Sn}	[83]	0.175 ± 0.020
Anti-analog giant dipole resonance	[84]	0.216 ± 0.048
Symmetry energy ^{208}Pb	[85]	0.158 ± 0.014
Dispersive optical model	[86]	$0.18^{+0.25}_{-0.12}$
Dispersive optical model	[67]	0.25 ± 0.05
Coupled cluster expansion	[66]	0.17 ± 0.03
r_{np}^{48}	[63,64], this paper	0.128 ± 0.040
α_D^{208}	[62], this paper	0.154 ± 0.019
α_D^{208}	[20,64], this paper	0.188 ± 0.017
^{208}Pb theoretical weighted mean		0.170 ± 0.008

Lattimer arXiv:2301.03666v1